

Intracellular regulation of Wnt and FGF signal transduction by the late endosomal compartment in *Xenopus laevis*

**Dissertation for Obtaining the Doctoral Degree
of Natural Sciences (Dr. rer. nat.)**

**Faculty of Natural Sciences
University of Hohenheim**

Institute of Biology, Dept. of Zoology (190z)

submitted by
Jennifer Kreis

from Herdecke
2022

Dean: Prof. Dr. Uwe Beifuss
1st reviewer: PD Dr. Kerstin Feistel
2nd reviewer: Prof. Dr. Armin Huber
Submitted on: 02.06.2022
Oral examination on: 15.11.2022

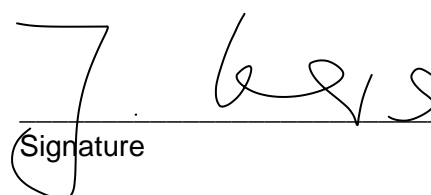
Affidavit according to Sec. 7(7) of the University of Hohenheim doctoral degree regulations for Dr. rer. nat.

1. For the dissertation submitted on the topic
“Intracellular regulation of Wnt and FGF signal transduction by the late endosomal compartment in *Xenopus laevis*”
I hereby declare that I independently completed the work.
2. I only used the sources and aids documented and only made use of permissible assistance by third parties. In particular, I properly documented any contents which I used – either by directly quoting or paraphrasing – from other works.
3. I did not accept any assistance from a commercial doctoral agency or consulting firm.
4. I am aware of the meaning of this affidavit and the criminal penalties of an incorrect or incomplete affidavit.

I hereby confirm the correctness of the above declaration: I hereby affirm in lieu of oath that I have, to the best of my knowledge, declared nothing but the truth and have not omitted any information.

Stuttgart, 02.06.2022

Place and date


Signature

Abstract

The endosomal network depicts a vast playground of multiple processing capabilities in terms of signaling. Distinct compartments of the endosomal machinery exert specific functions and thus contribute in signal termination, transduction, attenuation or amplification. Initially, these functions were attributed to early endosomes but recent research likewise considers late endosomes to be just as relevant in mediating such processes. Functionality as well as the molecular identity of these intracellular membranous platforms are orchestrated by a large superfamily of small Ras like GTPases. The collected data of this study particularly highlight the involvement of late endosomes and its associated regulator Rab7 in the early development of the African clawed frog *Xenopus laevis*.

In particular, the first two chapters address the Rab7-dependent specification of the mesodermal germ layer by regulating intracellular pathway activity of Wnt and FGF/MAPK signaling. After fertilization formation of the germ layers is one of the first processes to be initiated. An essential part of mesoderm development comprises subdivision into different mesodermal regions, thus clustering it into ventrolateral and dorsal mesoderm. This patterning is crucial to promote further differentiation into various tissues arising from the mesodermal germ layer. It turned out, Rab7 regulates ventrolateral fates in a Wnt-dependent manner. The small GTPase exerts its function upstream of the Wnt co-transcription factor Ctnnb1 to ensure its nuclear relocalization. In addition to that, Rab7-positive endosomes are likewise required to mediate intracellular FGF/MAPK signal transduction in order to specify dorsal mesoderm. Here, Rab7 regulates proper signaling at the level or downstream of Ras and upstream of Erk/Mapk1.

The last chapter then elicits further regulative properties of the late endosomal platform, concerning Cd63 function. The tetraspanin Cd63, which constitutes a transmembrane protein, associates with late endolysosomal compartments and exhibits a similar expression pattern like the small GTPase Rab7 in *Xenopus laevis*. Contrary to Rab7, function of Cd63 seems to be dispensable whilst gastrulation. However, the presented studies in this chapter suggest a vital function of the tetraspanin Cd63 during axial elongation and correct eye development. Therefore, these investigations regarding Cd63 demonstrated an involvement of the regulative function of late endosomes as signaling platforms for embryonic development beyond mesoderm specification and gastrulation.

Overall, the summarized data of this study provides further insights into the determining capacity of Rab7-positive endosomal platforms in intracellular signal transduction of different pathways during early embryonic development.

Zusammenfassung

Das endosomale Netzwerk stellt einen enormen Schauplatz für mannigfaltige Prozessierungsmöglichkeiten in Bezug auf Signalübertragung dar. Die verschiedenen Kompartimente der endosomalen Maschinerie üben spezifische Funktionen aus und tragen somit zur Signaltermination, -übertragung, -abschwächung oder -verstärkung bei. Anfänglich wurden diese Funktionen frühen Endosomen zugeschrieben, neuere Forschungen erachten jedoch auch späte Endosomen als gleichermaßen relevant für die Vermittlung solcher Prozesse. Sowohl die Funktionalität als auch die molekulare Identität dieser intrazellulären membranösen Plattformen werden durch eine große Superfamilie kleiner Ras ähnlicher GTPasen gesteuert. Die zusammengestellten Daten dieser Studie heben besonders die Beteiligung später Endosomen und des mit ihnen assoziierten Regulators Rab7 in der frühen Entwicklung des Afrikanischen Krallenfroschs *Xenopus laevis* hervor.

Die ersten zwei Kapitel thematisieren jeweils die Rab7-abhängige Spezifizierung des mesodermalen Keimblatts durch Regulation der intrazellulären Signalwegsaktivität von Wnt und FGF/MAPK Signalen. Nach der Befruchtung ist die Entstehung der Keimblätter einer der ersten initiierten Prozesse. Ein wesentlicher Teil der Mesodermentwicklung umfasst die Unterteilung in unterschiedliche mesodermale Bereiche, wodurch dieses in ventrolaterales und dorsales Mesoderm gegliedert wird. Diese Strukturierung ist essentiell um die weitere Differenzierung in die verschiedenen Gewebe, welche aus dem mesodermalen Keimblatt entstehen, voranzutreiben. Es stellte sich heraus, dass Rab7 ventrolaterales Schicksal in einer Wnt-abhängigen Weise reguliert. Die kleine GTPase vermittelt ihre Funktion oberhalb des Wnt Ko-Transkriptionsfaktors Ctnnb1 um wiederum dessen nukleare Relokalisierung zu gewährleisten. Darüber hinaus werden Rab7-positive Endosomen ebenfalls für die

intrazelluläre Vermittlung der FGF/MAPK Signaltransduktion benötigt um dorsales Mesoderm zu spezifizieren. Hier reguliert Rab7 die korrekte Signalgebung auf Ebene oder unterhalb von Ras beziehungsweise oberhalb von Erk/Mapk1.

Im letzten Kapitel werden die weiteren regulativen Eigenschaften später endosomaler Plattformen in Bezug auf die Funktion von Cd63, eruiert. Das Tetraspanin Cd63, welches ein Transmembranprotein darstellt, ist mit späten endolysosomalen Kompartimenten assoziiert und weist in *Xenopus laevis* ein ähnliches Expressionsmuster wie die kleine GTPase Rab7 auf. Im Gegensatz zu Rab7, scheint die Funktion von Cd63 während der Gastrulation entbehrlich zu sein. Allerdings lassen die in diesem Kapitel aufgeführten Studien eine entscheidende Funktion des Tetraspanins Cd63 während der axialen Elongation und der korrekten Augenentwicklung vermuten. Daher legen die Untersuchungen hinsichtlich Cd63 eine Beteiligung an der regulativen Funktion von späten Endosomen als Signalplattformen in der embryonalen Entwicklung dar, welche über die Mesodermspezifizierung und Gastrulation hinausgehen.

Insgesamt bieten die gesammelten Daten dieser Studie weitere Erkenntnisse über die entscheidende Kapazität Rab7-positiver endosomaler Plattformen in der intrazellulären Signaltransduktion verschiedener Signalwege während der frühen embryonalen Entwicklung.

Directory

Affidavit	1
Abstract	2
Zusammenfassung	4
Directory	6
Introduction	8
Signaling pathways in early development	8
Intracellular signaling via the endocytic pathway	12
Rab family members as regulators for intracellular signaling	16
Endosome maturation and Rab switch	17
LE-associated transmembrane protein Cd63	19
Aim of this work	21
Research chapter I: Rab7-mediated Wnt signal transduction	22
Rab7 is required for mesoderm patterning and gastrulation in <i>Xenopus</i>	23
Research chapter II: Rab7-mediated intracellular FGF signal transduction	46
The late endosomal regulator Rab7 is required for FGF-dependent mesoderm specification by regulating Ras-mediated MAPK activation	47
Research chapter III: Cd63 promotes developmental processes via late endosomal signaling platforms	75
The tetraspanin Cd63 is required for eye morphogenesis in <i>Xenopus</i>	76
Expression of an endosome-excluded Cd63 prevents axis elongation in <i>Xenopus</i>	82
Discussion	88
Rab7 knockdown does not affect development before zygotic gene activation ...	88

LE-associated Rab7 facilitates mesoderm specification after midblastula transition 89

LEs as crucial signaling platforms of Wnt and FGF pathway activation during mesoderm specification 93

Cd63 suggests a requirement of LEs in development beyond mesoderm specification 95

Conclusion 98

References 99

Author's contribution 116

Curriculum vitae 117

Danksagung 119

Introduction

Signaling pathways in early embryonic development

A well-orchestrated regulation of (intracellular) signaling processes denotes embryonic development in vertebrates. Signaling pathways often intertwine or operate up- and downstream of each other to drive early embryonic tissue specification and patterning. Positioning of the newly formed tissues is initiated during gastrulation whereby great structural rearrangements take place. These early developmental processes are mainly governed by a small number of evolutionary conserved signaling pathways, such as transforming growth factor (TGF)- β , its subgroup member bone morphogenetic protein (BMP) (Kishigami and Mishina, 2005; Yamamoto and Oelgeschläger, 2004), Wingless and Int1 (Wnt) and fibroblast growth factor (FGF). Albeit vertebrates share a conserved body plan, the interplay amongst these signaling pathways will be considered below in more detail during early development of the African clawed frog *Xenopus laevis*, as it is the utilized model organism in the studies presented hereafter.

As soon as fertilization takes place, one of the first signaling activities to occur is the shifting of Wnt signaling components from the vegetal hemisphere to the opposite side of sperm entry at the animal pole (De Robertis and Kuroda, 2004). Along parallel microtubule tracks, emanating from the sperm entry point, frequently rearranged in advanced T-cell lymphomas 1/Gsk3-binding protein (Frat1/Gbp) and Disheveled (Dvl) get translocated to the future dorsal side within the 1-cell embryo (Miller et al., 1999; Weaver et al., 2003). Shifting of these dorsalizing determinants is accompanied by a cortex rotation (Weaver and Kimelman, 2004). This motion process is stimulated by fertilization as well, whereby the eggs cortex rotates approximately 30° relative to its cytoplasm (De Robertis and Kuroda, 2004; Moon, 2005; Stennard et al., 1997). Wnt

pathway activity is mediated as consequence of shifted Frat1 and Dvl antagonizing glycogen synthase kinase 3 (Gsk3) function. Gsk3 negatively regulates Catenin beta 1 (Ctnnb1), a downstream Wnt signaling co-transcription factor, by targeting it for degradation (Moon, 2005; Yost et al., 1996). Eventually nuclear accumulation of Ctnnb1 throughout ongoing cell divisions accounts for dorsoventral axis establishment, whereas the site of Ctnnb1 accumulation and concomitant target gene activation now represents the dorsal side (Moon, 2005). Besides dorsal specification via Wnt components, signaling from the vegetal hemisphere induces endomesodermal tissue. Shortly after fertilization signals of the T-box transcription factor Vegt protein (Vegt) initially determine the vegetal cells fate to become endoderm (Zhang et al., 1998). The overlying equatorial marginal zone of such early blastula stage embryos develops into mesoderm, as Vegt further initiates mesodermal gene activity via Nodal paracrine factors (Dale, 1997; Skirkanich et al., 2011; Smith et al., 1993), thus introducing TGF- β signaling in the early developmental processes. By the time of late blastula stages a lack of inducing signals in the animal hemisphere specifies this remaining tissue as ectoderm. As the dorsoventral body axis is established and the germ layers are specified by Wnt and TGF- β signaling respectively, conjunction of these two pathways is essential for preliminary mesoderm patterning. Intersection of prior established Ctnnb1 signals with the TGF- β member growth differentiation factor 1 (Gdf1/Vg1) creates a gradient of Nodal proteins within the endoderm (Agius et al., 2000; Heasman et al., 1994; Schneider et al., 1996). Due to this gradient two mesodermal territories are formed within the equatorial marginal zone of blastula stage embryos, a small 60° and larger 300° arc section (Dale and Jones, 1999; Slack et al., 1990). The Nodal-related protein gradient is highest at the pathways overlapping region from which the small 60° arc dorsal mesoderm section originates. The remaining 300° arc of mesoderm derives from the non-overlapping pathway region with decreasing

Nodal-related protein concentrations and is referred to as ventrolateral mesoderm (Agius et al., 2000).

Dorsally, pathway activity of Wnt and TGF- β drives the formation of the Spemann organizer, a signaling center networking further patterning and developing properties (Agius et al., 2000; Kumar et al., 2021). In the ventral marginal zone, opposite to the currently established dorsal organizing center another signaling center emerges (De Robertis, 2009; De Robertis and Kuroda, 2004; Kumar et al., 2021; Niehrs and Pollet, 1999). Both organizing centers express a specific set of secreted factors, thus eliciting an antagonizing nexus between them. BMP inhibitors, namely Chordin, Noggin and Follistatin are released by the dorsal organizer to counteract ventrally secreted BMPs, e.g. Bmp4 (De Robertis, 2009). Hereby, another signaling pathway gains determining influence on early embryonic development by further patterning the established mesodermal territories. The inhibitory impact emanating from the Spemann organizer results in a gradient formation of Bmp4 within the ventrolateral mesoderm. Contemporaneous to ventrolateral Bmp4, spatially likewise distributed zygotic Wnt signaling confines the dorsal organizers extent (Ramel and Lekven, 2004). Starting by late blastula stages and lasting during gastrulation, graded BMP signals induce diverse mesodermal gene activities. Therefore, the most ventral mesoderm is characterized by high levels of Bmp4, lateral mesoderm is specified by intermediate to low signals and absent Bmp4 represents dorsal mesoderm (Dale and Jones, 1999; Dosch et al., 1997; Gawantka et al., 1995; Hemmati-Brivanlou and Thomsen, 1995). BMPs not only pattern mesodermal tissue, ectodermal cells receiving such signals are induced to become epidermis. Whereas restriction of BMP and Wnt signaling to the ventrolateral parts of the embryo permits neural tissue development on the dorsal side (Dale and Jones, 1999; Iemura et al., 1998; Piccolo et al., 1996; Wilson and Hemmati-Brivanlou, 1995; Zimmerman et al., 1996).

Although not being pivotal in this early developmental processes of initially inducing and patterning the germ layers, FGF signaling incorporates in mesoderm formation as well as it has been described as competence factor for this purpose (Böttcher and Niehrs, 2005; Dorey and Amaya, 2010; Fletcher and Harland, 2008; Kumar et al., 2021). Therefore, FGFs act in concert with TGF- β signaling specifically during mesoderm induction (Böttcher and Niehrs, 2005; Rodaway et al, 1999; Zhao et al, 2003). Mesodermal specification and maintenance are effected by interaction of FGF and Wnt signaling with the early pan-mesoderm marker T-box transcription factor (Tbxt) (Conlon et al., 1996; Schulte-Merker et al., 1995; Smith et al., 1991; Strong et al., 2000; Vonica and Gumbiner, 2002). Even dorsoventral patterning requires FGF signals, due to accumulating evidence in correlation with BMP signaling (Böttcher and Niehrs, 2005; Fürthauer et al., 1997; Kumar et al, 2018 and 2021). At the onset of gastrulation, where cells start to invaginate and thus passing through the dorsal organizer tissue, Spemann's organizer not only secretes BMP inhibitors but also Wnt antagonists (De Robertis, 2009; Glinka et al., 1997). Ongoing gastrulation and concomitant tissue rearrangement engender a Wnt gradient along the developing anterior to posterior axis, being lowest anterior and highest posterior (Kiecker and Niehrs, 2001). Inhibition of both, Wnt and BMP signals in the first involuting and later anterior most cells guaranties the formation of head and brain structures (De Robertis and Kuroda 2004; Niehrs, 2004 and 2010). Beyond mesodermal patterning within the marginal zone, FGFs differently participate in axial and paraxial mesoderm development (Dorey and Amaya, 2010). Especially in context of anterior to posterior specification FGF signals indirectly interact with the Wnt signaling pathway, as both pathways have been described to mediate caudal development (Pera et al., 2013; Wilson et al., 2009).

These early embryonic processes of germ layer induction and body axis establishment are governed by a plethora of cross-connections between different signaling pathways. Regarding this, the endocytic system could offer organizing platforms to regulate such tightly balanced intracellular signal transduction processes.

Intracellular signaling via the endocytic pathway

Endocytosis is generally addressed as procedure of internalizing extracellular or membranous cargo of different kinds and its subsequent translocation due to their multiple destinations. Processing throughout the endocytic pathway for instance includes sorting, recycling, storing, activating, silencing and often degrading of the endocytosed cargo (Huotari and Helenius, 2011). Signaling processes are often linked to various intracellular compartments such as endosomes. Recent studies have shown that endosomal compartments can either function as sorting platforms for signal termination or transduction (Platta and Stenmark, 2011). Initially, trafficking through the endocytic machinery is set up by local cell surface reorganization leading to an invagination of the plasma membrane. The primary endocytic compartments emerge by excision of the inward budding membrane. These newly formed vesicles then merge into/with early endosomes (EEs) and thereby membrane-anchored, carried along cargo like signaling receptors get internalized (Elkin et al., 2016; Sorkin and Zastrow, 2002). Within the endosomal network, EEs mark the first main platform for sorting-events, conducting stringent selection of uptaken cargo into recycling circuits or further passing through the degradative route (Elkin et al., 2016; Huotari and Helenius, 2011). Selection into either endosomal system results in distinct outcomes in context of the different signaling pathways. In terms of signal transduction and termination, recycling endosomes therefore mainly contribute to the maintenance of signaling capacity, whereas the more downstream, degradative endosomal system is largely considered

as termination platform for signaling activity (Cullen and Steinberg, 2018; Huotari and Helenius, 2011). Beyond the early endosomal sorting platform, EEs mature into late endosomes (LEs). Endosome maturation is accompanied by a change in the membrane composition and thus altered fusion partners occur. Moreover, their range of motion along microtubules shifts from the cell periphery to a more perinuclear area (Hoepfner et al., 2005; Huotari and Helenius, 2011; Nielsen et al., 1999). Large structural rearrangements distinguish the maturation process as well, whereby already EEs start to gain a multivesicular structure. Via inward budding of their limiting membrane endosomes form intraluminal vesicles (ILVs) and multivesicular bodies (MVBs)/LEs emerge during further maturation (Babst, 2011; Hurley and Hanson, 2010). Essential for ILV biogenesis is the endosomal sorting complexes required for transport (ESCRT) machinery, as its distinct complexes facilitate membrane rearrangement and cargo sorting (Huotari and Helenius, 2011; Schuh and Audhya, 2014). Acquisition of lysosomal components to LEs and fusion with each other and/or lysosomes constitute a point of no return in the endosomal pathway. In this progressed condition endolysosomes or lysosomes obtain a high density and exhibit a great number of hydrolases. Therefore, ultimate signaling termination and degradation of the transported cargo occurs when ILVs are subjected to lysosomal hydrolyses during fusion of endosomes and lysosomes (Elkin et al., 2016; Huotari and Helenius, 2011). Continuous acidification throughout the endosomal route from the plasma membrane to the lysosomal compartments provides functionality of the different compartments (Elkin et al., 2016). Decreasing pH within endosomal compartments promotes receptor ligand dissociation as well as hydrolase mediated digestion of the transported cargo placed in ILVs (Elkin et al., 2016; Huotari and Helenius, 2011; Mellman et al., 1996). The various platforms within the endosomal pathway constitute manifold options in terms of signaling attenuation, amplification, transduction and termination. Hereafter

Wnt and FGF signaling, two essential pathways in early developmental embryogenesis, will be introduced in context of the endosomal network.

Wnt signal transduction is tightly associated with downstream endocytic processes ensuring the nuclear translocation of the Wnt co-transcription factor Ctnnb1. Upon internalization of an activated Wnt receptor, subsequent recruitment of the Ctnnb1 destruction complex via Dvl to vesicular, receptor-bearing membranes takes place. Fusion of the vesicular structures to EEs, or so called signalosomes, is followed by the maturation into LEs/MVBs (Bilic et al., 2007). Endosome maturation is crucial to spatially separate the bound destruction complex from its target, preventing its continuous degradative turnover. Relocation of the Ctnnb1 destruction complex to ILVs of LEs eventually permits the sustained cytosolic accumulation of newly synthesized Ctnnb1, thus representing a signaling maintenance mechanism. Wnt signal transduction is obtained by Ctnnb1 nuclear translocation resulting in target gene activation (Platta and Stenmark, 2011; Taelman et al., 2010; Vinyoles et al., 2014).

Intracellular signal transduction facilitated by endosomal processes is not only associated with Wnt signaling, as there is evidence for a requirement in FGF signaling, too (Auciello et al., 2013). Especially the mitogen-activated protein kinase (MAPK) pathway, one intracellular branch of FGF and other signaling pathways utilizes endosomal compartments (Sorkin and Von Zastrow, 2000; Teis et al., 2002). Regulation of MAPK signaling linked to endosomes is best examined in the context of epidermal growth factor (EGF) signal transduction, which is closely related to FGF. Initially, binding of FGF/EGF ligands to protein tyrosine kinase receptors (PTKR) results in receptor dimerization, allowing cross-phosphorylation of their cytosolic residue (Fehrenbacher et al., 2009; Schlessinger, 2000). Along with the pathway initiation, formation of the ligand-receptor complex stimulates its internalization and thus, entry into the endocytic system (Oksvold et al., 2001). Association of growth

factor receptor-bound protein 2 (Grb2) to the cytosolic domain of such an activated membrane-bound receptor then in turn recruits the guanine nucleotide exchange factor (GEF) Son of Sevenless (Sos). This GEF facilitates a conformational switch of the membrane-associated Ras proto-oncogene serine/threonine kinase (Ras) GTPase between its guanine diphosphate- (GDP-) to guanine triphosphate- (GTP-) bound form. Direct interaction between activated Ras and Raf proto-oncogene serine/threonine kinase/mitogen-activated protein 3 kinase (Raf/Map3k) then initiates a subsequent kinase cascade, characterized by successive phosphorylation of downstream MAPK pathway components (Fehrenbacher et al., 2009). Besides PTKR, also the Grb2-Sos complex as well as Ras, have all been found in endosomal structures after pathway initiation (Di Guglielmo et al, 1994; Jiang and Sorkin, 2002; Oksvold et al., 2001; Sorkin et al., 2000). The more downstream late endosomal compartment in particular is commonly considered as signal termination platform. However, similar to Wnt signaling, this downstream endosomal transport route sustains signal transduction, as the internalized (EGF) receptors' activity maintains until its entire assimilation in the endolysosomal lumen (Burke et al., 2001; Oksvold et al., 2001; Wouters and Bastiaens, 1999). Endosomal receptor trafficking and concomitant recruitment of Ras and Raf/Map3k to late endosomal structures fosters the colocalization with a complex consisting of late endosomal/lysosomal adaptor mapk and mtor activator 2 (Lamtor2/p14), late endosomal/lysosomal adaptor mapk and mtor activator 3/Mek partner 1 (Lamtor3/Mp1) and mitogen-activated protein kinase/Erk kinase/mitogen-activated protein 2 kinase (Mek/Map2k; p14-mp1-map2k complex) (Lu et al., 2009). A stable anchoring of this complex to late endosomal membranes is facilitated via the lipid raft adaptor late endosomal/lysosomal adaptor mapk and mtor activator 1 (Lamtor1/p18) (Nada et al., 2009). The acquired spatial proximity between Raf/Map3k and the complex allows phosphorylation of Mek1/Map2k1 (Kolch, 2000; Lu et al.,

2009), which is essential for subsequent activation and phosphorylation of extracellular-signal regulated kinase/mitogen-activated protein kinase (Erk/Mapk) (Fehrenbacher et al., 2009; Platta and Stenmark, 2011). Activated Erk/Mapk dimerizes and translocates to the nucleus and eventually accomplishes signal transduction from the plasma membrane via the endocytic machinery by a final phosphorylation step of members belonging to the E26 transformation specific (Ets) family of transcription factors (Fehrenbacher et al., 2009).

The above mentioned signaling events depict the requirement of a well-orchestrated endocytosis machinery organizing the interplay of different membranous compartments, which is ensured by a various number of distinct organelle regulators. Many Ras-related in brain (Rab) family members, being enriched at those endosomal membranes, facilitate this regulatory function of intracellular membrane trafficking (Rink et al., 2005).

Rab family members as regulators for intracellular signaling

In 1983 the first *rab* gene has been identified by D. Gallwitz and colleagues in yeast (Gallwitz et al., 1983). Until today ongoing research lead to the discovery of at least 60 different Rab proteins encoded in the human genome (Stenmark and Olkkonen, 2001; Zerial and McBride, 2001). Various investigations identified individual Rab proteins being associated to discrete functions in subcellular membrane-associated transport. Moreover, the entirety of Rabs provide a specific identity to each membrane compartment involved in such endosomal trafficking events (Martinez and Goud, 1998; Rodman and Wandinger-Ness, 2000; Stenmark and Olkkonen, 2001). Rab proteins are at large evolutionary conserved from yeast to humans and further represent the largest family of monomeric small GTPases. Their carboxyl termini required for subcellular membrane targeting are least conserved in Rab proteins whereas the

guanine-nucleotide binding domains are highly preserved (Stenmark and Olkkonen, 2001). Membrane localization of these GTPases constitutes a transient state, as they oscillate between GDP- and GTP-bound conformations and therefore causing a dynamic equilibrium between a cytosolic and a membrane-associated entity (Rink et al., 2005; Zerial and McBride., 2001). Association with intracellular membranes functions via integration of a prenyl anchor and entails Rab proteins facing to the cytoplasm (Martinez and Goud, 1998; Stenmark and Olkkonen, 2001). Before entering the GDP/GTP cycle and performing repetitive rounds of membrane association and dissociation newly synthesized Rabs are bound by Rab escort proteins (REPs). REPs facilitate the initial delivery to appropriate intracellular membranes subsequent to presenting the small GTPase to a geranylgeranyl transferase. This enzyme catalyzes alterations in their cysteine motif at the carboxyl terminus, which are essential for proper membrane targeting. Once the GDP/GTP cycle is entered GTP/GDP exchange factor (GEF) mediates membrane binding by conversion from GDP to GTP and simultaneous release of REP. Vice versa conversion is rendered by GTPase-activating protein (GAP) and proximate membrane detachment is accompanied by GTPase dissociation inhibitor (GDI). Based on its structural similarity to REP and its higher abundance, GDI now functions as recycling factor in upcoming GDP/GTP cycles. GTP- and GDP-bound conformations are addressed as active and inactive states of Rab proteins. GTP-bound, membranous Rabs are regarded as active, due to their capability of interacting with downstream effectors in this conformation (Stenmark and Olkkonen, 2001).

Endosome maturation and Rab switch

Endosomal compartments often depict mosaic distributions of different Rab proteins. These non-intermixing populations of distinct Rabs illustrate intermediate stages of

ongoing endosomal dynamics (Stenmark, 2009; Zerial and McBride, 2001). Maturation from early to late endosomes elucidate such membrane-associated Rab protein turnover at transforming compartments within the endosomal dynamics. Early and late endosomes, participating in this most evaluated maturation process, are characterized by RAB5 Member RAS Oncogene Family (Rab5) and RAB7 Member RAS Oncogene Family (Rab7), respectively. The Rab switch occurring during endosome maturation involves proceeding decrease of Rab5 and concomitant increase of Rab7 at the same membrane (Rink et al., 2005). As there is no direct replacement of one GTPase by another, hybrid organelles evolve and Rab5 and Rab7 positive domains develop (Rink et al, 2005; Skjeldal et al., 2021; Vonderheit and Helenius, 2005). The current model proposes a two-phase Rab5 to Rab7 conversion process during maturation, one being independent of Rab7 and the other relying on its function. At first, EE-associated Rab5 briefly detaches from the endocytic membrane initiating the endosomal transition. Completing Rab5 dissociation then requires the appearance of downstream Rab7 at the endosomal membrane (Skjeldal et al., 2021). Gathering of Rab5 into domain like structures is assumed to activate the MON1 homolog A secretory trafficking associated-CCZ1 homolog vacuolar protein trafficking and biogenesis associated (Mon1-Ccz1) complex, which in turn facilitates recruitment of Rab7 (Langenmeyer et al., 2020; Skjeldal et al., 2021). Mon1-Ccz1 complex exerts a dual function by trespassing the Rab5 acquisition feedback loop and promoting homotypic fusion and protein-sorting (Hops) complex activation (Skjeldal et al., 2021). Disruption of the positive feedback loop is precipitated by displacing the Rab5 GEF from maturing endosomes, thus causing a further decrease of Rab5 levels (Poteryaev et al., 2010). On the contrary, complex interaction between Mon1-Ccz1 and Hops leads to Rab7 accumulation at maturing endosomal membranes since the Hops complex exerts GEF function towards this LE-associated GTPase (Langenmeyer et al., 2020; Poteryaev et

al., 2010; Skjeldal et al., 2021; Zhang et al., 2009). Once established, Rab7-positive compartments are referred to as mature LEs. Assimilation in the endosomal machinery reveals the significance of Rab7 in membrane trafficking and traffic dependent events, like biogenesis of endosomal compartments or signal processing. Even interaction with downstream effectors of Rab7 seems to be crucial, i.e. in distribution and movement of LEs and lysosomes (Zhang et al., 2009).

LE-associated transmembrane protein Cd63

Along with Rab7, Cluster of differentiation 63 (Cd63) was found abundantly present in downstream endosomal structures. Its presence in LEs and lysosomes suggests a regulatory function in membrane trafficking for this membrane-associated protein, too (Hurwitz et al., 2018; Pols and Klumperman, 2009). Transmembrane protein Cd63 belongs to the large superfamily of tetraspanins and was the first being characterized as such. In the human genome a total of 33 tetraspanins are encoded, whereas Cd63 classifies an own subunit due to its more ancient origin beyond the others (Pols and Klumperman, 2009). Tetraspanins exhibit a conserved structure, consisting of four hydrophobic transmembrane domains, divided in two extracellular, an intracellular loop and are terminated by two short intracellular tails (Lupia et al., 2014; Pols and Klumperman, 2009; Termini and Gillette, 2017). Cd63, like other tetraspanins, is synthesized in the endoplasmic reticulum and travels via the Golgi apparatus to the plasma membrane (Kobayashi et al., 2000; Pols and Klumperman, 2009). However, along with its cell surface accumulation, a predominant enrichment of Cd63 can be found in LEs and lysosomes, particularly in ILVs (Pols and Klumperman, 2009; van Niel et al., 2011). Cell surface-associated Cd63 relocates to late endosomal compartments via classical endocytosis. The ESCRT machinery participates in intravesicular assimilation of Cd63 in ILVs (Hurwitz et al., 2018; Saksena et al., 2007;

Trajkovic et al., 2008). Its localization in late endosomal compartments supposes a protective mechanism against degradation of this specific tetraspanin (Pols and Klumperman, 2009). In general, tetraspanins exert a function as membrane protein organizers, as they aggregate in tetraspanin enriched microdomains (TEMs) by rearrangement of the plasma membrane (Hurwitz et al., 2018; Termini and Gillette, 2017). Organized localization in TEMs facilitates the capacity of tetraspanins, e.g. Cd63 to interact with a various number of membrane proteins. Among this direct or indirect interaction partners are integrins, cadherins, kinases, signaling molecules, cell surface receptors, adaptor proteins and other tetraspanins (Hurwitz et al., 2018; Pols and Klumperman, 2009). Cd63s protein interactions and motile localization between the plasma membrane and the late endosomal system implies a participation in intracellular trafficking of such surface proteins (Hurwitz et al., 2018).

Aim of this work

Advancing research continuously reveals the importance of the endosomal machinery in intracellular signaling events. Initially endocytosis has been envisioned as a classical degradation pathway. Over time EEs emerged as crucial platforms in signal transduction and/or termination by constituting a first sorting nexus within the endocytic pathway. Nowadays even LEs increasingly come into focus in the context of intracellular signaling. So far, LEs for instance have been linked to signal transduction in Wnt and FGF signaling, two decisive pathways during early embryonic development. However, little is known about the regulation of this late endosomal mechanism. The studies listed here intended to elucidate the influence of intracellular membrane transport on early developmental processes governed by the LE-associated small GTPase Rab7 and the tetraspanin Cd63. Regarding Rab7, few *in vivo* studies have been accomplished, as its knockout causes early embryonic lethality in mice. Kawamura and colleagues could demonstrate, that in absence of Rab7 murine embryos die due to failure in gastrulation (Kawamura et al., 2012). Therefore, the main part of this work addresses the requirement of the LE regulator Rab7 for early signaling pathways in mesoderm patterning during gastrulation in the African clawed frog *Xenopus laevis*. The versatile use of this model organism allows comprehensive and tissue specific examination. Such investigations should enlighten how intracellular membrane transport via LEs drives early signaling pathways, in particular Wnt and FGF signaling. To further deepen the understanding about the regulatory capacity of the late endosomal membrane transport during embryonic development, the final part of the dissertation covers investigations of Cd63.

Research chapter I:

Rab7-mediated Wnt signal transduction

Rab7 is required for mesoderm patterning and gastrulation in *Xenopus*

RESEARCH ARTICLE

Rab7 is required for mesoderm patterning and gastrulation in *Xenopus*

Jennifer Kreis, Fee M. Wielath and Philipp Vick*

ABSTRACT

Early embryogenesis requires tightly controlled temporal and spatial coordination of cellular behavior and signaling. Modulations are achieved at multiple levels, from cellular transcription to tissue-scale behavior. Intracellularly, the endolysosomal system emerges as an important regulator at different levels, but *in vivo* studies are rare. In the frog *Xenopus*, little is known about the developmental roles of endosomal regulators, or their potential involvement in signaling, especially for late endosomes. Here, we analyzed a hypothesized role of Rab7 in this context, a small GTPase known for its role as a late endosomal regulator. First, *rab7* showed strong maternal expression. Following localized zygotic transcript enrichment in the mesodermal ring and neural plate, it was found in tailbud-stage neural ectoderm, notochord, pronephros, eyes and neural crest tissues. Inhibition resulted in strong axis defects caused by a requirement of *rab7* for mesodermal patterning and correct gastrulation movements. To test a potential involvement in growth factor signaling, we analyzed early Wnt-dependent processes in the mesoderm. Our results suggest a selective requirement for ligand-induced Wnt activation, implicating a context-dependent role of Rab7.

KEY WORDS: Rab7, Endosomes, Wnt, Mesoderm, Gastrulation, *Xenopus*

INTRODUCTION

Early embryonic processes like germ layer formation, induction of body axes, gastrulation, neural induction and tissue differentiation require tight control of cellular processes, including temporal and spatial activation of specific sets of signaling pathways. Regulation of endocytosis or membrane trafficking can control activation, intensity, or duration of signal transduction following receptor activation (Sigismund et al., 2012). However, this has only been analyzed in few developmental processes *in vivo*, as altering basic cellular processes can have dramatic effects.

Endocytosis of membrane receptors is considered a way of downregulation of signaling. Receptors are translocated to early endosomes (EE), which represent first intracellular sorting platforms (Platta and Stenmark, 2011). From here, receptor complexes can be inactivated and recycled back to the plasma membrane. Alternatively, they are retained in EE membranes while these organelles mature into

late endosomes (LE). There, transmembrane cargo can be translocated into intraluminal vesicles (ILV) by successive inward budding of the limiting membrane, a process characteristic for maturing LE, and which is performed by the endosomal sorting complexes required for transport (ESCRT) machinery (Hanson and Cashikar, 2012). Any cargo translocated into ILV is destined for acidic degradation, as LE fuse with lysosomes. Thus classically, LE represent an intermediate step between EE and degradation (Dobrowolski and De Robertis, 2011; Homer et al., 2018; Katzmann et al., 2002).


The role of endocytosis and endosomes for activation of signaling are much less understood. Several pathways require endocytosis for activation, or further transport to EE, where activating adapters are localized (Brunt and Scholpp, 2018; Butler and Wallingford, 2017; Dobrowolski and De Robertis, 2011; Fürthauer and González-Gaitán, 2009; Platta and Stenmark, 2011). A much rarer case is a positive role of LE for pathway activation, which has been suggested for epithelial growth factor (EGF) receptor-mediated mitogen-activated protein kinase (MAPK) activation (Platta and Stenmark, 2011; Teis et al., 2002). Further, for canonical Wnt signaling (from here on simply ‘Wnt signaling’), it has been demonstrated that LE are indispensable for maintaining intracellular signaling after endocytosis-mediated activation of the receptor complex (Platta and Stenmark, 2011; Taelman et al., 2010; Vinyoles et al., 2014).

Rab family proteins are a group of small GTPases that regulate membrane trafficking processes by transiently binding membranes and serving as process-specific molecular switches. Each Rab attaches to certain types of membrane or organelle and orchestrates recruitment of a specific set of effectors, thereby giving membranes an ‘identity’ and function (Stenmark, 2009). As judged by their general roles in cellular transport, many Rab proteins are categorized as ‘housekeeping genes’ (Houunkpe et al., 2021). However, they might be involved in tissue-specific processes requiring membrane transport.

The LE regulator Rab7a (from here on ‘Rab7’) and its low-expressed, tissue-specific paralog Rab7b are mainly found on LE. Thus, Rab7 is used as an LE marker, and, as a recruiter of many effectors, it is the main regulator of LE maturation and function (Huotari and Helenius, 2011; Stenmark, 2009). Concerning signaling pathways, it would thus be considered to be a permissive regulator of endolysosomal degradation, i.e. required for receptor degradation and termination of signaling (Platta and Stenmark, 2011). While this is straightforward logic, controlling activity of Rab7 could be a way of positively regulating downstream signal transducers as well. For instance, this might be the case for Wnt signaling, where functional LE have been shown to be required for sustained activation. In addition, the Wnt pathway has been reported to influence expression of endosomal regulators in a positive feedback loop, i.e. directly regulating Rab7 activity (Ploper and De Robertis, 2015; Ploper et al., 2015; Taelman et al., 2010).

Department of Zoology, Institute of Biology, University of Hohenheim, 70599 Stuttgart, Germany.

*Author for correspondence (philipp.vick@uni-hohenheim.de)

 P.V., 0000-0002-1430-4561

This is an Open Access article distributed under the terms of the Creative Commons Attribution License (<https://creativecommons.org/licenses/by/4.0/>), which permits unrestricted use, distribution and reproduction in any medium, provided that the original work is properly attributed.

Received 30 November 2020; Accepted 26 May 2021

Studies dealing with the *in vivo* function of Rab7 are rare, especially in a developmental context. Most information about its influence on cellular function derives from work in cell culture, i.e. from out-of-tissue contexts (Guerra and Bucci, 2016). This might be due to the general cellular role of Rab7, causing classical knockout (KO) approaches to result in embryonic lethality, as exemplified by work in the mouse. KO embryos had strong defects in endosomal transport in the anterior visceral endoderm (AVE), which resulted in antero-posterior (AP) patterning defects, and thus in failure to complete gastrulation (Kawamura et al., 2012). In a recent follow-up report, the authors further demonstrated that these phenotypes correlated with reduced Wnt signaling in the mesoderm, resulting in impaired mesoderm patterning (Kawamura et al., 2020).

In this work, we analyzed the *in vivo* function of *rab7* during *Xenopus* early embryogenesis, including a potential participation in Wnt pathway activation. In contrast to an expected general housekeeping role in all tissues, we found *rab7* mRNA specifically enriched in distinct types of tissues, reflecting dynamic changes of enhanced requirement. Using morpholino-mediated knockdown and CRISPR/Cas9-mediated genome editing, we found that loss of *rab7* specifically resulted in gastrulation defects without impacting

embryonic organizer induction. Furthermore, *rab7* was required endogenously for expression of Wnt-dependent genes in the dorsal and ventral mesoderm, as well as for ligand-mediated activation of exogenously induced Wnt signaling.

RESULTS

Loss of *rab7* results in gastrulation defects

We speculated *rab7* could show distinct spatial enrichment of mRNA expression during early development. If the case, such enhanced abundance would give indications about tissue- and process-specific requirements. Indeed, expression analysis by *in situ* hybridization (ISH) revealed very dynamic spatial and temporal signals. Strong maternal expression was found in the animal half of cleavage stages, a signal detected until the onset of zygotic transcription after midblastula transition (MBT) (Fig. 1A,B; Fig. S1A). At early gastrula stages, transcripts were mainly found in the deep mesodermal ring, omitting the dorsal lip, i.e. the anterior/head part of Spemann-Mangold organizer (Fig. 1C,D; Fig. S1B). During late gastrulation, stronger signals were detected in the neural plate ectoderm and in the axial, notochordal mesoderm, latter of which continued to be positive for *rab7* during neurulation

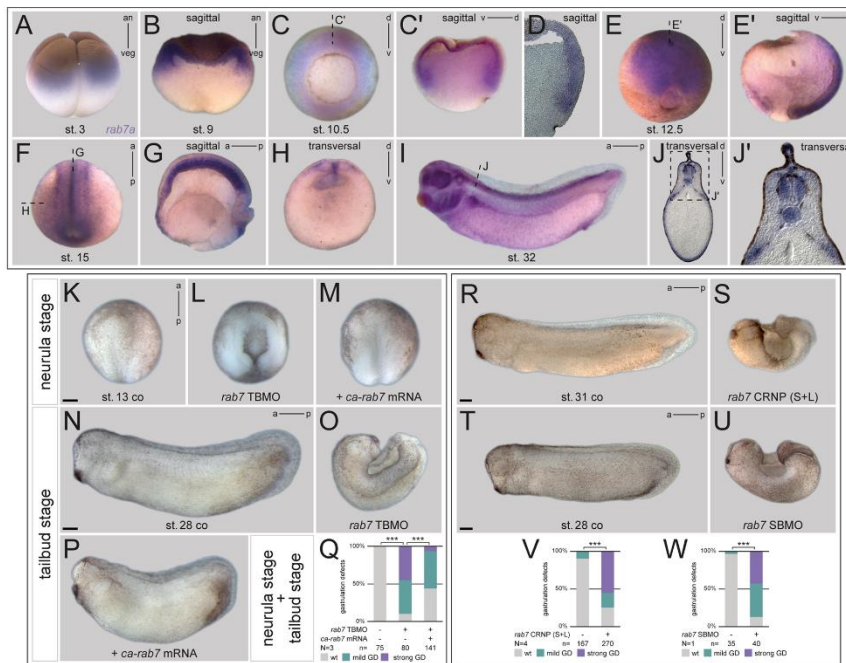


Fig. 1. *rab7* shows dynamic expression and inhibition resulted in gastrulation defects. (A,B) Expression of *rab7* mRNA in animal hemisphere at stage 3 and sagittal section of late blastula stage. (C) Upon gastrulation transcripts were enriched in deep mesodermal ring, (C') sagittal section as indicated in (C), (D) dorsal area close-up view of a vibratome-sectioned specimen. (E) At stage 12.5 *rab7* accumulates in neural plate ectoderm, (E') sagittal section of E. (F) During neurulation transcripts get restricted to notochord, neural tube and brain tissue, (G) sagittal and (H) transversal section indicated in F. (I) In tailbud stages transcripts were detected in the notochord and pronephric and head tissues, (J) transversal section indicated in I, (J') enlargement of J. (K,N) Control specimen at stages 13 and 28. (L,O) Injection of *rab7* TBMO in dorsal lineage caused gastrulation defects, resulting in severe dorsal phenotypes. (M,P) Co-injection of *ca-rab7* mRNA rescued loss of function phenotype of morphant embryos. (Q) Quantification of results in K–P. (R,T) Tailbud control embryos, (S,U) siblings treated with *rab7* CRNP (S+L) or *rab7* SBMO showing dorsal phenotypes. (V,W) Quantification of results in (R,S and T,U). a, anterior; an, animal; ca, constitutive active; co, control; CRNP, Cas9 Ribonucleoprotein; d, dorsal; GD, gastrulation defect; p, posterior; SBMO, splice blocking Morpholino Oligonucleotide; st., stage; TBMO, translation blocking Morpholino Oligonucleotide; v, ventral; veg, vegetal; wt, wild type. Scale bars: 250 μm.

(Fig. 1E; Fig. S1C). By then, ectodermal expression became more restricted to the lateral neural plate, and later in the deep cells of the neural tube and brain tissues (Fig. 1F-H; Fig. S1D-E). In following tailbud stages, *rab7* signals were detected in the cement gland and dermal areas, weaker in the notochord, and strong in the pronephric kidney, eyes, ventro-lateral neural tube, pharyngeal arches, trigeminal nerve complex, dorsal fin mesenchyme, and in the trunk neural crest cells (Fig. 1I,J; Fig. S1F,G; and data not shown). This analysis supported our hypothesis that *rab7* could be required for early embryonic development by participating in regulation of signaling activity in multiple tissues.

Next, we wanted to test an early *in vivo* requirement of *rab7* using a loss-of-function approach. We designed a morpholino oligomer (MO) targeting the 5'UTR of the L- and S-form of *Xenopus laevis rab7* to block translation of both homeologs (*rab7* TBMO). Morphant embryos passed through cleavage and blastula stages without detectable phenotypes (not shown). However, subsequent gastrulation movements were inhibited during gastrulation, causing complete failure to close the dorsal blastopore in about half of morphant embryos reaching early neurula stage (Fig. 1K,L). Other specimens displayed milder gastrulation phenotypes (not shown). The strong gastrulation defect became even more prevalent at tailbud stages, with further extension of the AP axis in control specimens, while morphant embryos remained wide open dorsally with strong dorsal curvature. By then, another 45% of specimens had developed milder phenotypes, recognizable mostly by impaired axial elongation (Fig. 1N,O,Q; and not shown). Importantly, co-injection of a constitutively-active (ca) *rab7* mRNA was able to rescue the strong gastrulation phenotype in a highly significant manner, demonstrating specificity of the observed MO effect. As tailbud stages, nearly all rescued embryos were able to close the blastopore and to elongate their AP axis, albeit with slightly reduced AP elongation (Fig. 1M,P,Q). To further underline specificity of this effect, we next designed single guide RNAs (sgRNA) to target the genomic loci of both *rab7* homeologs for CRISPR/Cas9-mediated mutagenesis, either in parallel, or individually. KO efficiency of injected embryos was determined by sequencing and subsequent analysis of indel distribution (Synthego ICE; for details see Materials and Methods). These analyses resulted in a predicted gene editing rate between 60% and 88% for L- or S-forms of the different sgRNAs (Fig. S2A-C). Genome editing of *rab7L/S* at the one-cell stage caused strong gastrulation defects, again resulting in tailbud stages with open dorsal part in 50% of specimens, resembling the phenotype shown for morphants (Fig. 1R,S,V). Interestingly, while selective targeting of homeolog L with sgRNA (L) also caused a similar phenotype in about 25% of injected specimen (Fig. S2D-F), no gastrulation defects were observed by only targeting homeolog S with sgRNA (S) (data not shown). Finally, we also designed a splice-blocking (SB) MO targeting the splice acceptor site at intron 2 of the *rab7* pre-mRNA to prevent splicing, and thus causing translational read-through and early termination (Fig. S2G). Successful inhibition of splicing could be demonstrated by RT-PCR for both homeologs, resulting in intron retention for each form (Fig. S2H). Injection of the *rab7* SBMO resulted in significant reduction of *rab7*-transcript amounts in morphant neurula or tailbud stage embryos, indicating nonsense-mediated decay of unspliced *rab7*, and thus successful knockdown of zygotic transcripts (Fig. S2I-L). Phenotypically, *rab7* SBMO injected embryos showed also gastrulation defects, but to a lower degree (Fig. 1T,U,W). Specimens that managed to close the blastopore were raised further. Such milder affected (or lower dose injected) morphants displayed deficits in AP elongation

(Fig. S2O,P). Finally, by raising the surviving sgRNA (S+L), or low-dose *rab7* TBMO injected embryos, this late phenotype could be phenocopied in early tadpole stages, again supporting specificity of the effect (Fig. S2M,N,Q,R). In summary, our loss-of-function approach demonstrated a requirement of *rab7* for early embryonic development.

Rab7 is required for axial mesoderm elongation and notochord morphogenesis

To better understand this gastrulation phenotype, we knocked down *rab7* specifically in the dorsal or ventro-lateral mesoderm. Thus for following experiments, *rab7* TBMO was co-injected along with a fluorescent lineage tracer specifically into the dorsal or ventral lineages, targeting the equatorial, i.e. mainly mesodermal progenitor areas (Fig. S3 for injection setup). Dorsal- or ventral-specific targeting was verified at early gastrula stages (Fig. S3A-J; see Materials and Methods). When mid-sagittal sections of dorsal *rab7* morphants were analyzed at early gastrula stages, such embryos formed a lip, but involution movements and archenteron formation were impaired (Fig. 2A-D; Fig. S3B-E). Interestingly, such bisections revealed a concomitant lack of Brachet's cleft, implying incorrect tissue remodeling during early gastrulation (Fig. 2C-F; Fagotto, 2020). These phenotypes became more apparent when morphants were analyzed for notochordal *noggin* (*nog*) expression at mid/late gastrula stage, illustrating strongly impaired axial elongation and reduced *nog* expression itself, also indicating a failure in maintaining notochordal fates in morphant tissue (Fig. 2G-J). Analysis of dorsal lips using an anti- β 1-Integrin antibody further revealed altered cell shapes and impaired tissue rearrangement in the involuting marginal zone of morphants (deep layers), i.e. exactly in that mesodermal area where we found enrichment of *rab7*, paralleling the lack of axial elongation and archenteron formation (Fig. 2K-O).

As these phenotypes indicated a failure in convergent extension (CE)-dependent processes, and thus, to form a proper elongated notochord subsequently, we examined notochord fate and appearance directly. When we checked expression of the marker *notochord homeobox* (*not*) in morphant embryos at early neurulation, lack of axial elongation was obvious, explaining the embryos' inability to close the dorsal part of the blastopore (Fig. 3A-C). When using the *rab7* SBMO for dorsal knockdown, a milder but significant effect was observed as well (Fig. S4A-C). Interestingly, while *not* expression was not reduced in the axial mesoderm but extended into the lateral somitic areas, analysis of *sonic hedgehog* (*shh*) in the same experiments revealed a different effect. Morphant embryos showed similar inhibition of axial elongation but expression intensity of *shh* was reduced in most cases, again suggesting partial lack of notochordal fate (Fig. 3D-F).

Some milder affected morphant embryos were grown to tailbud stages to analyze notochordal tissue differentiation. In these stages, *not* expression was also not reduced, but appeared enhanced in the mid-trunk area of such specimens, where in wild-type embryos expression had already faded by that stage (Fig. S4D-E'). Overall, notochordal appearance in sagittal sections confirmed attenuated CE. Stronger affected specimens again developed open dorsal tissues, but mostly retained *not* expression, often split as two separated areas relocated medially (Fig. S4G). Staining embryos with an MZ-15 antibody, which detects outer keratan sulphates of the notochordal sheet, revealed absent or strongly reduced signals, supporting a lack of notochord differentiation (Fig. S4H-K). These phenotypic analyses showed that early *rab7* function is required for

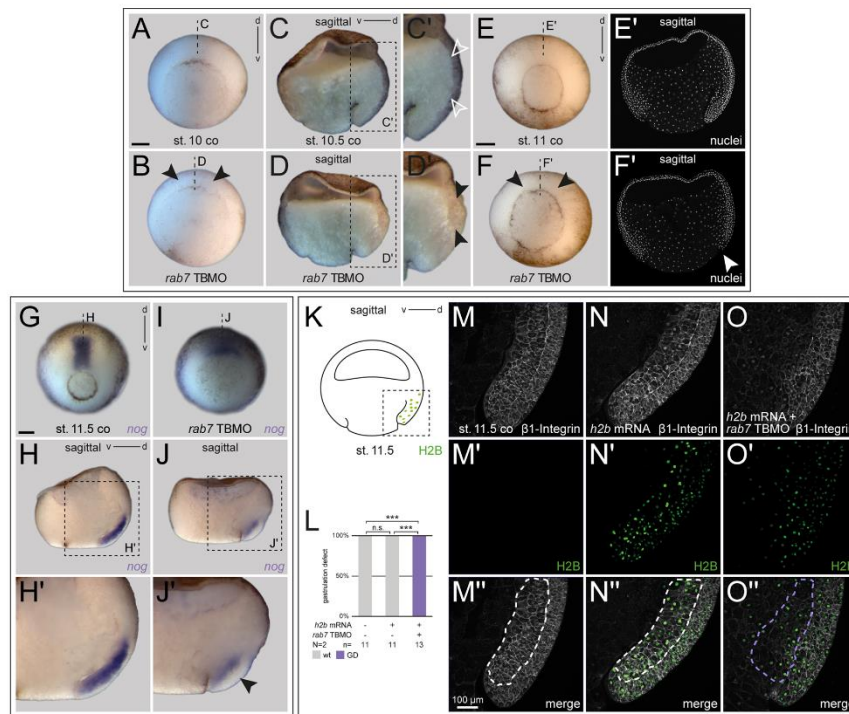


Fig. 2. *rab7* morphants show impaired dorsal lip formation. (A) Untreated embryos at the beginning of gastrulation forming a dorsal lip, (B) which can also be observed in *rab7* deficient siblings (black arrowheads). (C) In stage 10.5, sagittal sectioned control embryos revealed early involution movements. (C') Enlargement of the area in the dashed black box in C, showing formation of Brachet's cleft was visible (white outlined arrowheads), (D) dorsal *rab7* knockdown specimen rarely showed involution in sagittal sections or Brachet's cleft formation, (D') enlargement of the area in the dashed black box in D, (E) Older control embryo (mid-gastrula) with evenly shaped lip, (E') sagittal section with Hoechst stained nuclei revealed proceeded dorsal involution and archenteron formation. (F) Same-age morphant siblings developed irregularly shaped lips around the blastopore (black arrowheads), and (F') did not show any involuting tissue or archenteron formation in Hoechst stained sagittal section (white arrowhead). (G) Wild-type *nog* expression of control embryos and (I) reduced expression of *nog* and concomitant failed notochord elongation of dorsal *rab7* morphants. (H) Sagittal section and (H') enlargement of the area in the dashed black box in H) exhibited proceeded notochord elongation marked by *nog* in untreated embryos. (J) Sagittal section and (J') enlargement of the area in the dashed black box in J clearly depicted impaired *nog* expression (black arrowhead). (K) Schematic figure of sagittally bisected mid- to late gastrula embryo indicating view of dorsal lips shown in M-O'. (L) Quantification of overall embryonic phenotypes exemplified in M-O'. (M,N,O) bisected embryos stained for $\beta 1$ -Integrin (white). (M',N',O') Histone 2B (H2B) GFP signal used as lineage tracer (green). (M'',N'',O'') merged channels. (M,N) Normal distributed $\beta 1$ -Integrin in wild-type dorsal lips or *h2b* mRNA-injected specimen, indicating target site. (O) Axial *rab7* morphant cells revealed altered shapes and lack of involution behavior and archenteron formation. Scale bars: A-J', 250 μ m; M-O', 100 μ m.

axial tissue morphogenesis and involution during gastrulation, and thus for subsequent notochord formation.

Rab7 is required for dorsal mesoderm specification but not for organizer induction

To understand the role of *rab7* in this context, we next analyzed whether organizer induction was impaired by targeting this dorsal lineage. However, paralleling lack of *rab7* transcript enrichment in the anterior/head organizer area (Fig. 1C,D), neither knockdown with *rab7* TBMO or *rab7* SBMO, nor CRISPR-induced KO blocked organizer induction, as judged by *gooseoid* (*gsc*) and *chordin* (*chd*) expression (Fig. 4A-C; Fig. S5A-H). Next, we wanted to test if early, pre-gastrula dorso-ventral (DV) axis formation was altered in *rab7* morphants. Knockdown of *rab7* neither altered dorsal *chd*, nor ventral *ventx1* expression, indicating no alteration in

Bone Morphogenetic Protein (BMP) gradient formation (Fig. S5I-K and Fig. S4D-F). This suggested that *rab7* is dispensable for both, endogenous organizer induction and DV patterning.

The reduced expression pattern of *shh* suggested that *rab7* might be selectively required for other dorsal mesoderm genes as well. Therefore, we next checked expression patterns of *nodal3* and *forkhead box J1* (*foxj1*), two Wnt-dependent marker genes expressed in the superficial mesoderm (SM), i.e. the outer layer of the trunk organizer tissue (Glinka et al., 1996; Smith et al., 1995; Stubbs et al., 2008; Walentek et al., 2013). Interestingly, while very early expressed *nodal3* was reduced only in a fraction of embryos, *foxj1* was strongly reduced after loss of *rab7* (Fig. 4G-L). Further, dorso-lateral markers *myogenic differentiation 1* (*myod1*) and *myogenic factor 5* (*myf5*) (Kjolby and Harland, 2017; Shi et al., 2002) were strongly downregulated in their paraxial expression

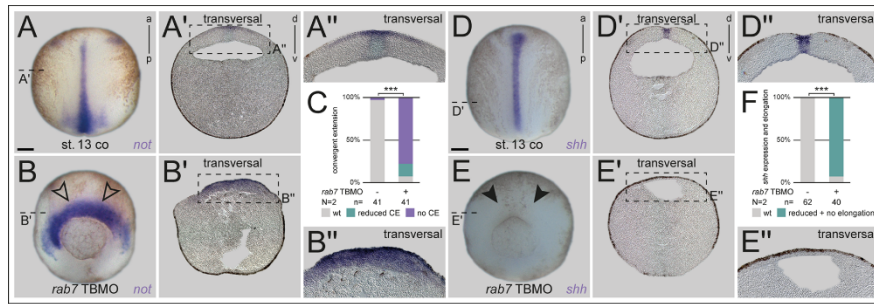


Fig. 3. *rab7* is required for axial elongation and notochord morphogenesis. (A,D) Early wild-type neurula embryos showing elongated notochords marked by the expression of *not* or *shh*. (A',D') Transversal sections indicated in (A,D) revealed *not* and *shh* expression in the axial neural plate and *shh* additionally throughout the whole notochord. (A',D') enlargement of the area in the dashed black boxes in A' and D', respectively. (B,E) Dorsal *rab7* TBMO injection resulted in embryos failing to elongate their notochord, although *not* expression intensity (black outlined arrowheads) was not reduced in comparison to *shh* (black arrowheads). (B') Transversal section of morphant embryos showed lateral expanded expression of *not* above the dorsal lip and (E') severely reduced *shh* expression. (B',E') enlargement of the area in the dashed black boxes in B' and E', respectively. (C,F) Quantification of results in A,B and D,E, respectively. Scale bars: 250 μm.

domains at early and mid-gastrulation (Fig. 4M-R). Co-injected β-gal lineage tracer suggested this to be a cell-autonomous effect, as the ventro-lateral aspect of *myoD1* (i.e. ventral lineage derived; compare Fig. S3I) was never inhibited in this injection approach (Fig. 4M-O). Together with the lateral extension of *not* into these areas, this indicated a potential shifting of paraxial fates (Fig. 3B). Finally, analysis of general mesoderm identity using *T-box transcription factor 1* (*tbx1*, also known as *brachyury*) revealed a significant reduction of expression after *rab7* knockdown in this area as well (Fig. 3S-U), explaining the morphogenetic phenotype in the axial mesoderm (Figs 2 and 3). The selective down-regulation of some marker genes suggested a specific requirement of *rab7* for dorsal mesoderm development, probably downstream or in parallel of endogenous organizer induction.

Rab7 is required for specification of the ventro-lateral mesoderm

Organizer induction was not blocked after loss of *rab7*, yet, dorsal mesoderm specification was significantly impaired. Therefore, we asked if *rab7* also participated in subsequent ventro-lateral mesoderm specification, a process known to be dependent on zygotic *wnt8a* (Hoppler and Moon, 1998). During gastrulation, the organizer secretes Wnt antagonists dorsally in the axial mesoderm, while *wnt8a* activity is limited to the ventro-lateral mesoderm. Using targeted injections on the ventral side, we blocked *rab7* only in this area to test the possibility that it was required for mesoderm specification (Fig. S3F-J). Morphant embryos developed mild gastrulation phenotypes with low lethality rates, and thus the majority could be raised until tadpole stages. Such embryos showed ventro-posterior malformations, which became more pronounced as early tadpoles, when tail formation was strongly inhibited in most cases (Fig. 5A-C; Fig. S6A,B). Next, we analyzed ventro-lateral gene expression during late gastrulation, to test whether *rab7* was required for specification of these fates. Expression of *myoD1* and *T-box 6* (*tbx6*), two of such marker genes, were strongly inhibited or lost in morphants, demonstrating a requirement of *rab7* for ventral mesoderm identity as well. Co-injection of β-gal lineage tracer demonstrated loss of expression only in the targeted part of the mesoderm, not dorso-laterally, i.e. again supporting a cell-autonomous effect on signal perception (Fig. 5D-G; Fig. S6C-E).

To get a first indication, whether this lack of ventral specification is related to inhibition of endogenous Wnt signaling in the mesoderm, we performed epistasis experiments using suboptimal doses of the *rab7* TBMO in combination with a well-established *ctnnb1* (*β-catenin*) MO (Heasman et al., 2000). While injection of effective doses of *ctnnb1* MO resulted in loss of *myoD1* expression, i.e. phenocopying, *rab7* morphants (Fig. 5J,L), low-dose injections of either *ctnnb1* MO or *rab7* TBMO both had only minor effects on ventral *myoD1* (Fig. 5I,L). When both MOs were combined using low doses, *myoD1* expression was lost in all double-morphants examined, supporting the conclusion of an epistatic interaction of Rab7 and Ctnnb1 (Fig. 5K,L). Together, our experiments support the conclusion that *rab7* participates in specification of ventral mesodermal fates during gastrulation, potentially by regulating endogenous Wnt8a-activated signaling.

Rab7 acts epistatically with the endosomal regulator Vps4

In most contexts, Rab7 acts via its well-studied role as a regulator of late endosomal function. However, in some cases it has been shown to perform a cellular role independent of LE, and, potentially not in the endo-lysosomal pathway (Guerra and Bucci, 2016). Therefore, we aimed to address this point as well, by testing if other late endosomal regulators, which have also been demonstrated to be required for Wnt function, regulate ventral fates in concert with Rab7. We chose two components of the ESCRT machinery (Horner et al., 2018), which have previously been characterized in Wnt signal transduction in *Xenopus*, i.e. *hepatocyte growth factor-regulated tyrosine kinase substrate* (*hrs*) and *vacuolar protein sorting 4 homolog* (*vps4*) (Taelman et al., 2010). Using doses that have been shown to block double axis formation, we knocked down *hrs* ventrally, targeting the ventral mesoderm (Fig. S6F-H), or overexpressed a dominant-negative version of *vps4* (*dn-vps4*) (Bishop and Woodman, 2000), to analyze LE-dependent mesoderm patterning. In both cases, loss of these regulators caused strong reduction of *myoD1* in the ventral part, supporting a necessity for correct LE, and possibly Wnt function in this tissue (Fig. 6A,E; Fig. S6F-H). As this implicated a functional cooperation with Rab7 on LE, we performed an epistatic analysis to demonstrate interaction. Either low-dose injection of *dn-vps4* mRNA, or that of *rab7* TBMO caused minor reduction of *myoD1* expression, however,

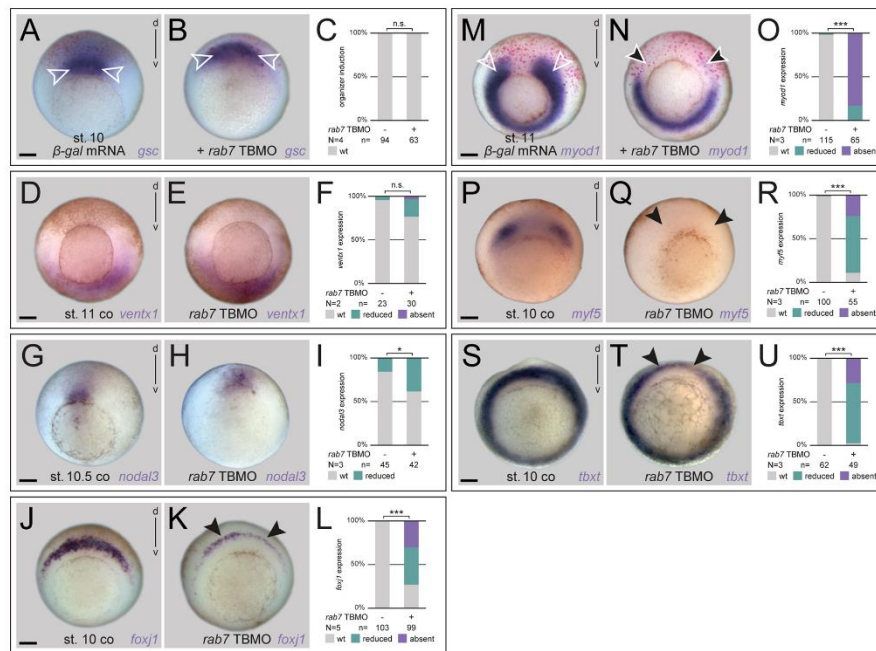


Fig. 4. Dorsal mesoderm specification requires Rab7 independent of the organizer. (A,D,G,J,M,P,S) Untreated control specimen, or *β-gal* mRNA control injections confirming dorsal targeting (white outlined arrowheads in A,M) with wild-type *gsc*, *ventx1*, *nodal3*, *foxj1*, *myod1*, *myf5* and *tbxt* expression, respectively. (B,E) *rab7* loss of function in dorsal or ventral lineage did not alter *gsc* or *ventx1* expression, respectively. (H) *nodal3* expression was slightly reduced in some *rab7* morphant embryos. (K,N,Q,T) expression of *foxj1*, *myod1*, *myf5* and *tbxt* were severely affected in specimen with *rab7* deficiency (black arrowheads). (C,F,I,L,O,R,U) Quantification of results in A,B,D,E,G,H,J,K,M,N,P,Q,S,T. Scale bars: 250 μm.

parallel injection of both caused strong inhibition of *myod1* in a significant manner (Fig. 6B-E). From these results we conclude that Rab7 should act in a canonical manner as an endosomal regulator in the ventral mesoderm, together with LE effectors known to be required for Wnt activation.

Rab7 is required for canonical Wnt pathway activation in vivo

In order to investigate directly whether the loss of *rab7* interfered with endogenous Wnt signals in the mesoderm, and to bypass the possibility that any putative maternal *rab7* mRNA or protein would ‘cover’ its requirement for organizer induction in our experiments, we activated Wnt signaling exogenously. First, we used radial injections of *wnt8a* mRNA, which is well known to dorsalize the embryo (Hikasa and Sokol, 2013; Smith and Harland, 1991). Injections caused radial expression of dorsal-specific organizer genes and crased that of ventral-specific *ventx1* (Fig. 7A,B,D; Fig. S7A-H). Importantly, co-injection of *rab7* TBMO restored the DV-axis highly significantly, again without impacting on endogenous organizer-specific expression of *chd* or *nog* (Fig. 7C,D; Fig. S7C,D). Early gastrula embryos tested for *ventx1* showed phenotypic restoration of their DV axis, yet *ventx1* expression stayed partially reduced (Fig. S7G,H). These results suggest that *rab7* is required for ligand-dependent activation of Wnt signaling, upstream of exogenously induced organizer genes.

If *rab7* participated in Wnt pathway activation *in vivo*, then knockdown should prevent induction of secondary axes, a classical

readout for canonical Wnt pathway in *Xenopus* (Sokol et al., 1991). Co-injection of *rab7* TBMO was sufficient to prevent *wnt3a*-induced double axis induction in a highly significant manner (Fig. 7E-H). Importantly, the efficiency of *ctnbl1* to induce double axes was not altered after *rab7* knockdown (Fig. S7I-M). To further rule out the hypothesis that this effect was due to impairment of processes downstream of organizer induction, we analyzed these secondary organizers for expression of *gsc*, which clearly demonstrated inhibition of Wnt-induced organizers (Fig. S7N-P). These results were further supported using the Wnt-specific β-catenin activated reporter (BAR) (Biechele et al., 2009) in animal caps, where *wnt8a*-induced activation was also blocked by *rab7* inhibition (Fig. 7I). The same reporter blockage after loss of *rab7* was found endogenously, when the BAR construct was directly injected into the Wnt-dependent ventral mesoderm. Loss of *rab7* reduced signals by 90%, indicating that the loss of ventral markers was caused by Wnt pathway inhibition upstream of β-catenin-mediated transcriptional activation (Fig. S7I). In a final approach, we wanted to test if induced activation of zygotic Wnt signaling was sufficient to rescue the loss of paraxial marker genes after *rab7* knockdown. Thus, we incubated dorsal morphants in 0.2 M LiCl at the begin of gastrulation, i.e. after organizer induction. For both, *myod1* and *myf5*, LiCl treatment was partially able to rescue expression in the paraxial mesoderm, while LiCl-induced ectopic expression in the axial areas was not inhibited by inhibition of *rab7*, supporting a role upstream of β-catenin activated

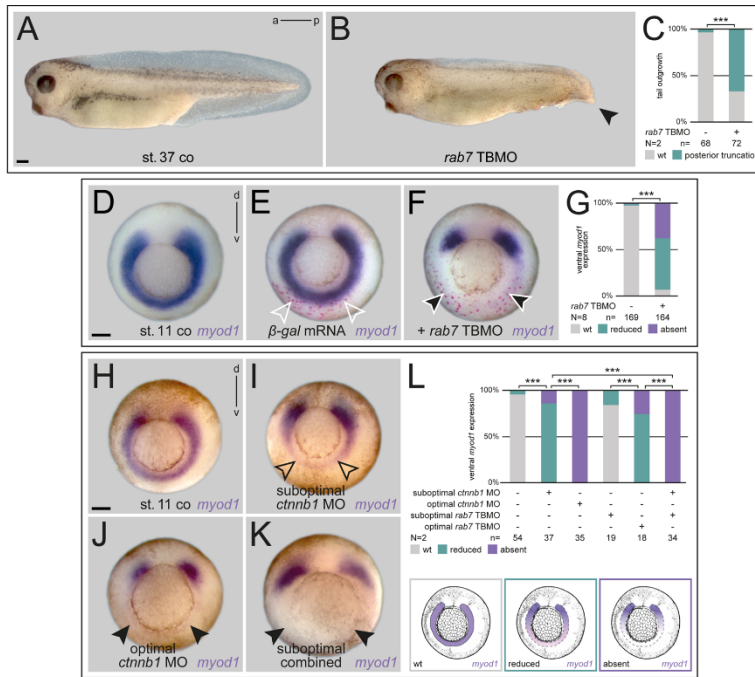


Fig. 5. Specification of the ventral mesoderm requires Rab7.

(A) Untreated early tadpoles with normal tail development, which was impaired by *rab7* loss of function in ventral lineage resulting in posterior truncations (B, black arrowhead). (C) Quantification of results in A,B. (D) Mid-gastrula control embryo depicting wild-type *myoD1* expression, (E) injected β -gal mRNA marks ventrally targeted area (outlined white arrowheads). (F) Co-injection of β -gal mRNA and *rab7* TBMO revealed reduced or absent ventral *myoD1* expression in most specimen at corresponding target site (white outlined black arrowheads). (G) Quantification of results in D-F. (H) Ventro-lateral mesoderm shown by wild-type *myoD1* expression. (I) Ventral injection of suboptimal doses of *ctnnb1* MO resulted in minor reduction of *myoD1* (black outlined arrowheads), (J) whereas optimal doses caused complete loss of ventro-lateral expression (black arrowheads). (K) Parallel injection of *rab7* TBMO and *ctnnb1* MO, both in suboptimal doses, lead to absence of *myoD1* (black arrowheads). (L) Quantification of epistatic function of Rab7 and Ctnnb1 in ventro-lateral mesoderm, different manifestations of *myoD1* expression exemplified below. Scale bars: 250 μ m.

transcription (Fig. 7J-Q). These results support the conclusion that *rab7* participates in mediating early *Xenopus* Wnt signals in a context-dependent manner. Altogether, we therefore conclude from our experiments that loss of the small GTPase Rab7 can interfere with Wnt pathway activation in early frog embryos, upstream of Ctnnb1 stabilization.

DISCUSSION

In this study, we analyzed the *in vivo* role of the small GTPase Rab7 in the frog *Xenopus* with focus on its role in early patterning and regulation of morphogenetic processes during gastrulation. We were able to demonstrate a requirement for dorsal and ventral gastrulation processes, which were both strongly impaired after loss of *rab7*. Further, our results implicate that Rab7 participates in mesodermal patterning processes in the early embryo, at least partially in a Wnt-dependent manner, explaining the observed morphogenetic phenotypes.

***rab7* has distinct activity pattern throughout embryonic development**

In developmental studies, genes with categorized housekeeping function are mostly used as molecular tools – developmental expression is rarely included, as it is considered to be ubiquitous, with little temporal or spatial fluctuations by definition (‘housekeeping genes’, Hounkpe 2021; Kim et al., 2012; Lee and Harland, 2010 for Rab coding examples). Our analysis of *rab7* revealed strikingly dynamic and spatially restricted expression patterns throughout early development, suggesting a tissue- and

context-specific requirement. Therefore, we would predict that many other of such classified genes show tissue-specific and developmentally regulated function as well, and should therefore be used carefully and classified as strict housekeeping genes. Alternatively, for clarity, such examples could be given a separate subcategory within the term ‘housekeeping gene’. In context of membrane trafficking, expression of different endosomal regulators (e.g. *hrs* or *vps4*) could reveal distinct *endosomal synexpression groups*, following a concept proposed before (Niehrs and Pollet, 1999). Such analyses could reveal novel roles for endosomal regulation of developmental processes or pathways, in line with a shared co-transcriptional regulation, as demonstrated for genes coding endosomal components (Ploper et al., 2015; Sardiello et al., 2009). In the case of *rab7*, strong signals in the neural plate border (Fig. 1F-H), pronephric kidney, and cranial and trunk neural crest (Fig. 1I,J) suggest such possible roles, also in other Wnt-regulated tissues (Borday et al., 2018; Burstyn-Cohen et al., 2004; Honoré et al., 2003; Pla and Monsoro-Burq, 2018; Villanueva et al., 2002; Zhang et al., 2011).

Rab7 is required for dorsal mesoderm specification and tissue remodeling during gastrulation

We performed loss of function of *rab7* using antisense oligos and CRISPR/Cas9-mediated genome editing. Reflecting the late expression in diverse tissues, mildly affected, or low-dose injected tadpoles displayed shortened AP axes, head and eye defects, and edema formation, the latter putatively due to loss of *rab7* in the pronephric system (Fig. 1; Fig. S2; Wessely and Tran, 2011). Yet,

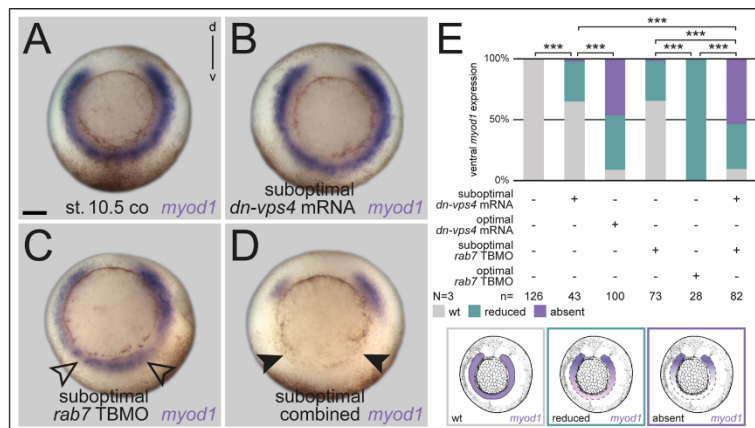


Fig. 6. Small GTPase Rab7 acts epistatically with the LE regulator Vps4. (A) Untreated specimen; (B) Injection of *dn-vps4* mRNA or (C) *rab7* TBMO in suboptimal dose led to minor reduction of *myod1* expression on ventral side (black outlined arrowheads in C). (D) Parallel suboptimal injection of *rab7* TBMO and *dnvps4* mRNA resulted in absent *myod1* expression (black arrowheads). (E) Quantification of results, different manifestations of *myod1* expression in analysis are exemplified below quantification. Scale bar: 250 μ m.

while developing no phenotypes during cleavage or blastula stages, the most prominent developmental defects of *rab7*-deficient embryos became apparent during gastrulation, as a result of incorrect mesoderm patterning. The lack of very early phenotypes, despite the presence of a large supply of maternal *rab7* mRNA in cleavage and blastula stages suggest that this pool might also be required after MBT, i.e. at least partially during gastrulation. This is supported by the fact that the *rab7* TBMO was more efficient in causing gastrulation defects than the *rab7* SBMO.

Interestingly, work in mice supports evolutionary conservation of the role of *rab7* in this context (Kawamura et al., 2012). Here, *rab7* KO also prevented gastrulation, resulting in early embryonic death. More importantly, the authors demonstrated recently that this phenotype was caused by lack of proper mesoderm formation, recognizable by defects in tissue remodeling and subsequent germ layer formation (Kawamura et al., 2020). These cellular phenotypes are highly reminiscent of our observations in the dorsal mesoderm after loss of *rab7*, where cellular arrangements were disorganized as well, and correct formation of Brachet's cleft was impaired, i.e. germ layers also failed to separate correctly (Fig. 2; Fig. S4). Another indication for a conserved role of *rab7* in these processes might be the alteration of cell adhesion we observed (Fig. 2K-O). In the mouse, such altered cell adhesion was also observed after loss of *rab7*, paralleling the failed tissue remodeling (Kawamura et al., 2020).

From work in cell culture it is known that Rab7 is required for correct activation and localization of β 1-Integrin at the cell membrane in a permissive way, i.e. as a component required for transport towards the membrane (Arjonen et al., 2012; Margiotta et al., 2017). Thus, such a function of Rab7-mediated transport could specifically explain changes of β 1-Integrin after *rab7* inhibition (Fig. 2O). Yet, we cannot clearly distinguish whether the alterations of cell adhesion in the dorsal mesoderm is a direct result of loss of Rab7-mediated transport of adhesion components, or an indirect consequence of the lack of mesodermal specification. The significant downregulation of *tbxt* in most embryos argues for the second possibility (Fig. 4S-U), which suffices to explain the observed problems of tissue remodeling, axial elongation and notochord morphogenesis, since *Tbxt* is a well-known upstream regulator of mesoderm specification and non-canonical Wnt pathways required for CE (Bruce and Winklbauer, 2020; Schulte-Merker and Smith, 1995; Tada and Smith, 2000).

Rab7 mediates dorsal development independent of the organizer

Strikingly, we did not observe a change in organizer induction as judged by expression of *gsc* or *chd* at early gastrulation. Whether such a Rab7-deficient organizer is fully functional, i.e. capable of inducing a secondary axis in a classical transplantation assay, is not clear from these analyses. Yet, embryos show no signs of ventralization or dorsalization, neither phenotypically, nor when analyzed for mid-gastrula expression of DV-specific genes *ventx1* or *chd* (Fig. 4D-F; Fig. S5F-K). These results argue against an involvement of *rab7* in early Wnt-mediated Nieuwkoop center/organizer induction (Fagotto et al., 1997; Heasman et al., 1994) or in transforming growth factor beta (TGF- β)/Nodal pathway-induced activation of organizer genes, nor in BMP-mediated ventral development (De Robertis, 2009). These conclusions are supported by the recent report also showing no alteration of Nodal or BMP signaling in *rab7* KO mice (Kawamura et al., 2020). So far, neither involvement of Rab7, nor of LE in general has been linked to activation of TGF- β signaling, a finding we would also conclude from our *Xenopus* analyses.

In contrast to wild-type expression of organizer genes, we found that *rab7* was clearly necessary for *foxj1*, *myod1*, *myf5*, and *tbxt*, and partially for correct *nodal3* expression (Fig. 4G-U). Most of these genes are known to depend on active Wnt signaling (with uncertainty for *tbxt*), however, to what extent maternally or zygotically activated Wnt signals contribute to their activation is not fully understood (Shi et al., 2002; Smith et al., 1995; Stubbs et al., 2008; Vonica and Gumbiner, 2002; Walentek et al., 2013). *nodal3* expression, which was impacted least after *rab7* inhibition, is initiated just after MBT and thought to be a direct Wnt target (Glinka et al., 1996; Smith et al., 1995). Therefore, these results might indicate a role for Rab7 only for processes relying on zygotic Wnt activation. In the recently analyzed *rab7* KO mouse, gastrulation phenotypes and lack of *tbxt* expression have been demonstrated as well, and these phenotypes were related to inhibition of Wnt signaling by reduced degradation of the Wnt antagonist Dickkopf (*Dkk*) (Kawamura et al., 2020). It is not clear whether Rab7 participates in *Dkk* degradation in *Xenopus* development. However, excess *Dkk* protein caused by loss of Rab7 can neither explain inhibition of induced double axes, nor blockage of transcriptional Wnt reporter activation in animal caps,

Biology Open

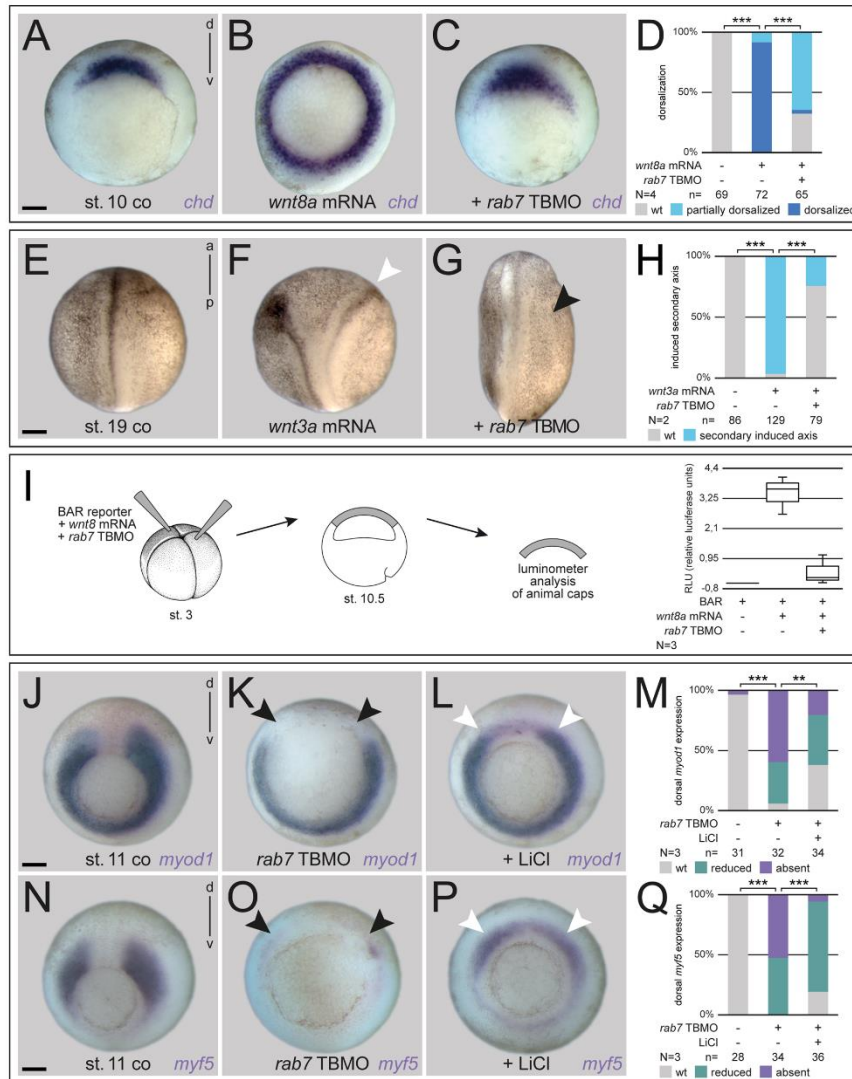


Fig. 7. Rab7 is required for canonical Wnt pathway activation. (A) Wild-type dorsal expression of *chd* in comparison to specimen with (B) radial injected *wnt8a* mRNA showing an extended *chd* expression domain around the blastopore. (C) Co-injection of *rab7* TBMO restricted additional *chd* expression to normal wild-type state. (D) Quantification of results in A-C. (E) Untreated control specimen, (F) in comparison to induced double axis (white arrowhead) after ventral *wnt3a* mRNA injection, (G) parallel injection of *rab7* TBMO inhibited secondary axis formation (black arrowhead). (H) Quantification of results in E-G. (I) Luciferase-based Wnt reporter assay analysis at stage 10.5 illustrated that *wnt8a* induced reporter activity was blocked by *rab7* loss of function in animal caps. (J,N) Wild-type expression of *myod1* and *myf5* in stage 11 control embryos. (K,Q) Absent dorsal *myod1* expression and lost domains upon *rab7* loss of function (black arrowheads). (L,P) Treatment with LiCl partially rescues dorsal expression of *myod1* and *myf5* in *rab7* morphant embryos (white arrowheads). Please note that LiCl-induced ectopic expression in the axial mesoderm was not inhibited by the *rab7* TBMO. (M,Q) Quantification of results in J-L and N-P, respectively. Scale bars: 250 μ m.

which are devoid of *dkk* transcripts (Fig. 7; Glinka et al., 1998). Further, *dkk* is not expressed endogenously in the ventral mesoderm, i.e. accumulated protein can therefore not explain *rab7*

knockdown-induced loss of ventral marker genes (Fig. 5; Fig. S6). We therefore conclude that at least in these contexts, Rab7 should participate in Wnt ligand-induced signal transduction, probably as

part of a late endosomal machinery-mediated signal maintenance mechanism (Fig. 6, Taelman et al., 2010, and below).

Rab7 is necessary for Wnt activation in *Xenopus* in a context-dependent manner

The unexpected lack of ventralization phenotype contradicted the reported role of LE for Wnt pathway activation, as we expected Rab7 to be also required for maternal, Wnt-dependent organizer induction (Taelman et al., 2010; Vinyoles et al., 2014). This was even more puzzling, as we could demonstrate an absolute requirement for exogenously induced activation of Wnt-dependent processes, i.e. double axis assay, Wnt reporter activation, and the restoration of the DV axis after Wnt8a-mediated dorsalization (Fig. 7; Fig. S7). The last result exemplified this discrepancy, as exogenously induced Wnt-dependent dorsal fates were blocked after loss of *rab7*, while the endogenous, organizer-induced expression of *chd* and *nog* stayed unaltered (Fig. 7A-D; Fig. S7A-D). A compensatory action by the paralogous *rab7b* can be excluded, as it is not present in the early embryo (Peshkin et al., 2019 preprint; Session et al., 2016; our preliminary results). One straightforward explanation would be that endogenous maternal Wnt activation does not require ligand-mediated receptor activation and endocytosis, which we used for exogenous Wnt pathway induction. This could include a mechanism bypassing the endolysosomal system, what would be in agreement with the fact that injection of *dickkopf-1* mRNA, which blocks extracellular Wnt receptor activation, does not ventralize the embryo either (Glinka et al., 1998). In cell culture and *Xenopus* embryos, LE have been reported to be necessary to establish a robust Wnt output, i.e. to maintain continuous inhibition of glycogen synthase kinase 3 (GSK3), and thus Wnt pathway activation. However, endogenous organizer induction has not been analyzed in these experiments (Niehrs and Acebrón, 2010; Taelman et al., 2010). In fact, we cannot exclude that early Wnt activation might only rely on 'fast-acting', LE-independent mechanisms (like Axin inhibition), which have been suggested to be required for GSK3-inhibition and Wnt activation (Clevers and Nusse, 2012; Li et al., 2012). Alternatively, the *Xenopus* zygote might already contain fully or partially matured LE, as proposed before, whose functionality we are not able to interfere with using embryonic injections (Dobrowolski and De Robertis, 2011).

In contrast to the rather complex involvement of Rab7 for dorsal fates, we could show a requirement for endogenous ventro-lateral mesoderm patterning, as all marker genes (*myf5*, *myo1*, *thx6*) were strongly downregulated after loss of *rab7* (Fig. 4M-R, Fig. 5D-G; Fig. S6C-E). These genes have all been shown to depend on a ventral source of Wnt, mediated by Wnt8a (Hoppler and Moon, 1998; Hoppler et al., 1996; Kjolby and Harland, 2017; Shi et al., 2002), which was supported by the epistatic effect of *rab7* knockdown with *ctmb1* knockdown (Fig. 5H-L). Furthermore, we could also demonstrate that *rab7* knockdown blocked endogenous Wnt target gene activation, as monitored using a ventral mesodermal BAR reporter signal (Fig. S7I). From these experiments, we suggest that *rab7* participates in ventral mesoderm specification, at least partially as a necessary factor for Wnt target gene activation. This effect on mesoderm specification was phenocopied by loss of LE-associated ESCRT factors *vps4* and *hvs*, which are also known to be required for Wnt pathway activation (Taelman et al., 2010). As we could demonstrate an additive relationship with loss of *rab7* (Fig. 6), we suggest Rab7 fulfills this role as an endosomal regulator required for correct LE-mediated Wnt transduction (Dobrowolski and De Robertis, 2011; Hikasa and Sokol, 2013).

The connection of Rab7 to other signaling pathways – beyond Wnt activation

Our findings implicate a role of Rab7 for exogenously induced Wnt activation, and for endogenous ventral mesoderm specification, probably in a Wnt-dependent function. Yet, some results obtained with our dorsal analyses might indicate further, potentially Wnt-independent roles during gastrulation. While dorsal loss of *rab7* resulted in subsequent gastrulation and axial elongation defects, selective downregulation of *shh* seems puzzling (Fig. 3). Regulation of *shh* in the ventral neural tube is well analyzed (Dessaud et al., 2008), however, little was reported about the induction and maintenance of its notochordal expression. Activin was shown to be able to induce *shh* in animal caps, but not endogenously in the mesoderm (Yokota et al., 1995), and we have no evidence for a participation of Rab7 in TGF- β pathways either. Yet, in the well-studied limb bud, Wnt7a has been shown to be required for induction and/or maintenance of *shh*, offering a potential link to our observations (Parr and McMahon, 1995; Yang and Niswander, 1995). Another interesting aspect also comes from the limb bud, where fibroblast growth factor (FGF) signaling was reported both to induce and to maintain *shh* expression (Scherz et al., 2004; Vogel et al., 1996; Yang and Niswander, 1995). FGF signaling is known to cooperate with Wnt in different contexts, and both are required additionally to induce *myf5* in the somitic mesoderm (e.g. Shi et al., 2002). Thus, if *rab7* additionally participated in FGF pathway activation, this would explain the strong effect on *myf5* and *myo1* after loss of function (Fig. 4M-R), the partial ability to rescue *myf5* and *myo1* by LiCl treatment (Fig. 7J-Q), and the differential impact on *nodal3* versus *foxj1* and *thx* (Fig. 4G-L and S-U). The last three genes depend on Wnt signaling, but only *thx* and *foxj1* have also been shown to be regulated by the FGF pathway dorsally, downstream of Nodal3-induced activation of Fgf receptor 1 (Glinka et al., 1996; Schneider et al., 2019; Smith et al., 1995; Vick et al., 2018; Yokota et al., 2003).

MATERIALS AND METHODS

Xenopus laevis care and maintenance

Frogs were purchased from Nasco (901 Janesville Avenue P.O. Box 901 Fort Atkinson, WI, USA). Handling, care and experimental manipulations of animals was approved by the Regional Government of Stuttgart, Germany (V349/18ZO 'Xenopus Embryonen in der Forschung'), according to German regulations and laws (§6, article 1, sentence 2, number 4 of the animal protection act). Animals were kept at the appropriate conditions (pH=7.7, 20°C) at a 12 h light cycle in the animal facility of the Institute of Zoology of the University of Hohenheim. Female frogs (4-12 years old) were injected subcutaneously with 300-700 units of human chorionic gonadotropin (hCG; Sigma-Aldrich), depending on weight and age, to induce ovulation. Sperm of male frogs was gained by dissection of the testes that was stored at 4°C in 1× MBSH (Modified Barth's saline with HEPES) solution. Embryos were staged according to Nieuwkoop and Faber (1994). Only clutches of embryos from healthy females were used for the experiments reported here, provided the early embryonic stages showed normal survival rates as well. Individual embryos from one batch were randomly picked and used either as control or test specimens. If control groups displayed unusual developmental defects later in development, such clutches were excluded as well, based on empirical judgement.

Lineage-specific microinjections

For lineage-specific experiments, embryos were injected at the four-cell stage into the marginal (equatorial) region of either both dorsal or both ventral blastomeres, to target the dorsal or ventro-lateral mesoderm specifically (Fig. S3A,F). Using a Harvard Apparatus setup, drop size was calibrated to 4 nl per injection. For verification of dorsal-specific or ventral knockdown,

a lineage tracer (fluorescein-dextran, mGFP mRNA, H2B-GFP mRNA, or β -gal mRNA) was added. For both targeted injections into the dorsal and ventral mesoderm, embryos were cultivated until early gastrula stages (stage 10-10.5), when the DV axis is easily recognized by dorsal lip formation, and verified for correct targeting of dorsal or ventral lineages, respectively (Fig. S3A-J). In dorsal experiments analyzing somitic (paraxial) marker genes (*myoD1*, *myf5*), injections were targeted slightly more lateral into the same blastomere (not shown). For experiments with analyses at mid to late gastrula (stage 11-12.5), embryos were checked at early gastrula, then fixed at later stages (Fig. S3D-E', I-J'). For all targeted knockdown analyses, embryos of all treatments (uninjected specimens of the same batch, and control-injected or treatment-injected specimens) were cultivated for exactly the same time under the same temperature-controlled conditions before fixation and analysis. Thus, any apparent differences in staging within one experiment should represent phenotypic alterations caused by the treatment itself.

Morpholino design and microinjections

The *rab7a*-5'UTR-TBMO was designed using the sequence of the S-form from the genomic sequence as deposited in gene bank (one mismatched base pair for the L-Form; no binding to *X. laevis rab7b* mRNA). TBMO-sequence is 5'-GTCTCCGCTCTCTACCCCTGCCAGC-3'. The *rab7a* SBMO was designed using the sequence of the L-Form from the genomic sequence as deposited in gene bank (three mismatched base pairs for the S-Form). Splice acceptor site at intron 2 of the *rab7a* pre-mRNA is targeted by SBMO (5'-GCCAACCCCTAGAAATGGAGATACAA-3'). Further MOs used in this study were *ctnbn1* and *hrs* MO as published (Heasman et al., 2000; Taelman et al., 2010) or a random co-MO as a MO fill up for epistatic analyses. Total amounts of injected MOs were: 0.4 pmol *ctnbn1* MO (suboptimal dose), 0.8 pmol *ctnbn1* MO (optimal dose), 1.6-2.0 pmol *hrs* MO, 0.7 pmol *rab7* TBMO (suboptimal/low dose), 1.0-1.4 pmol *rab7* TBMO (optimal dose), 1.4-4.0 pmol *rab7* SBMO.

mRNA synthesis and microinjections

Plasmids were linearized with NotI and transcribed *in vitro* (Sp6 polymerase) using Ambion message machine kit. Drop size was calibrated to 4 nl per injection. Total amounts of injected mRNA per embryo are as followed: 80 pg *ca-rab7a* (*Canis lupus*) mRNA, 400 pg *dn- ν ps4* mRNA, 400 pg mGFP mRNA, 400 pg H2B-GFP mRNA, 160 pg *wnt8a* mRNA, 400 pg β -gal mRNA.

sgRNA design and microinjections

Two single-guide RNAs were designed for the *Xenopus laevis rab7a* gene, *rab7* CRNP (S+L), target sequence: 5'-GGTGATGGTGGATGACAGATTGG-3' (on exon 3), and *rab7* CRNP (L), target sequence: 5'-GGGACACAGCTGGGACAGAA AGG-3' (on exon 4), using the publicly available 'CRISPCan' software. sgRNAs were transcribed with the MEGashortscript T7 Kit from synthetic DNA oligomers and purified with the MEGAclear Transcription Clean-Up Kit (both ThermoFisher).

Oligos for synthesis were: *rab7*-CRNP (S+L) forward: 5'-GCAGCTAA-TACGACTCACTATAGGTGATGGTGGATGACAGATGTTTATAGAGC-TAGAAATAGCAAG-3', *rab7* CRNP (L) forward 5'-GCAGCTAATAC-GACTCACTATAGGGACACAGCTGGGACAGGAAGTTTATAGAGCTA-GAAATAGCAAG-3', and general reverse 5'-AAAAGCACC-GACTCGGTGCCACTTTTCAAGTTGATAACGGACTAGCCT-TATTTAACTTGCTATTTCTAGCTCTAAAC-3'.

Embryos were injected with 1 ng Cas9 protein (PNA Bio) and 300 pg sgRNA at the one-cell stage and cultivated at room temperature (RT) until desired stage. DNA was isolated from ten mutant and five control embryos. For verification of successful genome editing, isolated DNA was proceeded by RT-PCR and sequenced. Analysis of sequenced DNA was analyzed via Synthego ICE. PCR-Primers for sequencing were the following: *rab7* CRNP(S+L), L-form (FP 5'-AGCCGATTTCTTTGTTGTGCCA-3'; RP 5'-ATTCAGGTGCAGTGAGATGT-3'), *rab7* CRNP(S+L), S-form (FP 5'-TGAGTCATTGTGCTGTGTG-3'; RP 5'-CCCCATTGAAAACCT-GAAGAGAG-3'), *rab7* CRNP(L), (FP 5'-ACGGGACGAGATTAATA-GGACA-3'; RP 5'-CTTGGACTGCCTGGATGAG-3').

PCR-based verification of efficient intron retention for the SBMO

For verification of SBMO, a standard RT-PCR was performed. SBMO was injected in all four blastomeres of four-cell embryos, cultivated until stage 13, and fixed for RNA isolation. The following PCR primers were used: forward 5'-CCTCCAGGAATATGCAGGAA-3'; reverse 5'-CTGCATTG-TGACCAATCTGTC-3'.

Luciferase-based Wnt assay

For Luciferase-based Wnt assay (Promega Dual-Luciferase[®] Reporter Assay System), embryos were injected into two animal or ventral blastomeres at the four-cell stage (80 pg BAR reporter DNA plus 40 pg Renilla DNA). For exogenously induced reporter activity, embryos were injected of 240 pg *wnt8a* mRNA +/- 1.4 pmol *rab7* TBMO and cultivated until stage 10.5, then animal caps were dissected and further processed. For endogenous analysis, embryos were co-injected with *rab7* TBMO, cultivated until stage 12, then the ventral halves were dissected. Dissection of tissues was performed in 0.1x MBSH. Extracted tissues (ten animal caps or ventral halves) were transferred into lysis buffer (Promega) and incubated for 15 min. Lysates were centrifuged repeatedly for 15 min, then supernatant transferred in triplets onto a 96-well plate for Luciferase analysis by the GloMax Explorer system. Relative Luciferase units (RLU in %) were calculated by the ratio of Luciferase and Renilla values.

In situ hybridization

For *in situ* mRNA detection, ISH was performed after fixation in MEMFA for 2-3 h at RT and processed following a customized standard protocol (Sive et al., 2000; customization after R. Rupp, personal communication). PCR primer pair for cloning of *X. laevis rab7a* were: forward: 5'-ATCAATACGCGTCAACAACC-3'; reverse: 5'-ACAGGTGTCAGTATT-CATTGG-3'. Cloned full length coding region was sequenced. *X. laevis rab7a* shows no significant overlap with *rab7b*, excluding mixed signals during ISH. RNA *in situ* probes were transcribed using SP6 or T7 polymerases.

Axis induction assay

Double axis assay was performed by single injection of 0.8 pg *wnt3a* mRNA +/- 0.7 pmol *rab7* TBMO into one ventral mesodermal blastomere at the four-cell stage as described (Beyer et al., 2012). Embryos were raised until gastrulation or neurula stage. Double axes were scored empirically by second ventral *gsc* expression (early gastrula) and for visible induction of secondary axes (late neurulas).

Embryo sections

For vibratome sections, embryos were embedded in a glutaraldehyde-crosslinked gelatin-albumin mix and razor-blade sectioned. Hoechst stained vibratome sections were incubated on microscope slide before imaging (1:10,000 Hoechst). Bisections of embryos was performed using a razor blade.

Immunofluorescence analysis

Co-injected fluorescein dextran (70,000 MW, ThermoFisher, D1822) was used as lineage tracer for dorsal lips in IF analyses. For IF analyses, embryos were fixed in 4% paraformaldehyde for 1 h at RT, followed by two washes in 1x PBS for 15 min each. For staining of animal caps or bisected specimens, embryos were manually dissected horizontally or sagittally after fixation, transferred to 24-well plates, and washed twice for 15 min in PBST (PBS/0.1% Triton X-100). After blocking for 2 h at RT in CAS-Block (1:10 in PBST; ThermoFisher, #008120) blocking reagent was replaced by antibody solution (diluted in CAS-Block) for incubation ON at 4°C. Antibodies used were: β 1-Integrin (DSHB α 8-s; 1:70), MZ15 (DSHB; 1:200). Then antibody solution was removed and explants washed twice for 15 min in PBS. Secondary antibodies (ThermoFisher, all 1:1000 in CAS-Block) were incubated for 2 h at RT. Cell borders were visualized using AlexaFluor[™]Plus 405 Phalloidin (ThermoFisher A30104) overnight at 4°C (1:100 in PBS-). For photo documentation, bisected embryos or caps were transferred onto microscope slides or positioned in low melt agarose on a Petri dish (0.5% low melt agarose in 1x PBS-).

Photo documentation

LSM images of IF data were taken with a Zeiss LSM 700 Axioplan2 Imaging microscope and then adjusted using the Zeiss Zen 2012 Blue edition. All other pictures were taken with a Zeiss SteREO Discovery V12 microscope or an Axioplan2 inverted microscope using AxioVision 4.6. Afterwards Adobe Photoshop CS6 was used for cropping and careful brightness adjustments. All figures were arranged using Adobe Illustrator CS6.

Statistical analysis

Statistical calculations of marker gene expression patterns were performed using Pearson's chi-square test (Bonferroni corrected, if required). $*-P<0.05$, $**P<0.01$, $***P<0.001$ were used for all statistical analyses, as well as the declaration N —the number of experiments (i.e. number of biological replicates of batches of embryos from different fertilizations), and n —the number of embryos analyzed (i.e. number of biological replicates of embryos).

Acknowledgements

We like to thank T. Ott for technical advice and valuable feedback, V. Andre, M. Maerker, J.-L. Plouhinec, A. Schäfer-Kosulja, and S. Vogel for technical assistance, and M. Blum and Lab members for continuous valuable feedback. Further, we want to thank Drs E. De Robertis, R. Harland, T. Hollemann, C. Kintner, R. Moon, R. Rupp, B. van Deurs, and P. Woodman for sharing constructs.

Competing interests

The authors declare no competing or financial interests.

Author contributions

Conceptualization: P.V.; Validation: J.K., P.V.; Formal analysis: J.K., F.M.W.; Investigation: J.K., F.M.W., P.V.; Data curation: J.K.; Writing - original draft: P.V.; Writing - review & editing: J.K., F.M.W.; Visualization: J.K., F.M.W.; Supervision: P.V.; Project administration: P.V.

Funding

J.K. was a recipient of a PhD fellowship from the Landesgraduiertenförderung Baden-Württemberg.

References

Arjonen, A., Alanko, J., Veltel, S. and Ivaska, J. (2012). Distinct recycling of active and inactive $\beta 1$ integrins. *Traffic* **13**, 610-625. doi:10.1111/j.1600-0854.2012.01327.x

Beyer, T., Danilchik, M., Thumberger, T., Vick, P., Tisler, M., Schneider, I., Bogusch, S., Andre, P., Ulmer, B., Walentek, P. et al. (2012). Serotonin signaling is required for Wnt-dependent GRP specification and leftward flow in Xenopus. *Curr. Biol.* **22**, 33-39. doi:10.1016/j.cub.2011.11.027

Biechele, T. L., Adams, A. M. and Moon, R. T. (2009). Transcription-based reporters of Wnt/beta-catenin signaling. *Cold Spring Harb. Protoc.* **2009**, pdb.prot5223. doi:10.1101/pdb.prot5223

Bishop, N. and Woodman, P. (2000). ATPase-defective mammalian VPS4 localizes to aberrant endosomes and impairs cholesterol trafficking. *Mol. Biol. Cell* **11**, 227-239. doi:10.1091/mbc.11.1.227

Borday, C., Parain, K., Thi Tran, H., Vleminckx, K., Perron, M. and Monsoroburq, A. H. (2018). An atlas of Wnt activity during embryogenesis in Xenopus tropicalis. *PLoS ONE* **13**, e0193606. doi:10.1371/journal.pone.0193606

Bruce, A. E. and Winklbauer, R. (2020). Brachyury in the gastrula of basal vertebrates. *Mech. Dev.* **163**, 103625. doi:10.1016/j.mod.2020.103625

Brunt, L. and Scholpp, S. (2018). The function of endocytosis in Wnt signaling. *Cell. Mol. Life Sci.* **75**, 785-795. doi:10.1007/s00018-017-2654-2

Burstyn-Cohen, T., Stanleigh, J., Sela-Donenfeld, D. and Kalcheim, C. (2004). Canonical Wnt activity regulates trunk neural crest delamination linking BMP/noggin signaling with G1/S transition. *Development* **131**, 5327-5339. doi:10.1242/dev.01424

Butler, M. T. and Wallingford, J. B. (2017). Planar cell polarity in development and disease. *Nat. Rev. Mol. Cell Biol.* **18**, 375-388. doi:10.1038/nrm.2017.11

Clevers, H. and Nusse, R. (2012). Wnt/beta-catenin signaling and disease. *Cell* **149**, 1192-1205. doi:10.1016/j.cell.2012.05.012

De Robertis, E. M. (2009). Spemann's organizer and the self-regulation of embryonic fields. *Mech. Dev.* **126**, 925-941. doi:10.1016/j.mod.2009.08.004

Dessaud, E., McMahon, A. P. and Briscoe, J. (2008). Pattern formation in the vertebrate neural tube: a sonic hedgehog morphogen-regulated transcriptional network. *Development* **135**, 2489-2503. doi:10.1242/dev.009324

Dobrowolski, R. and De Robertis, E. M. (2011). Endocytic control of growth factor signalling: multivesicular bodies as signalling organelles. *Nature Publishing Group* **13**, 53-60. doi:10.1038/nm3244

Fagotto, F. (2020). Tissue segregation in the early vertebrate embryo. *Semin. Cell Dev. Biol.* **107**, 130-146. doi:10.1016/j.semcdb.2020.05.020

Fagotto, F., Guger, K. and Gumbiner, B. M. (1997). Induction of the primary dorsalizing center in Xenopus by the Wnt/GSK/beta-catenin signaling pathway, but not by Vg1, Activin or Noggin. *Development* **124**, 453-460. doi:10.1242/dev.124.2.453

Fürthauer, M. and González-Gaitán, M. (2009). Endocytic regulation of notch signalling during development. *Traffic* **10**, 792-802. doi:10.1111/j.1600-0854.2009.00914.x

Glinka, A., Delius, H., Blumenstock, C. and Niehrs, C. (1996). Combinatorial signalling by Xwnt-11 and Xnr3 in the organizer epithelium. *Mech. Dev.* **60**, 221-231. doi:10.1016/S0925-4773(96)00624-7

Glinka, A., Wu, W., Delius, H., Monaghan, A. P., Blumenstock, C. and Niehrs, C. (1998). Dickkopf-1 is a member of a new family of secreted proteins and functions in head induction. *Nature* **391**, 357-362. doi:10.1038/34848

Guerra, F. and Bucci, C. (2016). Multiple roles of the small GTPase Rab7. *Cells* **5**, 34. doi:10.3390/cells5030034

Hanson, P. I. and Cashikar, A. (2012). Multivesicular body morphogenesis. *Annu. Rev. Cell Dev. Biol.* **28**, 337-362. doi:10.1146/annurev-cellbio-092910-154152

Heasman, J., Crawford, A., Goldstone, K., Garner-Hamrick, P., Gumbiner, B., McCrear, P., Kintner, C., Noro, C. Y. and Wylie, C. (1994). Overexpression of cadherins and underexpression of beta-catenin inhibit dorsal mesoderm induction in early Xenopus embryos. *Cell* **79**, 791-803. doi:10.1016/0092-8674(94)90069-8

Heasman, J., Kofron, M. and Wylie, C. (2000). beta-catenin signaling activity dissected in the early Xenopus embryo: a novel antisense approach. *Dev. Biol.* **222**, 124-134. doi:10.1006/dbio.2000.9720

Hikasa, H. and Sokol, S. Y. (2013). Wnt signaling in vertebrate axis specification. *Cold Spring Harbor Perspect. Biol.* **5**, a007955-a007955. doi:10.1101/cshperspect.a007955

Honoré, S. M., Aybar, M. J. and Mayor, R. (2003). Sox10 is required for the early development of the prospective neural crest in Xenopus embryos. *Dev. Biol.* **260**, 79-96. doi:10.1016/S0012-1606(03)00247-1

Hoppler, S. and Moon, R. T. (1998). BMP-2/4 and Wnt-8 cooperatively pattern the Xenopus mesoderm. *Mech. Dev.* **71**, 119-129. doi:10.1016/S0925-4773(98)00004-5

Hoppler, S., Brown, J. D. and Moon, R. T. (1996). Expression of a dominant-negative Wnt blocks induction of MyoD in Xenopus embryos. *Genes Dev.* **10**, 2805-2817. doi:10.1101/gad.10.21.2805

Horner, D. S., Pasini, M. E., Beltrame, M., Mastrodonato, V., Morelli, E. and Vaccari, T. (2018). ESCRT genes and regulation of developmental signaling. *Semin. Cell Dev. Biol.* **74**, 29-39. doi:10.1016/j.semcdb.2017.08.038

Hounkpe, B. W., Chenou, F., de Lima, F. and De Paula, E. V. (2021). HRT Atlas v1.0 database: redefining human and mouse housekeeping genes and candidate reference transcripts by mining massive RNA-seq datasets. *Nucleic Acids Res.* **49**, D947-D955. doi:10.1093/nar/gkaa609

Huotari, J. and Helenius, A. (2011). Focus review endosome maturation. *EMBO J.* **30**, 3481-3500. doi:10.1038/emboj.2011.286

Katzmann, D. J., Odorizzi, G. and Emr, S. D. (2002). Receptor downregulation and multivesicular-body sorting. *Nat. Rev. Mol. Cell Biol.* **3**, 893-905. doi:10.1038/nm973

Kawamura, N., Sun-Wada, G.-H., Aoyama, M., Harada, A., Takasuga, S., Sasaki, T. and Wada, Y. (2012). Delivery of endosomes to lysosomes via microautophagy in the visceral endoderm of mouse embryos. *Nat. Commun.* **3**, 1071-1010. doi:10.1038/ncomms2069

Kawamura, N., Takaoka, K., Hamada, H., Hadjantonakis, A.-K., Sun-Wada, G.-H. and Wada, Y. (2020). Rab7-mediated endocytosis establishes patterning of Wnt activity through inactivation of Dkk antagonism. *CellReports* **31**, 107733. doi:10.1016/j.celrep.2020.107733

Kim, K., Lake, B. B., Harembak, T., Weinstein, D. C. and Sokol, S. Y. (2012). Rab11 regulates planar polarity and migratory behavior of multiciliated cells in Xenopus embryonic epidermis. *Dev. Dyn.* **241**, 1385-1395. doi:10.1002/dvdy.23826

Kjølby, R. A. S. and Harland, R. M. (2017). Genome-wide identification of Wnt/beta-catenin transcriptional targets during Xenopus gastrulation. *Dev. Biol.* **426**, 165-175. doi:10.1016/j.ydbio.2016.03.021

Lee, J.-Y. and Harland, R. M. (2010). Endocytosis is required for efficient apical constriction during xenopus gastrulation. *Curr. Biol.* **20**, 253-258. doi:10.1016/j.cub.2009.12.021

Li, V. S. W., Ng, S. S., Boersema, P. J., Low, T. Y., Karthaus, W. R., Gerlach, J. P., Mohammed, S., Heck, A. J. R., Maurice, M. M., Mahmoudi, T. et al. (2012). Wnt signaling through inhibition of beta-catenin degradation in an intact Axin1 complex. *Cell* **149**, 1245-1256. doi:10.1016/j.cell.2012.05.002

Margliotta, A., Progidia, C., Bakke, O. and Bucci, C. (2017). Rab7a regulates cell migration through Rac1 and vimentin. *BBA Mol. Cell Res.* **1864**, 367-381. doi:10.1016/j.bbamcr.2016.11.020

Niehrs, C. and Acebron, S. P. (2010). Wnt signaling: multivesicular bodies hold GSK3 captive. *Cell* **143**, 1044-1046. doi:10.1016/j.cell.2010.12.003

- Niehrs, C. and Pollet, N. (1999). Synexpression groups in eukaryotes. *Nature* **402**, 483-487. doi:10.1038/990025
- Nieuwkoop, P. D. and Faber, J. (1994). *Normal Table of Xenopus laevis*. New York: Garland.
- Parr, B. A. and McMahon, A. P. (1995). Dorsalizing signal Wnt-7a required for normal polarity of D-V and A-P axes of mouse limb. *Nature* **374**, 350-353. doi:10.1038/374350a0
- Peshkin, L., Lukyanov, A., Kalocsay, M., Gage, R. M., Wang, D., Pells, T. J., Karimi, K., Vize, P. D., Wühr, M. and Kirschner, M. W. (2019). The protein repertoire in early vertebrate embryogenesis. *Preprint, bioRxiv* **1865**, 571174. doi:10.1101/571174
- Pla, P. and Monsoro-Burg, A. H. (2018). The neural border: Induction, specification and maturation of the territory that generates neural crest cells. *Dev. Biol.* **444** Suppl. 1, S36-S46. doi:10.1016/j.ydbio.2018.05.018
- Platta, H. W. and Stenmark, H. (2011). Endocytosis and signaling. *Curr. Opin. Cell Biol.* **23**, 393-403. doi:10.1016/j.cob.2011.03.008
- Ploper, D. and De Robertis, E. M. (2015). The MITF family of transcription factors: Role in endosomosomal biogenesis, Wnt signaling, and oncogenesis. *Pharmacol. Res.* **99**, 36-43. doi:10.1016/j.phrs.2015.04.006
- Ploper, D., Taelman, V. F., Robert, L., Perez, B. S., Titz, B., Chen, H.-W., Graeber, T. G., von Eeuw, E., Ribas, A. and De Robertis, E. M. (2015). MITF drives endosomosomal biogenesis and potentiates Wnt signaling in melanoma cells. *Proc. Natl. Acad. Sci. USA* **112**, E420-E429. doi:10.1073/pnas.1424576112
- Sardiello, M., Palmieri, M., di Ronza, A., Medina, D. L., Valenza, M., Gennarino, V. A., Di Malta, C., Donaudy, F., Embrione, V., Polishchuk, R. S. et al. (2009). A gene network regulating lysosomal biogenesis and function. *Science* **325**, 473-477. doi:10.1126/science.1174447
- Scherz, P. J., Harfe, B. D., McMahon, A. P. and Tabin, C. J. (2004). The limb bud Shh-Fgf feedback loop is terminated by expansion of former ZPA cells. *Science* **305**, 396-399. doi:10.1126/science.1098966
- Schneider, I., Kreis, J., Schweickert, A., Blum, M. and Vick, P. (2019). A dual function of FGF signaling in Xenopus left-right axis formation. *Development* **146**, dev173575. doi:10.1242/dev.173575
- Schulte-Merker, S. and Smith, J. C. (1995). Mesoderm formation in response to Brachyury requires FGF signalling. *Curr. Biol.* **5**, 62-67. doi:10.1016/S0960-9822(95)00017-0
- Session, A. M., Uno, Y., Kwon, T., Chapman, J. A., Toyoda, A., Takahashi, S., Fukui, A., Hikosaka, A., Suzuki, A., Kondo, M. et al. (2016). Genome evolution in the allotetraploid frog *Xenopus laevis*. *Nature* **538**, 336-343. doi:10.1038/nature19840
- Shi, D.-L., Bourdelas, A., Umbhauer, M. and Boucaut, J.-C. (2002). Zygotic Wnt/β-catenin signaling preferentially regulates the expression of Myf5 gene in the mesoderm of *Xenopus*. *Dev. Biol.* **245**, 124-135. doi:10.1006/dbio.2002.0633
- Sigismund, S., Confalonieri, S., Ciliberto, A., Polo, S., Scita, G. and Di Fiore, P. P. (2012). Endocytosis and signaling: cell logistics shape the eukaryotic cell plan. *Physiol. Rev.* **92**, 273-366. doi:10.1152/physrev.00005.2011
- Sive, H. L., Grainger, R. M. and Harland, R. M. (2000). *Early Development of Xenopus Laevis*. CSHL Press.
- Smith, W. C. and Harland, R. M. (1991). Injected Xwn1-8 RNA acts early in *Xenopus* embryos to promote formation of a vegetal dorsalizing center. *Cell* **67**, 753-765. doi:10.1016/0092-8674(91)90070-F
- Smith, W. C., McKendry, R., Ribisi, S. and Harland, R. M. (1995). A nodal-related gene defines a physical and functional domain within the Spemann organizer. *Cell* **82**, 37-46. doi:10.1016/0092-8674(95)90050-0
- Sokol, S., Christian, J. L., Moon, R. T. and Melton, D. A. (1991). Injected Wnt RNA induces a complete body axis in *Xenopus* embryos. *Cell* **67**, 741-752. doi:10.1016/0092-8674(91)90069-B
- Stenmark, H. (2009). Rab GTPases as coordinators of vesicle traffic. *Nature Publishing Group* **10**, 513-525. doi:10.1038/nm2728
- Stubbs, J. L., Oishi, I., Izpisua-Belmonte, J. C. and Kintner, C. (2008). The forkhead protein Foxj1 specifies node-like cilia in *Xenopus* and zebrafish embryos. *Nat. Genet.* **40**, 1454-1460. doi:10.1038/ng.267
- Tada, M. and Smith, J. C. (2000). Xwn11 is a target of *Xenopus* Brachyury: regulation of gastrulation movements via Dishevelled, but not through the canonical Wnt pathway. *Development* **127**, 2227-2238. doi:10.1242/dev.127.10.2227
- Taelman, V. F., Dobrowolski, R., Plouhinec, J.-L., Fuentealba, L. C., Vorwald, P. P., Gumper, I., Sabatini, D. D. and De Robertis, E. M. (2010). Wnt signaling requires sequestration of glycogen synthase kinase 3 inside multivesicular endosomes. *Cell* **143**, 1138-1148. doi:10.1016/j.cell.2010.11.034
- Teis, D., Wunderlich, W. and Huber, L. A. (2002). Localization of the MP1-MAPK scaffold complex to endosomes is mediated by p14 and required for signal transduction. *Dev. Cell* **3**, 803-814. doi:10.1016/S1534-5807(02)00364-7
- Vick, P., Kreis, J., Schneider, I., Tingler, M., Getwan, M., Thumberger, T., Beyer, T., Schweickert, A. and Blum, M. (2018). An early function of polycystin-2 for left-right organizer induction in *Xenopus*. *iScience* **2**, 76-85. doi:10.1016/j.isci.2018.03.011
- Villanueva, S., Glavic, A., Ruiz, P. and Mayor, R. (2002). Posteriorization by FGF, Wnt, and retinoic acid is required for neural crest induction. *Dev. Biol.* **241**, 289-301. doi:10.1006/dbio.2001.0485
- Vinyoles, M., Del Valle-Pérez, B., Curto, J., Viñas-Castells, R., Alba-Castellón, L., García de Herreros, A. and Duñach, M. (2014). Multivesicular GSK3 sequestration upon Wnt signaling is controlled by p120-catenin/cadherin interaction with LRP5/6. *Mol. Cell* **53**, 444-457. doi:10.1016/j.molcel.2013.12.010
- Vogel, A., Rodríguez, C. and Izpisua Belmonte, J. C. (1996). Involvement of FGF-8 in initiation, outgrowth and patterning of the vertebrate limb. *Development* **122**, 1737-1750. doi:10.1242/dev.122.6.1737
- Vonica, A. and Gumbiner, B. M. (2002). Zygotic Wnt activity is required for Brachyury expression in the early *Xenopus laevis* embryo. *Dev. Biol.* **250**, 112-127. doi:10.1006/dbio.2002.0786
- Walentek, P., Schneider, I., Schweickert, A. and Blum, M. (2013). Wnt11b is involved in cilia-mediated symmetry breakage during *Xenopus* left-right development. *PLoS ONE* **8**, e73646-e9. doi:10.1371/journal.pone.0073646
- Wessely, O. and Tran, U. (2011). *Xenopus* pronephros development—past, present, and future. *Pediatr. Nephrol.* **26**, 1545-1551. doi:10.1007/s00467-011-1881-2
- Yang, Y. and Niswander, L. (1995). Interaction between the signaling molecules WNT7a and SHH during vertebrate limb development: dorsal signals regulate anteroposterior patterning. *Cell* **80**, 939-947. doi:10.1016/0092-8674(95)90297-X
- Yokota, C., Mukasa, T., Higashi, M., Odaka, A., Muroya, K., Uchiyama, H., Eto, Y., Asashima, M. and Momoi, T. (1995). Activin induces the expression of the *Xenopus* homolog of sonic hedgehog during mesoderm formation in *Xenopus* explants. *Biochem. Biophys. Res. Commun.* **207**, 1-7. doi:10.1006/bbrc.1995.1144
- Yokota, C., Kofron, M., Zuck, M., Houston, D. W., Isaacs, H., Asashima, M., Wylie, C. C. and Heasman, J. (2003). A novel role for a nodal-related protein: Xnr3 regulates convergent extension movements via the FGF receptor. *Development* **130**, 2199-2212. doi:10.1242/dev.00434
- Zhang, B., Tran, U. and Wessely, O. (2011). Expression of Wnt signaling components during *Xenopus* pronephros development. *PLoS ONE* **6**, e26533. doi:10.1371/journal.pone.0026533

Biology Open (2021); doi:10.1242/bio.056887; Supplementary information

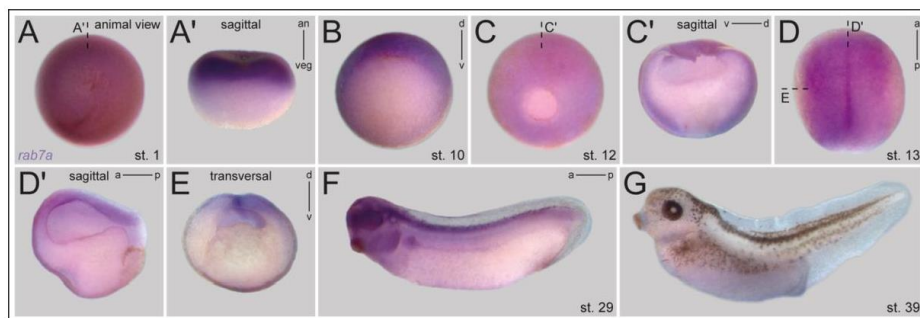


Fig. S1. *rab7* exhibits dynamic expression pattern.

(A) *rab7* expression in animal hemisphere of st. 1 embryo, (A') sagittal section of (A). (B,C) Early and late gastrula stages displayed transcripts in deep mesoderm, (C') sagittal section of (C). (D) Onset of neurulation with *rab7* restricted to neural plate and notochord, (D') sagittal section of (D), (E) transversal section as indicated in (D). (F,G) Tailbud stage expression in the notochord, trunk neural crest, eyes, pronephric and head tissues and in dorsal fin mesenchyme. a, anterior; an, animal; d, dorsal; p, posterior; st., stage; v, ventral; veg, vegetal.

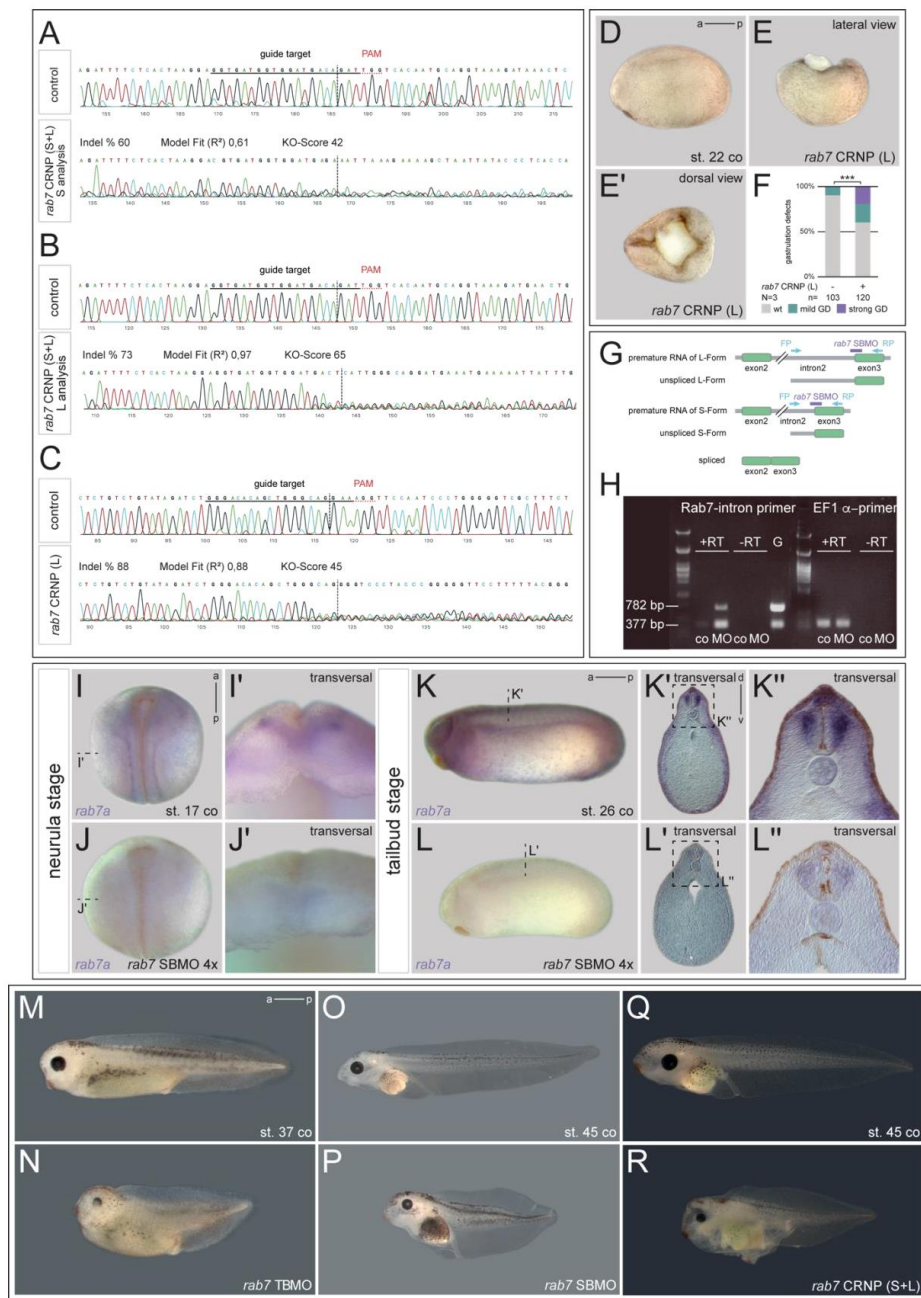


Fig. S2. Loss of *rab7* caused gastrulation and axis elongation defects.

(A-C) Synthego ICE CRISPR analysis of *rab7* sgRNAs targeting both S and L alleles or L alone. (D) Wildtype control embryo compared to lateral view of *rab7* CRNP (E) treated specimen with severe gastrulation defects, (E') dorsal view. (F) Quantification of results in (D-E). (G) Scheme of binding sites of *rab7* SBMO targeting both homeologs. (H) RT-PCR of knockdown by *rab7* SBMO

Biology Open (2021); doi:10.1242/bio.056887; Supplementary information

demonstrated successful inhibition of splicing. (I,K) Wildtype neurula and tailbud control specimen with stage specific *rab7* transcripts, (I',K') transversal sections of (I,K), (K'') blow-up of (K'). (J,L) Radial knockdown of *rab7* by SBMO caused significant reduction of *rab7* expression in neurula and tailbud stages, respectively, (J',L') transversal sections of (J,L), (L'') blow-up of (L'). (M,O,Q) Untreated control tadpoles and (N,P,R) milder affected morphant embryos, suffering from AP-axis defects, knockdown was induced using (N) *rab7* TBMO, (P) *rab7* SBMO and (R) *rab7* CRNP (S+L). a, anterior; an, animal; co, control; CRNP, Cas9 Ribonucleoprotein; d, dorsal; EF1 α , Elongation factor 1 alpha; FP, forward primer; G, genomic DNA; GD, gastrulation defect; p, posterior; RP, reverse primer; RT, reverse transcriptase; st., stage; v, ventral; veg, vegetal; wt, wildtype.

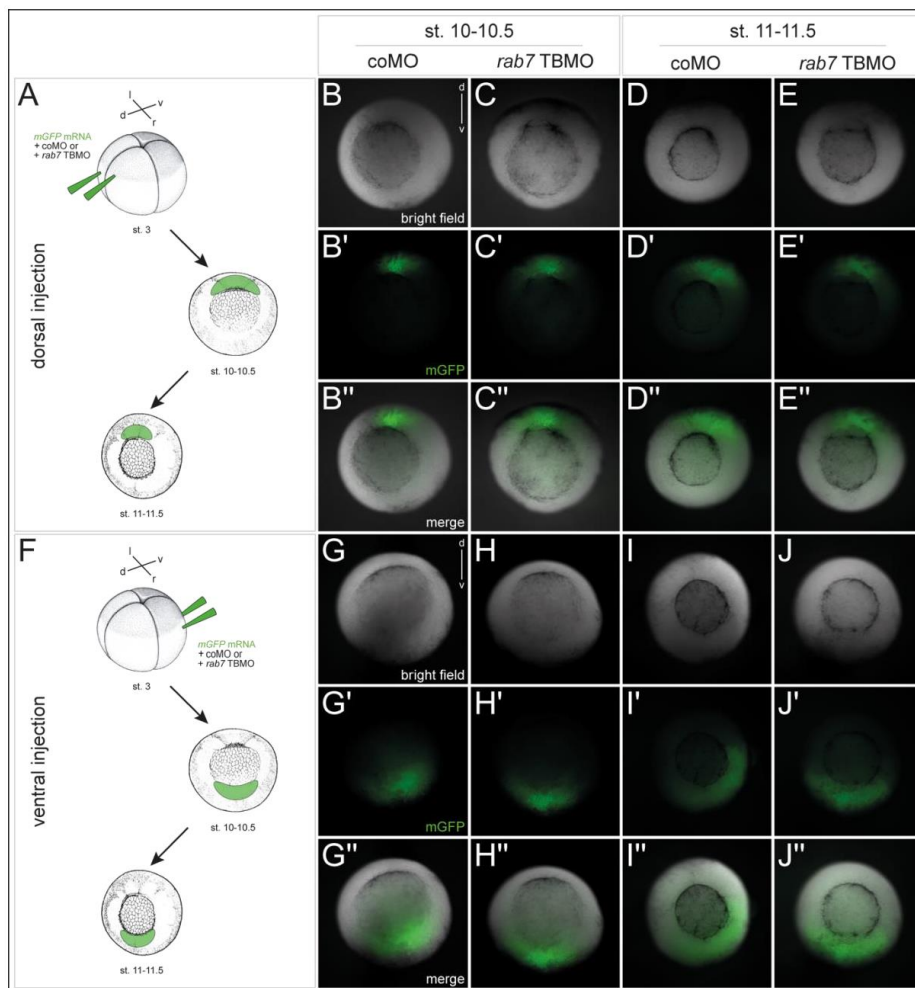


Fig. S3. Lineage-specific knockdown of *rab7* in the dorsal or ventral mesoderm.

(A,F) Lineage tracing scheme of injection site (dorsal or ventral) in st. 3 embryos; tested st. 10-10.5 illustrates observed localization of injected material at correct target side (dorsal or ventral), and approximately one stage later before fixation (for late gastrula analyses). *mGFP* mRNA lineage tracer was co-injected with coMO (B,D,G,I) or *rab7* TBMO (C,E,H,J), correct targeting and corresponding phenotypes visualized via fluorescent mGFP (B'-E',G'-J'), brightfield (B-E,G-J) and merged channels (B''-E'',G''-J''). coMO injected specimen depicted normal gastrulation at st. 10-10.5 and 11-11.5, both, when injected dorsally (B,D) or ventrally (G,I). (C,E) Impaired dorsal lip formation of *rab7* morphant embryos at onset of gastrulation, with increasing severeness during gastrulation. (H) Ventral injected specimen did not show altered tissue at st. 10-10.5, (J) impaired lip formation at later gastrula stages with diffuse appearance of ventral lip.

coMO, control Morpholino Oligonucleotide; d, dorsal; p, posterior; st., stage; TBMO, translation blocking Morpholino Oligonucleotide; v, ventral; veg, vegetal.

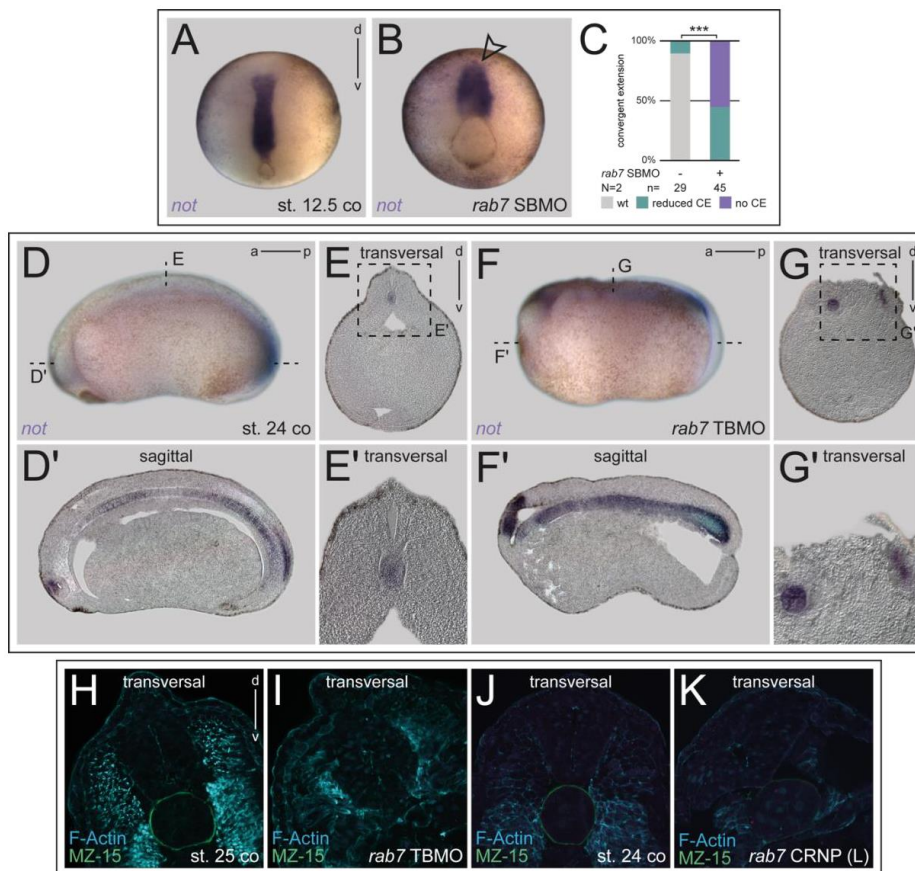


Fig. S4. *rab7*-deficient embryos develop axial elongation defects and impaired notochord morphogenesis.

(A) Elongated notochords of control embryos highlighted by *not* expression (B) in comparison to dorsal *rab7* SBMO injection, which resulted in reduced notochord elongation (arrowhead). (C) Quantification of results in (A-B). (D) Tailbud stage embryos revealed *not* expression throughout the notochord, (D') also shown in sagittal and (E) transversal section and (E') blow-up of (E). (F) *rab7* knockdown in dorsal lineage did not reduce *not* expression, (F') but affected notochord morphogenesis depicted in thicker notochord as shown in sagittal section. (G) Transversal sections revealed some morphant specimen also developed split notochords, (G') blow-up highlighting open dorsal tissue. (H-K) Transversal sections of st. 24/25 embryos stained for F-Actin (blue) and MZ-15 (green). (H,J) control specimen displayed wildtype outer sheets of notochords (green), (I) MZ-15 staining was absent in *rab7* TBMO injected or (K) reduced in *rab7* CRNP treated embryos. a, anterior; CE, convergent extension; co, control; CRNP, Cas9 Ribonucleoprotein; d, dorsal; n.s., not significant; p, posterior; st., stage; v, ventral; wt, wildtype.

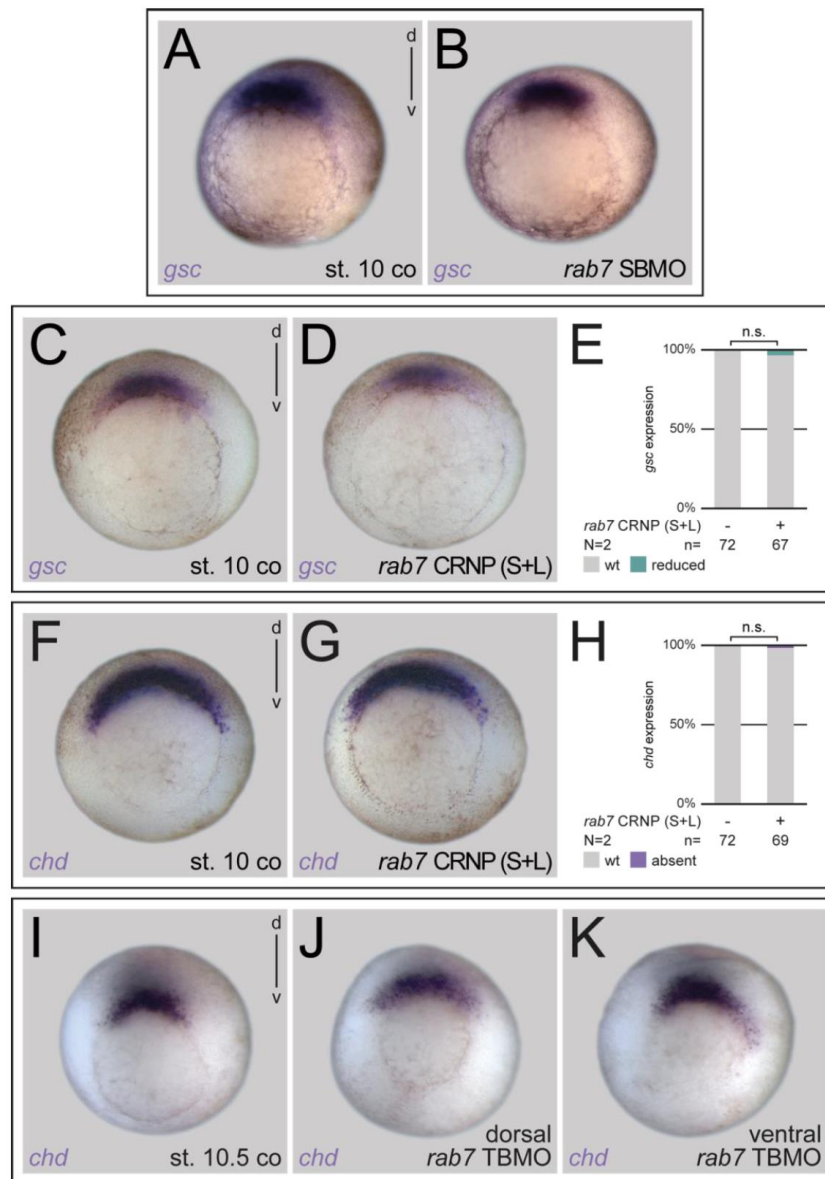


Fig. S5. Loss of Rab7 does not impact organizer gene expression or DV patterning. (A,C) St. 10.5 untreated controls showing wildtype *gsc* expression (B,D) comparable to embryos either injected with *rab7* SBMO or *rab7* CRNP (S+L). (E) Quantification of results in (C-D). (F) Wildtype *chd* expression in control embryos were unaffected in embryos injected with (G) *rab7* CRNP (S+L). (H) Quantification of results in (F-G). (I) DV range of *chd* expression of control embryos was unaltered in embryos injected with *rab7* TBMO in (J) dorsal or (K) ventral lineage. co, control; CRNP, Cas9 Ribonucleoprotein; d, dorsal; n.s., not significant; v, ventral; wt, wildtype.

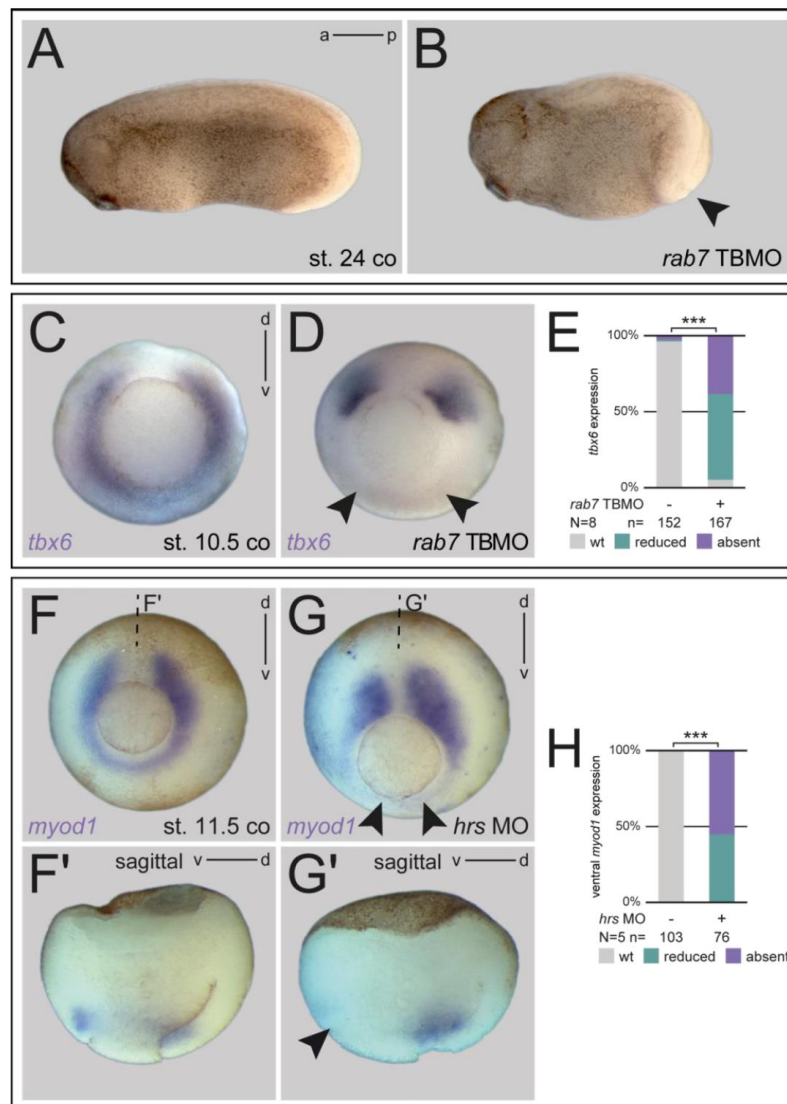


Fig. S6. A Specification of the ventro-lateral mesoderm requires proper Rab7 function and *hrs* knockdown in the ventral mesoderm phenocopies loss of *rab7*.

(A) Untreated specimens with normal tail development. (B) Impaired posterior development after loss of *rab7* in ventral lineage (black arrowhead). (C) Control embryo depicting wildtype *tbx6* expression, (D) ventral *rab7* knockdown inhibited *tbx6* expression (black arrowheads). (E) Quantification of results in (C-D). (F) Wildtype *myod1* expression in control specimen, (F') sagittal section of (F) showing ventral expression. (G) Ventral injection of *hrs* MO (0,8-1 pmol) caused loss of *myod1* (black arrowheads), (G') sagittal section as indicated in (G) with absent ventral expression (black arrowhead). (H) Quantification of results. a, anterior; co, control; d, dorsal; MO, morpholino oligonucleotide; p, posterior; st., stage; v, ventral; wt, wildtype.

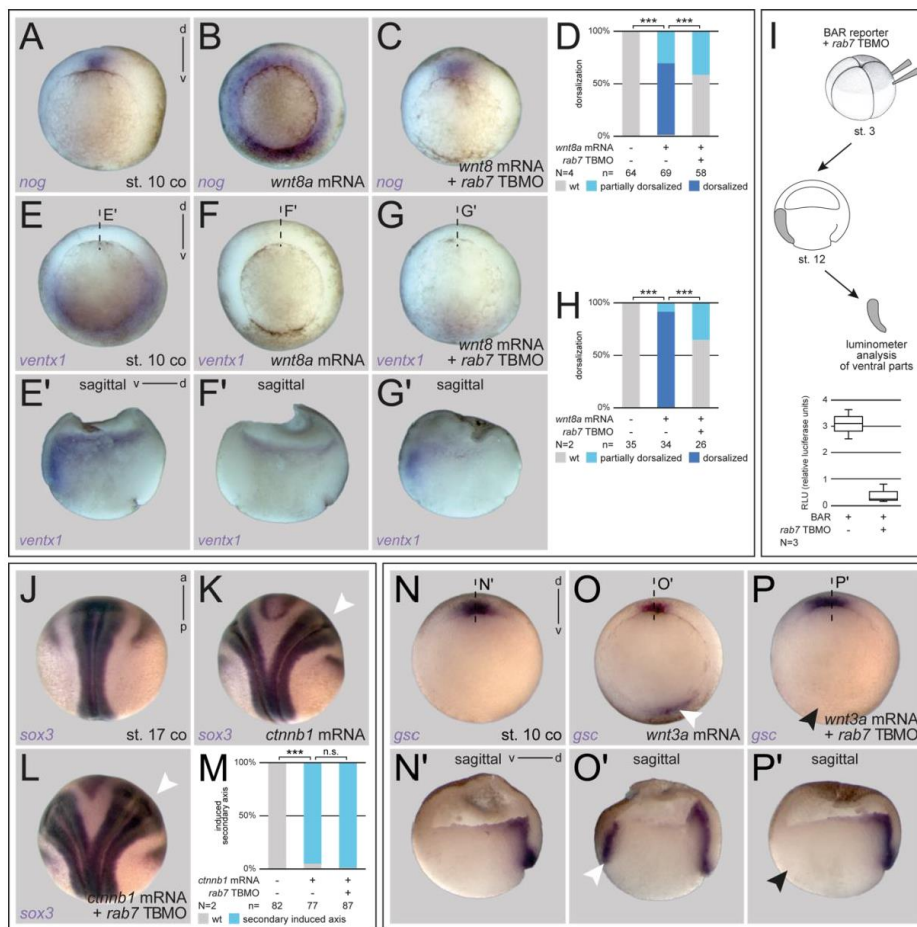


Fig. S7 Rab7 is required for exogenous activation of canonical Wnt pathway.

(A) Wildtype dorsal expression of *nog* in st. 10 embryos in comparison to specimen with (B) radial injected *wnt8a* mRNA showing complete dorsalization by extended *nog* expression around the blastopore. (C) Co-injection of *rab7* TBMO restricted *nog* expression to normal wildtype area again. (D) Quantification of results in (A-C). (E) Wildtype ventral expression of *ventx1* in st. 10 embryos, (E') sagittal section as indicated in (E) showing *ventx1* expression domain. (F) Loss of *ventx1* expression upon radial *wnt8a* mRNA injection, (F') highlighted in bisected embryo. (G) Co-injection of *rab7* TBMO partially restored lost *ventx1* expression, (G') which in the sagittal section remained smaller and weaker on ventral side. (H) Quantification of results in (E-G). Please note premature (st. 10) appearance of fully radial lips in (B,F) but not in (A,C,E,G) in same age specimens. (I) Late gastrula Luciferase-based BAR-reporter assay (bottom) demonstrating tissue-specific inhibition of endogenously induced Wnt reporter activity in the ventral mesoderm (middle) after co-injection of *rab7* TBMO into the ventral mesodermal lineage at 4-cell stage (top). (J) Wildtype AP axis in control specimen. (K) *ctnnb1* induced right-sided secondary axis (white arrowhead), (L) which was not inhibited by *rab7* knockdown (white arrowhead). (J-L) Axes highlighted by *sox3* expression. (M) Quantification of results in (J-L). (N) Control embryos showing normal dorsal *gsc* expression, (N')

Biology Open (2021); doi:10.1242/bio.056887; Supplementary information

confirmed in sagittal section indicated in (N). (O) Ventral *wnt3a* mRNA injection induced second organizer marked by *gsc* (white arrowhead), (O') sagittal section revealed additional ventral *gsc* positive domain (white arrowhead). (P) Lost second *gsc* expression upon parallel *rab7* TBMO injection (black arrowhead), (P') highlighted in sagittal section (black arrowhead). a, anterior; co, control; d, dorsal; n.s., not significant; p, posterior; v, ventral; wt, wildtype.

Research chapter II:

Rab7-mediated intracellular FGF signal transduction

The late endosomal regulator Rab7 is required for FGF-dependent mesoderm specification by regulating Ras-mediated MAPK activation

Abstract

Gastrulation denotes an important developmental step, as this process includes great structural tissue rearrangements and patterning events shaping the emerging organism. Specification of the mesoderm at the onset of gastrulation involves a variety of signaling pathways and further patterning demands subtle regulation among these. Endocytosis and the endosomal machinery offer manifold platforms for intracellular pathway regulation, and especially LEs claim increasing attention. LE-associated Rab7 has been linked to mesoderm specification and patterning during gastrulation, as a positive regulator of canonical Wnt signaling. Distinct axial defects due to compromised dorsal mesoderm development in *rab7*-deficient *Xenopus laevis* embryos suggested an additional requirement of Rab7 for FGF/MAPK signaling. Here, we specifically addressed such a role of Rab7 by using different FGF/MAPK pathway components. We suggest a hierarchical placement of Rab7 upstream of MAPK dependent activation of the transcription factor Ets2, most likely at the level of the small GTPase Ras. Visualization of intracellular Ras relocalization upon FGF receptor activation supported a requirement of Rab7 in this process. Thus, this study affords an insight on how the Rab7-regulated endosomal machinery could participate in FGF/MAPK signal transduction to enable correct dorsal mesoderm specification.

Introduction

Mesoderm development involves a variety of well-orchestrated signaling events at multiple levels. After mesoderm induction, patterning of the newly formed germ layer takes place. Initial identity of dorsal mesoderm depends on Wnt signaling (Moon, 2005), specification of ventrolateral mesoderm however is mediated by signals of BMP and Wnt (Dale and Jones, 1999; Dosch et al., 1997; Hemmati-Brivanlou and Thomsen, 1995). At the onset of gastrulation, dorsal Wnt activity gets downregulated in the dorsal most mesoderm to allow FGF/MAPK-dependent dorsal axial and paraxial tissue development (Amaya et al., 1993; Dorey and Amaya, 2010; Glinka et al., 1997; Itoh and Sokol, 1999).

One way of regulating intracellular signal transduction is offered by endosomal membrane trafficking. For a long time, translocation of activated receptors from the plasma membrane through the endosomal system to their final degradation via lysosomes, was only considered in the context of signal termination (Platta and Stenmark, 2011). However, today's degree of knowledge understands individual endosomal compartments as potential or even crucial signaling platforms.

In case of proper MAPK signal activation LEs are assumed to be critical mediating platforms (Platta and Stenmark, 2011; Teis et al., 2002). Ligand binding following receptor activation results in recruitment of further pathway components in order to form a complex. Through endocytosis relocalization of the receptor complex to EEs is initiated. Furthermore, complex formation promotes transition of the membrane-anchored small GTPase Ras in its activated state. Interaction of Ras with the downstream kinase Raf/Map3k, enables the kinase to initiate the MAPK signaling cascade. In the course of early to late endosome maturation, the receptor complex accompanied by interacting Ras and Raf/Map3k persists on the vesicular membrane.

Recruitment of a scaffold complex consisting of Lamtor2/p14, Mp1 and Mek1 to these late endosomal membranes leads to the phosphorylation of Mek/Map2k by Raf/Map3k, which in turn phosphorylates Erk/Mapk (Morrison, 2012; Teis et al., 2002). This last kinase forms dimers and eventually enters the nucleus to ensure transcription of target genes by phosphorylating the transcription factor Ets2 (Fehrenbacher et al., 2009).

Trafficking within the endosomal system is regulated by a family of Rab proteins. Transient attachment of these small GTPases to their corresponding endosomal compartments orchestrates effector recruitment and provides membrane identity and functionality (Stenmark, 2009). The regulative function of LEs in terms of membrane trafficking is facilitated by Rab7. Interestingly, experimental examination of Rab7 null mice already demonstrated a specific role in mesoderm development. Knockout mice suffer from defective anteroposterior patterning paralleled by disruptive gastrulation leading to early embryonic death (Kawamura et al., 2012 and 2020).

Knockdown analyses of *rab7* in *Xenopus laevis* revealed similar results, as we demonstrated a role for Rab7 during gastrulation in regulating mesodermal specification (Kreis et al., 2021). Patterning of the ventrolateral marginal zone was linked to canonical Wnt signaling in a Rab7-dependent manner. However, the encountered dorsal phenotypes could not solely be linked to impaired Wnt signaling. Therefore, we hypothesized a function for Rab7 in other signaling pathways, specifically in terms of dorsal mesoderm development. The most auspicious candidate was FGF signaling, since the expression of several mesodermal genes requires MAPK signal transduction. Furthermore, *rab7*-deficient embryos developed an axial elongation phenotype reminiscent of tadpoles suffering from a FGF receptor loss-of-function (LOF) (Amaya et al., 1991 and 1993; Kreis et al., 2021).

Due to this, we focused on a potential role of Rab7 for FGF-dependent dorsal mesoderm specification in *Xenopus*. We found that Rab7 is required for Ets2-

dependent induction of mesodermal identity upstream of MAPK activation. Loss of *rab7* blocked dorsal mesodermal marker genes and inhibited downstream elongation of axial mesoderm in animal cap explants. Using FGF/MAPK pathway components in gain-of-function (GOF) analyses we concluded that Rab7 functions at the level or downstream of the GTPase Ras. Further, we demonstrate that loss of Rab7 interferes with FGF-induced translocation of endogenous Ras from the plasma membrane to intracellular vesicular membranes, suggesting a Rab7-dependent membrane trafficking mechanism required for MAPK activation.

Results

Ets2 or activated Erk/Mapk1 rescues mesodermal identity in *rab7* morphants

We previously showed that depletion of *rab7* via a translation blocking Morpholino oligomere (TBMO) in *Xenopus* embryos resulted in mesodermal patterning defects which were reminiscent of a loss of FGF signaling. Such embryos developed severe gastrulation defects (GDs) and failed to elongate their anteroposterior axis compared to their wildtype siblings (Figure 1A, B, D). To test our hypothesis that FGF signaling contributes to the observed phenotype, rescue experiments with the downstream transcription factor Ets2 were conducted in a dorsal *rab7* LOF setting. Although, survival rates in tailbud stage morphants were low, introduction of *ets2* mRNA was able to partially rescue the GDs, but failed in restoring the elongation of the body axis (Figure 1C, D).

Hence, the rescue capacity of *ets2* was evaluated in the context of mesodermal marker genes during gastrulation. First, specificity of *ets2* was substantiated by dorsal *ets2* misexpression followed by a mesodermal marker analysis of *tbxt* and *myogenic differentiation 1 (myod1)*, which encode for two transcription factors mediating mesodermal and somitic identity. Misexpression resulted in an ectopic *myod1* activation within the more anterior midline region of gastrulae, recapitulating recently reported findings (Supplement Figure 1A-C; Kjolby et al., 2019). Expression of *tbxt* and *myod1* were severely diminished in *rab7* morphants (Figure 1F, H; Supplement Figure 1E, G), but *ets2* was sufficient to compensate for the *rab7* deficiency and partially restored expression of both factors (Figure 1G, H; Supplement Figure 1F, G). Again, an expansion of the *myod1* expression domain in the anterior midline of rescued embryos was detectable (Supplement Figure 1F).

Activation of Ets2 is mediated through phosphorylation by the upstream kinase Erk/Mapk1. To further confirm the functional requirement of Rab7 for MAPK-dependent induction of mesodermal identity, rescue experiments with a stabilized Erk/Mapk1 kinase were performed in the same experimental setting as before. *erk/mapk1* mirrored the competence of *ets2* to compensate for the marked reduction of *tbxt* and *myod1* transcripts after dorsal *rab7* LOF (Figure 1I-L; Supplement Figure 1H-K).

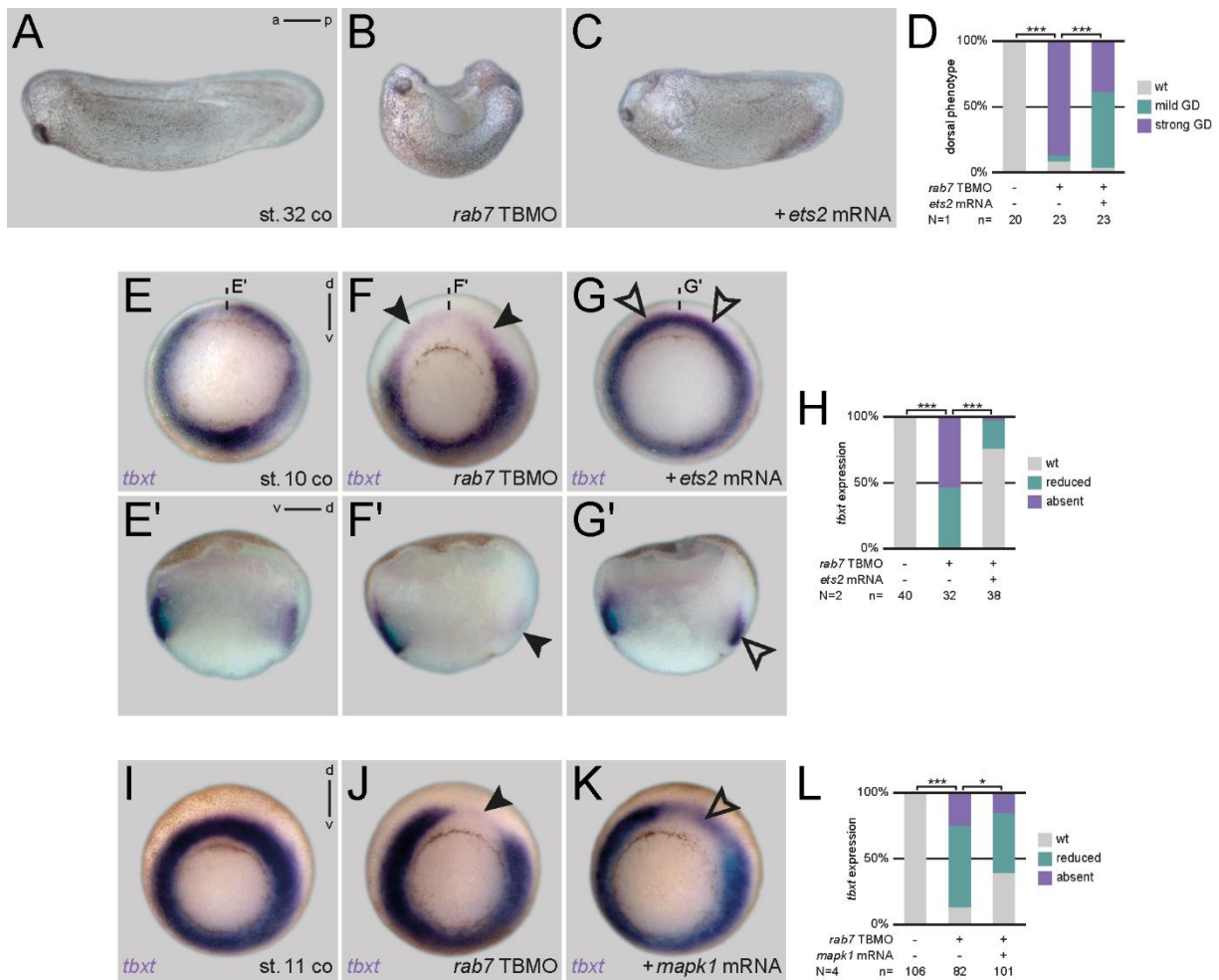
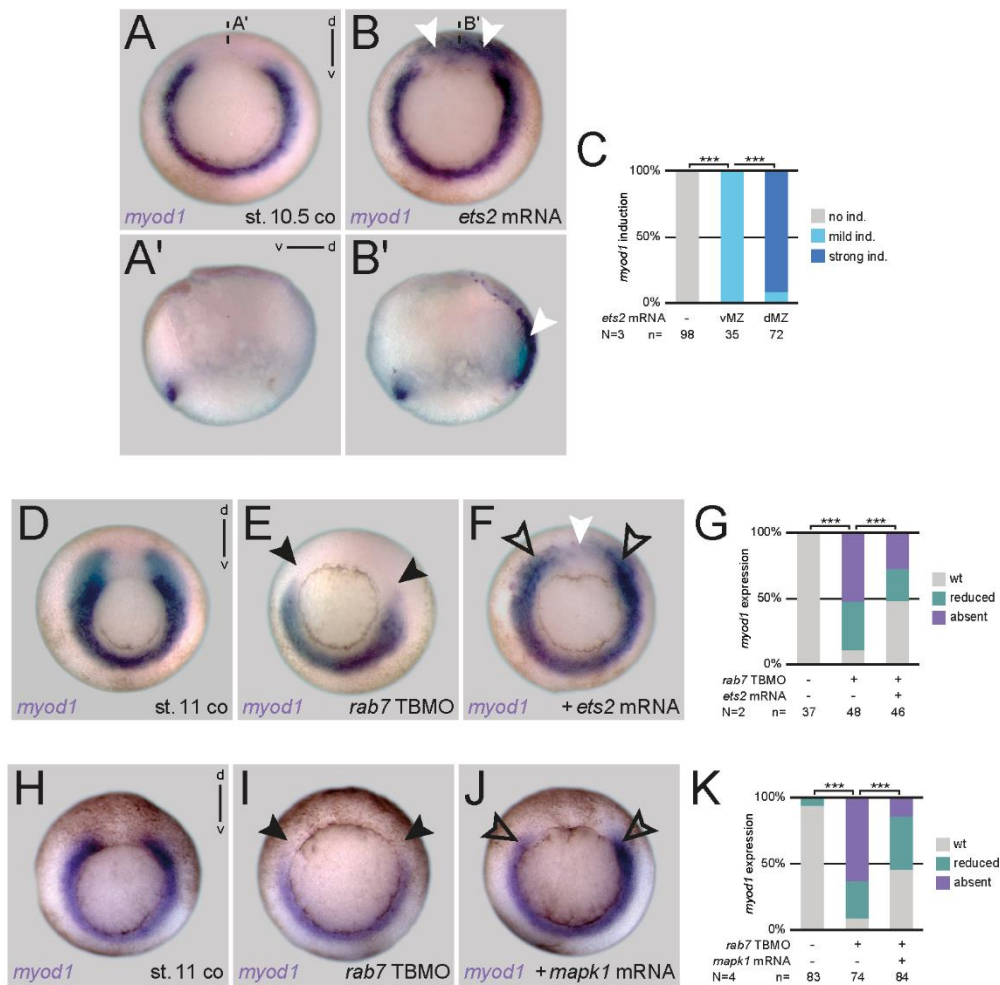


Figure 1: Downstream FGF pathway components rescued GDs and pan-mesoderm marker *tbxt*.

(A, B, D) *Xenopus* st. 32 tadpoles suffering from axial elongation and GDs due to dorsal *rab7* deficiency compared to untreated siblings. (C) Severe manifestation of GDs attenuated by coinjection of *ets2* mRNA. (D) Quantification of dorsal phenotype. (E) Uniform circular appearance of *tbxt* expression of st. 10 *Xenopus* embryos (F) faded due to dorsal knockdown of *rab7* (black arrows). (G) Rescue injection of *ets2* mRNA restored expression almost back to wildtype level (outlined black arrows). (E'-G') Panels beneath depict corresponding sagittal sections. (H) Quantification of *tbxt* expression rescued by *ets2* mRNA. (I) Circular *tbxt* expression of st. 11 specimen (J) faded upon dorsal *rab7* LOF (black arrow). (K) Coinjection of *erk/mapk1* mRNA in morphant embryos partially restored lost dorsal *tbxt* expression (black outlined arrow). (L) Quantification of *tbxt* expression rescued by *erk/mapk1* mRNA.



Supplement Figure 1: Downstream FGF pathway components rescued paraxial *myod1* expression.

(A) Dorsal gap of wildtype *myod1* expression of st. 10.5 embryos (B) depicted ectopic *myod1* induction upon *ets2* mRNA overexpression (white arrows), (A', B') clarified in sagittal sections respectively. (C) Quantification of dorsal *myod1* induction. (D) *myod1* horseshoe-shaped expression of st. 10 specimen (E) displayed downregulated paraxial transcripts after dorsal loss of *rab7* (black arrows). (F) *ets2* mRNA injected dorsally rescued the paraxial mesoderm identity (outlined black arrows), moreover a gained expression pattern in animal areas above the dorsal gap was observed (white arrow). (G) Quantification of *myod1* expression rescued by *ets2* mRNA. (H) Horseshoe *myod1* expression of st. 11 specimen (I) faded upon dorsal *rab7* LOF (black arrows). (J) Coinjection of *erk/mapk1* mRNA in morphant embryos partially restored lost dorsal *myod1* expression (black outlined arrows). (K) Quantification of *myod1* expression rescued by *erk/mapk1* mRNA.

Rab7 acts upstream of Erk/Mapk1 within the FGF signaling pathway

The previous collected data implied a hierarchical placement of Rab7 in the MAPK signaling cascade upstream of Erk/Mapk1. Interestingly, ligand free FGF pathway activation due to cellular remodeling events occurs in the posterior neural plate of late gastrulae/early neurulae (Kinoshita et al., 2020). Since Rab7 is required for MAPK-dependent mesoderm patterning and presumably morphogenetic processes, putatively downstream of FGF receptor activation, neural plates were investigated (Figure 2A) in *rab7*-depleted embryos. As pathway activity is mediated by phosphorylated Erk/Mapk (pErk/pMapk1), immunofluorescence intensity of pErk/pMapk1 was evaluated in a Rab7-dependent manner to confirm its upstream requirement of Erk/Mapk1 (Figure 2B-D). The amount of nuclear and cellular pErk/pMapk1 of neural plate cells decreases via *rab7* knockdown compared to wildtype siblings (Figure 2B, C, D). These results underline the role of Rab7 in FGF/MAPK-related patterning events and morphogenetic cell movements in the dorsal mesoderm upstream of Erk/Mapk1.

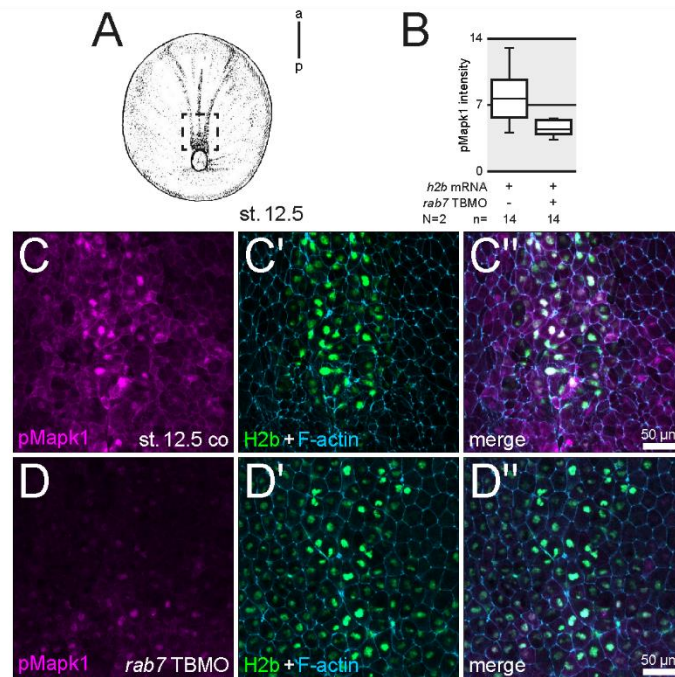


Figure 2: Rab7 acts upstream of Erk/Mapk1 activation.

(A) Localization of the imaged tissue of st. 12.5 embryos and (B) intensity quantification of pErk/pMapk1 signal. (C, C'') Nucleic and cytosolic accumulation of pErk/pMapk1 (magenta) at posterior neural plate of wildtype specimen. (D, D'') Downregulation of pErk/pMapk1 signal intensity in *rab7*-morphant neural plates. (C', D') For lineage tracing and nuclear staining coinjection of *h2b* RNA (green) was performed, cell borders are highlighted by F-actin (blue).

Rab7 is required for FGF-dependent dorsal mesoderm induction and axial elongation

Specification of the dorsal mesoderm in the endogenous setting is not interpretable in a Wnt-independent manner. In order to test Rab7 function in a setup without potential crosstalk of the Wnt signaling pathway, an assay based on artificial mesoderm/organizer induction in animal caps was utilized (Kurth and Hausen, 2000). Late blastula/early gastrula animal caps lack Wnt signaling activity, but exhibit FGF pathway activity (Kurth and Hausen, 2000; Slack et al., 1990), therefore providing an appropriate tissue for more precise examinations. Mesodermal organizer-like tissue was induced by a single injection of *nodal homolog 1 (nodal1)* mRNA into the animal hemisphere of early embryos (Figure 3A, B, D). Concomitant with endogenous organizer induction and dorsal lip formation, injected cells condensed pigment at the injection site, mimicking bottle cell formation, while surrounding cells ectopically expressed *tbxt*, as previously described (Figure 3B, D; Kurth and Hausen, 2000). Both, artificial bottle cell formation as well as circular expression of *tbxt* failed to emerge in the *rab7* LOF situation (Figure 3B, E). A similar outcome was observed, when artificial organizers were induced via constitutive active *smad family member 2 (smad2)*, excluding a potential upstream effect of LE-related Rab7 on Nodal1/TGF- β signal transduction itself (Supplement Figure 2A-D). Blocked circular *tbxt* expression and pigment condensation of artificial organizers in *rab7*-morphant caps revealed a participation of this small GTPase for general mesoderm specification, most likely in a FGF-dependent fashion. Importantly, equivalent results were achieved when a dominant negative FGF receptor (*dn-fgfr*) was utilized to counteract mesoderm induction (Figure 3B, F), thus strongly supporting the hypothesis of a Rab7-specific function in the FGF signaling pathway during mesodermal induction/maintenance.

Results of a second animal cap assay, moreover depicting elongation processes, underlined these findings. In terms of dorsal mesoderm behavior, this assay could state an involvement of Rab7 for such processes, too. Animal caps of either wildtype or *rab7*-morphant stage 9 embryos were dissected and subsequently incubated with or without Activin (Figure 3G). Induced elongation of animal caps via Activin treatment, resembled the convergent extension movement of the endogenous dorsal marginal zone during gastrulation and the ring-shaped *tbxt* expression encircling the artificial organizers (Figure 3H, J; Symes and Smith, 1987), whereas untreated caps merely formed roundish tissue (Figure 3H, I). Loss of *rab7* severely diminished elongation of animal caps (Figure 3H, L), thereby recapitulating the observed *in vivo* situation of impaired axial elongation upon *rab7* deficiency (Figure 1B).

Taken together, both assays suggest a role for Rab7 in mesoderm specification and furthermore an involvement in dorsal mesoderm rearrangements by facilitating FGF signaling in both processes.

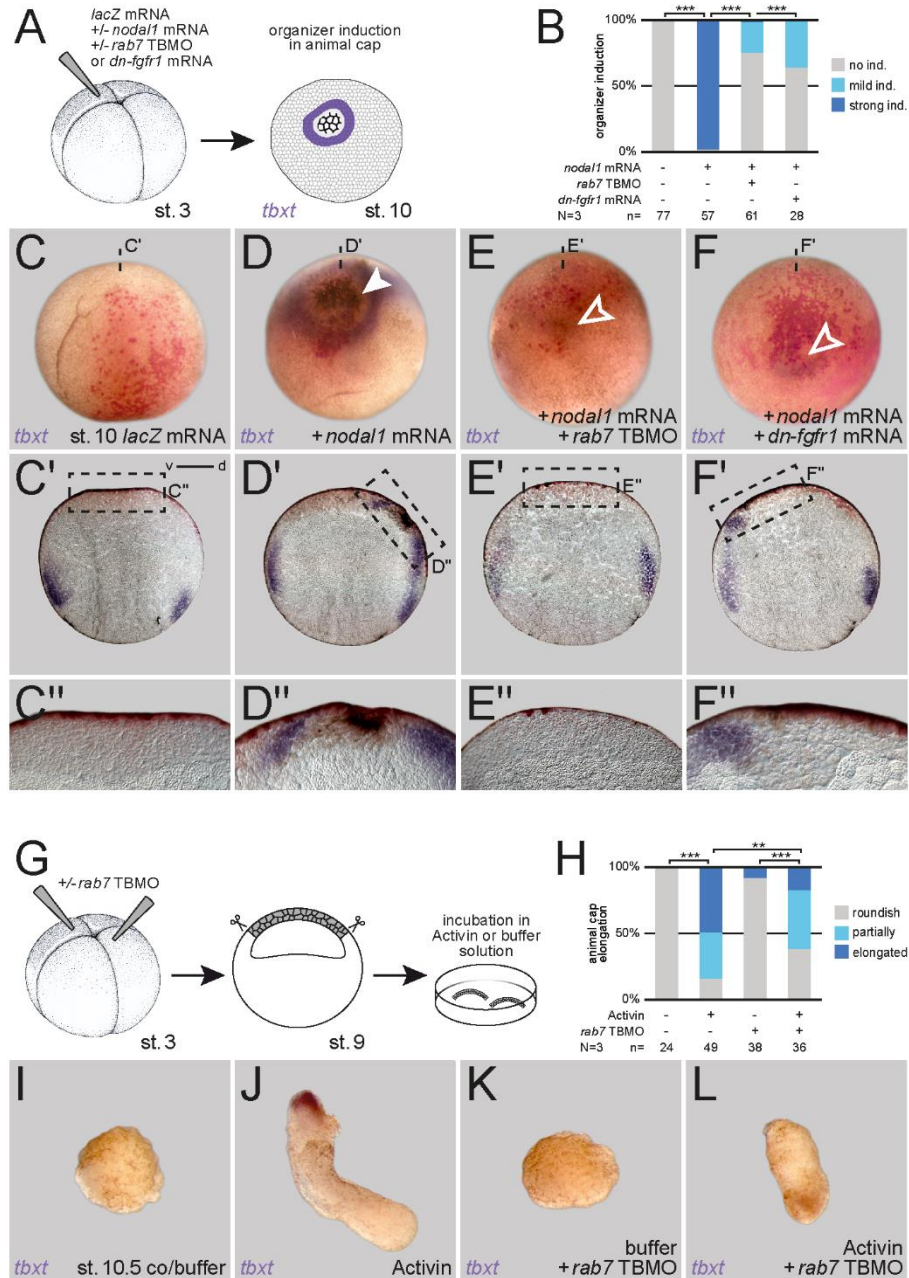
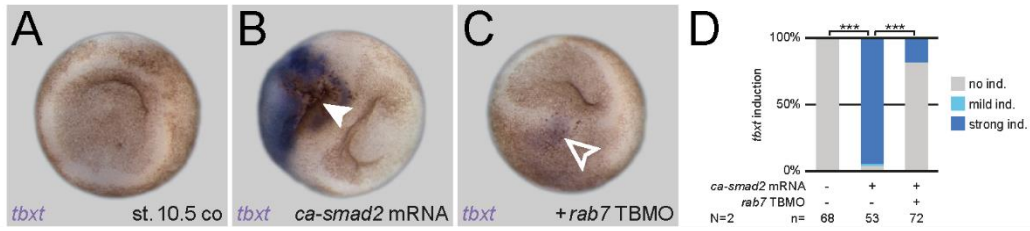


Figure 3: Dorsal mesoderm induction and axial elongation depends on Rab7.

(A) Experimental setup of artificial organizer induction in animal caps. (B) Quantification of induced artificial organizers in animal caps. (C) Wildtype animal caps of st. 10 embryos. (D) *nodal1* mRNA injection induced pigment accumulation, indicating organizer induction (white arrow), induction site is spheroid by *tbxt* expression. (E, F) Coinjection of either *rab7* TBMO or *dn-fgfr1* mRNA resulted in artificial organizer inhibition (outlined white arrows) and blocked *tbxt* expression in animal caps. (C'-F') Panels beneath show half sections of treated tissues and (C''-F'') zoom-ins of potential organizer induction sites, respectively. (C-F) For lineage tracing *lacZ* staining was used. (G) Experimental setup of animal cap elongation assay. (H) Quantification of animal cap elongation. (I) Untreated animal caps dissected of st. 10.5 embryos (J) elongated upon Activin treatment. (K) *rab7*-deficient, untreated animal caps remained in a roundish shape, (L) treated ones depicted partial or complete inhibition of elongation. (J) *tbxt* expression was only observed in Activin treated, elongated caps.



Supplement Figure 2: Rab7 is required for mesoderm induction downstream of TGF-β signaling.

(A) Uniform animal caps of st. 10.5 specimen (B) exhibited artificial organizer and *tbxt* induction upon *ca-smad2* mRNA injection (white arrow). (C) Induction was blocked in *rab7*-morphant animal caps. (D) Quantification of *tbxt* induction.

Loss of Rab7 blocks FGF-induced mesodermal identity at the level of Ras activation

Rab7 seems to act upstream of Erk/Mapk1, since mesodermal marker gene expression was restored in rescue experiments (Figure 1I-L; Supplement Figure 1H-K) and pErk/pMapk1 levels were strongly reduced in *rab7* morphants (Figure 2B-D). Therefore, FGF pathway components in the receptor's vicinity were utilized to narrow down the hierarchical localization of this small GTPase within FGF-activated MAPK signaling. Mesodermal tissue was induced in animal caps of 4-cell stage embryos via the FGF ligand Fgf8 or constitutively active viral Ras (vRas) (Figure 4B, D, F, H), a membrane-associated GTPase known to interact with activated receptor complexes (Jiang and Sorkin, 2002). Exogenous induction of mesoderm was traced by *tbxt* expression in animal caps of gastrulating specimens (Figure 4B, D, F, H; Whitman and Melton, 1992). Intriguingly, in both cases parallel repression of *rab7* efficiently prevented mesoderm induction (Figure 4C, D, G, H), supporting the conclusion that Rab7 acts downstream of FGF ligands and intracellular Ras to mediate MAPK activation in the mesoderm.

Rab7 participates in FGF-induced Ras translocation *in vivo*

The previous analyses of the small GTPase Rab7 enclosed its potential function at the level or downstream of Ras and upstream of Erk/Mapk1 (Figure 1I-L; Supplement Figure 1H-K; Figure 4A-H). As it was shown that some pools of Ras relocate from the plasma membrane to endosomes during activation (Jiang and Sorkin, 2002; Teis et al., 2002), a potential Rab7-dependent subcellular shift of Ras was analyzed via immunofluorescence (Figure 4I). Intracellular distribution of Ras was evaluated in animal caps of gastrula stage embryos injected with membrane-anchored green fluorescent protein (mGFP) to highlight cell borders and membranes of intracellular

vesicular structures (Figure 4K-M). In untreated cells Ras localized mainly to cell borders and small vesicular structures (Figure 4J, K). Upon FGF pathway activation via a constitutively active Fgfr1 (ca-fgfr1) (Neilson and Friesel, 1996), Ras was enriched at enlarged intracellular mGFP-positive vesicles (Figure 4J, L). Depletion of *rab7* greatly reduced the vesicle size and intracellular accumulations of Ras (Figure 4J, M). These results suggest that Rab7 is required to facilitate membrane trafficking events involving Ras to allow signal propagation of the FGF/MAPK pathway.

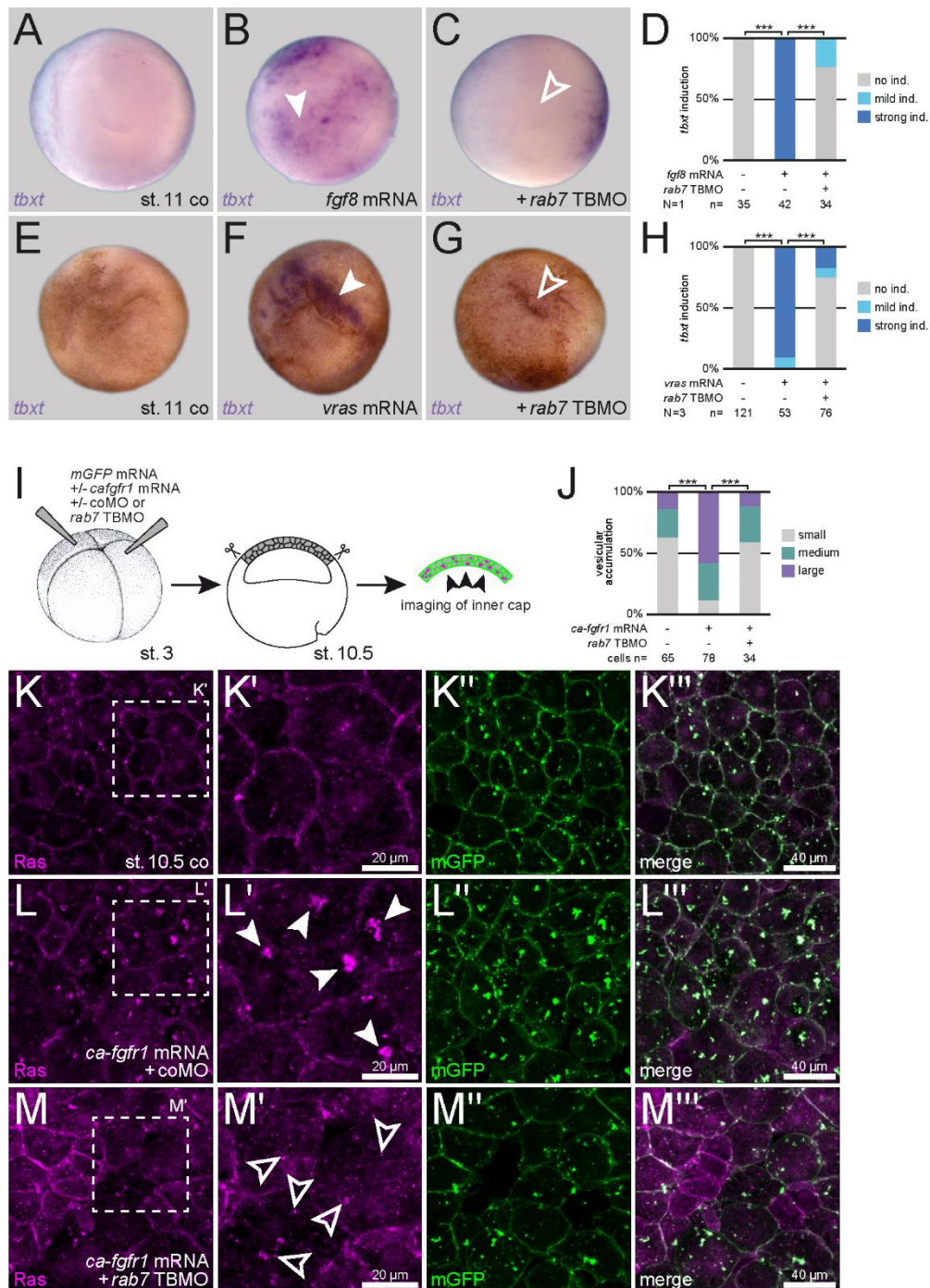


Figure 4: Rab7 acts at the level or downstream of Ras in MAPK signaling.

(A, E) Wildtype animal caps of st. 11 embryos. (B) Induction of *tbxt* expression (white arrows) in animal caps by *fgf8* or (F) *vras* mRNA overexpression. (C, G) Loss of *rab7* in those animal caps blocked *tbxt* induction (white outlined arrows). (D, H) Quantification of *tbxt* induction via *fgf8* or *vras* mRNA. (I) Experimental setup and (J) size quantification of vesicular structures within st. 10.5 animal caps. (K) Distribution of wildtype Ras protein (magenta) at the plasma membrane and mostly small intracellular vesicles. (L) Pathway activation via *ca-fgfr1* mRNA coinjected with a coMO led to enriched distribution of Ras in larger vesicles. (M) Concomitant knockdown of *rab7* reversed Ras accumulation to wildtype vesicular size. (K', L', M') High magnifications as indicated in (K, L, M); (K'', L'', M'') for lineage tracing coinjection of *mGFP* RNA (green) was performed; (K''', L''', M''') merged fluorescent channels.

Discussion

Tissue rearrangements during gastrulation are substantially involved to shape the appearance of a post gastrula embryo and the later arising mature organism. Appropriate specification of the mesoderm is an essential precondition for this to occur. As the mesoderm gets subdivided into various regions, the demand of different signaling pathways becomes evident for such patterning events (Dale and Jones, 1999; Slack et al., 1990; Smith, 1989). Hence, a balanced orchestration of the involved signaling pathways at tissue and even cellular level is key. Regulators of the endosomal machinery, namely Rab proteins, can mediate such intracellular signal transduction processes (Platta and Stenmark, 2011; Stenmark, 2009). Our previous data already revealed a function of the small GTPase Rab7 for ventral mesoderm specification, in a Wnt-dependent manner (Kreis et al., 2021). Concerning the specification of dorsal mesoderm, the obtained results of this study show a role for Rab7 in FGF/MAPK signaling, too.

Rab7 is crucial for FGF/MAPK signaling during mesoderm development

First implications were drawn from the bent and concomitant shortened anteroposterior axis upon dorsal *rab7* LOF, which mirrored the phenotype observed in embryos overexpressing a dominant negative FGF receptor (Amaya et al., 1991 and 1993). The curved axis emerged as the defective FGF receptor-harboring cells fail to differentiate into muscle, somites and notochord and thus these embryos are lacking the sustaining tissues to form their elongated shape (Amaya et al., 1993). Besides failed specification, defects of morphogenetic rearrangements during gastrulation could likewise account for the formation of shortened axis (Wallingford et al., 2002). In agreement with that, *rab7* knockout mice display GDs presumably due to misregulated morphogenetic

signaling, which resulted in early embryonic lethality (Kawamura et al., 2012). Their follow-up analyses considered that the observed GDs were caused by failed Wnt-dependent mesodermal patterning (Kawamura et al., 2020). This was in line with our own observation that mesoderm differentiation was lost in *rab7*-depleted embryos based on marker gene expression. However, the only partial rescue of dorsal gene expression at the onset of gastrulation with lithium chloride, a known Wnt agonist, suspected another pathway to be involved in dorsal mesoderm specification (Kreis et al., 2021).

Our animal cap assay, which based on artificial mesoderm/organizer induction, confirmed a role of Rab7 function during FGF-dependent mesoderm development in absence of Wnt signaling. Mesoderm induction via *ca-smad2*, a transcriptional effector of TGF- β signaling, further argued against a potential role for Rab7 in transducing this pathway, too. This was especially important, because analyses in animal caps are otherwise challenging in terms of differentiation between TGF- β and FGF signaling, as both pathways are necessary in exogenous mesoderm induction (Kimelman and Kirschner, 1987; Kurth and Hausen, 2000; Paterno and Gillespie, 1989; Slack et al., 1990). The absence of ventralized or dorsalized phenotypes in *rab7*-deficient embryos likewise argues against a regulatory function within the TGF- β signaling pathway (De Robertis, 2009; Moos et al., 1995), nor has TGF- β signal transduction been linked to a late endosomal function or its regulator Rab7, yet. This, together with the remarkable rescue capacity of downstream FGF pathway components, demonstrates the regulative function of Rab7 for FGF/MAPK signaling during dorsal mesoderm differentiation.

Rab7 acts at the level or downstream of endosome-associated Ras

Rescued mesodermal marker genes as well as attenuated pErk/pMAPK1 levels of morphant embryos led to the conclusion of Rab7 acting upstream of Erk/Mapk1. A more accurate placement of Rab7 function within the FGF signaling pathway was feasible by the use of more upstream signaling cascade components. *rab7* LOF-mediated inhibition of mesoderm specification induced by a FGF ligand or vRas in animal caps, likely localizes the Rab protein function at the level or downstream of Ras. Generally, Ras is found evenly at plasma membranes and intracellular compartments like e.g. vesicular structures (Jiang and Sorkin, 2002; Lu et al., 2009). EGF-stimulated cells unveiled that this GTPase was also found in the same endosomal structures as endocytosed receptor complexes (Jiang and Sorkin, 2002). According to the current knowledge, distribution of membrane-associated pathway components into the endocytic machinery could indicate (early) endosome dependent signal transduction (Platta and Stenmark, 2011). We show Ras accumulation at intracellular vesicles under FGF pathway-activated conditions. The observed colocalization of Ras and mGFP suggests that the accumulated vesicular structures are of (early) endosomal character as mGFP harbors a Glycosylphosphatidylinositol (GPI) anchor, which functions as a sorting determinant for internalization into endosomal compartments (Chatterjee and Mayor, 2001; Sabharanjak et al., 2002). This is line with results of another study demonstrating increased Ras localization at early endosome antigen 1 (EEA1)-positive vesicular structures in EGF-stimulated cells (Lu et al., 2009). Of note, activated epidermal growth factor receptors (EGFRs) and their associated signal transducers were also detectable at/in multivesicular compartments being positive for Cd63 and Lysosome-associated membrane glycoprotein-1 (Lamp-1), both identifying more downstream structures within the late endosomal machinery. Such pathway components even persisted throughout the maturation from early to late endosomes

as intact complexes (Oksvold et al., 2001), indicating potential signaling activity at LEs. Therefore, the absence of Rab7 may affect transport of receptor complexes along endocytic routes, thus resulting in impaired signal transduction.

Loss of Rab7 could impact signaling via disturbed late endosome formation

Induced accumulation of Ras in larger intracellular structures dispersed when *rab7* was downregulated. Hence, we assumed a LE-dependent function of Rab7 for Ras translocation to facilitate FGF/MAPK signal transduction.

Downregulation of *rab7* most likely affects the integrity of LEs as signaling platforms or even prevents LE formation in its entirety. Endosome maturation is a crucial step of LE formation, whereas the stepwise detachment of the EE regulator Rab5 is mediated by Rab7 (Skjeldal et al., 2021). Absence of Rab7 in the endosomal system may lead to an inability of LE synthesis, as Rab5 remains at the endosomal membranes and thus no maturation process takes place. Subsequently, Rab7-dependent recruitment of effectors promoting signal transduction would not occur. EEs may then constitute a dead end for further signal transduction or its maintenance, although this scenario probably entails an increased recycling circuit activity. Ras exiting EEs via recycling endosomes could explain the dispersion from larger to smaller vesicular structures upon Rab7 deficiency at an apparent constant Ras level. Defective endosome maturation or lost late endosomal identity may as well impact on even earlier endocytic events in a way that Ras accumulation does not occur at all.

The here reported data suggest LEs as signaling platforms for FGF-induced MAPK signal transduction in *Xenopus*, as it was already assumed for intracellular EGF signaling (Oksvold et al, 2001). Rab7-positive endosomes could provide the spatial environment for certain pathway components to meet and exert their specific function to maintain the signaling cascade (Figure 5). To start the MAPK signaling cascade,

direct interaction of Ras and Raf/Map3k is essential (Kolch, 2000; Lu et al., 2009; Morrison, 2012). First initiated by Raf/Map3k, further phosphorylation steps of downstream kinases have been suggested to take place at LEs after recruitment of such kinases to their limiting membranes (Lu et al., 2009; Nada et al., 2009; Teis et al., 2002). The *rab7* LOF analyses of this study hierarchically placed Rab7 between Ras and Erk/Mapk1, two pathway components found on LEs, actively mediating signal transduction here. Inhibition of *rab7* vastly impaired mesoderm specification and correct tissue rearrangement of the dorsal mesoderm as well. Altogether, this implicates that Rab7 is crucial to obtain the functionality of LEs serving as platforms for FGF/MAPK signal transduction during dorsal mesoderm specification in *Xenopus* embryos.

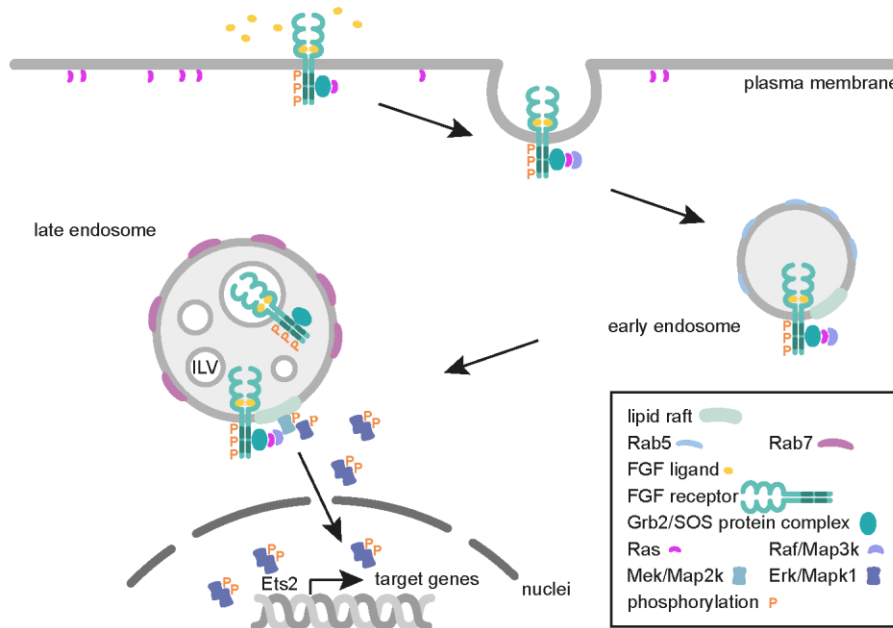


Figure 5: Model for Rab7-dependent FGF/MAPK signal transduction via LEs.

After ligand activation receptor complex formations occurs. Receptor complex is transferred to Rab5-associated EEs via endocytosis. Upon endosome maturation translocation of the activated receptor complex to Rab7-positive LEs occurs. This places Raf/Map3k in direct proximity to Mek/Map2k on LEs, which allows the MAPK phosphorylation cascade to start. Phosphorylated Erk/Mapk1 then forms dimers and dissolves from LEs to translocate to the nucleus to activate members of Ets family of transcription factors, eventually mediating transcription of target genes.

Material and Methods

Animal treatment and handling

Xenopus laevis frogs were purchased from Nasco (901 Janesville Avenue P.O. Box 901 Fort Atkinson) and treated as approved by the Regional Government Stuttgart, Germany (V349/18ZO 'Xenopus Embryonen in der Forschung'), according to German regulations and laws (§6, article 1, sentence 2, nr. 4 of the animal protection act). Animals were held in the animal facility of the Department of Zoology of the University of Hohenheim at the appropriate conditions as follows: pH=7.7, 20°C and a 12 h light cycle. To induce ovulation in *Xenopus* females subcutaneously injection of 300-700 units of human chorionic gonadotropin (hCG; Sigma) was performed. *Xenopus* males were sacrificed to gain sperm for fertilization, testes were stored at 4°C in 1x MBSH (Modified Barth's saline with HEPES) solution. Staging of embryos was based on Nieuwkoop and Faber, 1994.

Microinjection setup

For microinjections a Harvard Apparatus setup was used and drop size was set to 4 nl per injection. For lineage specific verification fluorescein dextran, *mGFP* mRNA, *h2b* mRNA or *lacZ* mRNA was coinjected and validated as described earlier (Kreis et al., 2021). Embryos were injected at the 4-cell stage either in the animal hemisphere or in the dorsal marginal zone.

Microinjections

The *rab7a* TBMO was used as published (Kreis et al., 2021); sequence is 5'-GTCTCCGCTTCCTACCCCTGCCAGC-3'. A random control Morpholino oligomere (coMO) was used as a MO fill up in this study. Total amount of injected MO was:

0.7-1.4 pmol *rab7* TBMO. For mRNA synthesis plasmids were linearized with NotI and transcribed in vitro (Sp6 polymerase) using Ambion message machine kit. Total amounts of injected mRNA per blastomere are as follows: 200 pg *ca-smad2* mRNA, 80 pg *dn-fgfr1* mRNA, 400-480 pg *ets2* mRNA, 400 pg *fgf8* mRNA, 400 pg *h2b-GFP* mRNA, 400 pg *lacZ* mRNA, 12-20 pg *mapk1/erk* mRNA, 400 pg *mGFP* mRNA, 20 pg *nodal1* mRNA, 8 pg *vras* mRNA.

Immunofluorescence analysis and quantification

For IF analyses of animal caps or dorsal neural plates, *mGFP* mRNA or *h2b-GFP* mRNA was coinjected as lineage tracer, respectively. After reaching the appropriate stage, embryos were fixed in MEMFA for 1 h at room temperature, this was followed by 2 washes in 1x PBS- (phosphate buffered saline) for 15 min. Animal caps were dissected horizontally upon fixation. Afterwards whole mounts or animal caps were transferred to 24 well plates and washed two times for 15 min in PBST (PBS/0.1% Triton X-10). Then blocking for 2 h at room temperature in CAS-Block (1 : 10 in PBST; ThermoFisher, # 008120) was performed, blocking reagent was replaced by antibody solution (diluted in CAS-Block) for incubation over night at 4°C. Primary antibodies were used as follows: anti-pErk/pMapk1 (Cell Signaling, # 4370, 1 : 200), anti-Ras (Abcam, EP1125Y; 1 : 500). Antibody solution was removed by washing twice for 15 min in 1x PBS-. Secondary antibodies (ThermoFisher, all 1 : 1000 in CAS-Block) were applied for 2 h at room temperature or overnight at 4°C. F-actin was directly visualized via using AlexaFluorTMPlus 405 Phalloidin (ThermoFisher, A30104; 1 : 200 in PBS-) for cell boarder detection. Photo documentation was performed with whole mounts or animal caps being transferred to microscope slides. Fluorescence intensity of pErk/pMapk1 was measured with a Zeiss LSM 700 Axioplan2 Imaging microscope running the Zeiss Zen 2012 Blue Edition. Each neural plate was

imaged with the same settings and box plot quantification was performed by using Excel 2016.

Animal cap elongation assay

Rab7 TBMO was injected 2x at the 4-cell stage into the animal hemisphere. Embryos were raised until stage 9 in 0,1x MBSH solution. Animal caps were manually dissected and individually transferred to 24 well plates, containing an Activin solution (10ng/mL in 0,5x MBSH) or buffer and incubated until stage 13-15. Used well plates have been coated with 2% BSA (bovine serum albumin) in 1x PBS- (pH=7,4). For subsequent *in situ* hybridization and photo documentation animal caps were fixed in 2-3 h at room temperature in MEMFA.

***In situ* Hybridization**

RNA *in situ* probes were synthesized by using SP6 or T7 polymerases. Embryos were fixed 2-3 h at room temperature for *in situ* mRNA detection and further processed according to a customized (after R. Rupp, personal communication) standard protocol.

Embryo sections

Bisections of embryos were performed by using a razor blade. For more high-quality sections embryos were embedded in a glutaraldehyde-crosslinked gelatin-albumin mix and sectioned with a Leica VT1000S vibrating blade microtome.

Photo Documentation

IF images were taken by using a Zeiss LSM 700 Axioplan2 Imaging microscope and adjustment of such images was performed with the Zeiss Zen 2012 Blue Edition. Zeiss SteREO Discovery V12 microscope or Axioplan2 inverted microscope were used to

document all other experiments. Afterwards image editing was performed with Adobe Photoshop CS6 and Adobe Illustrator CS6.

Statistical analysis

Any probability of the collected data was calculated with Pearson's chi-square test (Bonferroni corrected, if required). Significance levels of all statistical analyses were grouped as follows: $*=p<0.05$, $**=p<0.01$, $***=p<0.001$. N= or n= declares respectively number of experiments or number of embryos analyzed.

Acknowledgements

The chapter “The late endosomal regulator Rab7 is required for FGF-dependent mesoderm specification by regulating Ras-mediated MAPK activation” was written as a draft for publication. Parts of the integrated data depicted here, emerged during a bachelor thesis by Celine Camuto under my supervision.

Research chapter III:

Cd63 promotes developmental processes via late endosomal signaling platforms

The tetraspanin Cd63 is required for eye morphogenesis in *Xenopus*

11/25/2020 - Open Access

The tetraspanin Cd63 is required for eye morphogenesis in *Xenopus*Jennifer Kreis¹, Ramona Bonk¹ and Philipp Vick^{1§}¹Institute of Biology, University of Hohenheim, 70599 Stuttgart, Germany

§To whom correspondence should be addressed: philipp.vick@uni-hohenheim.de

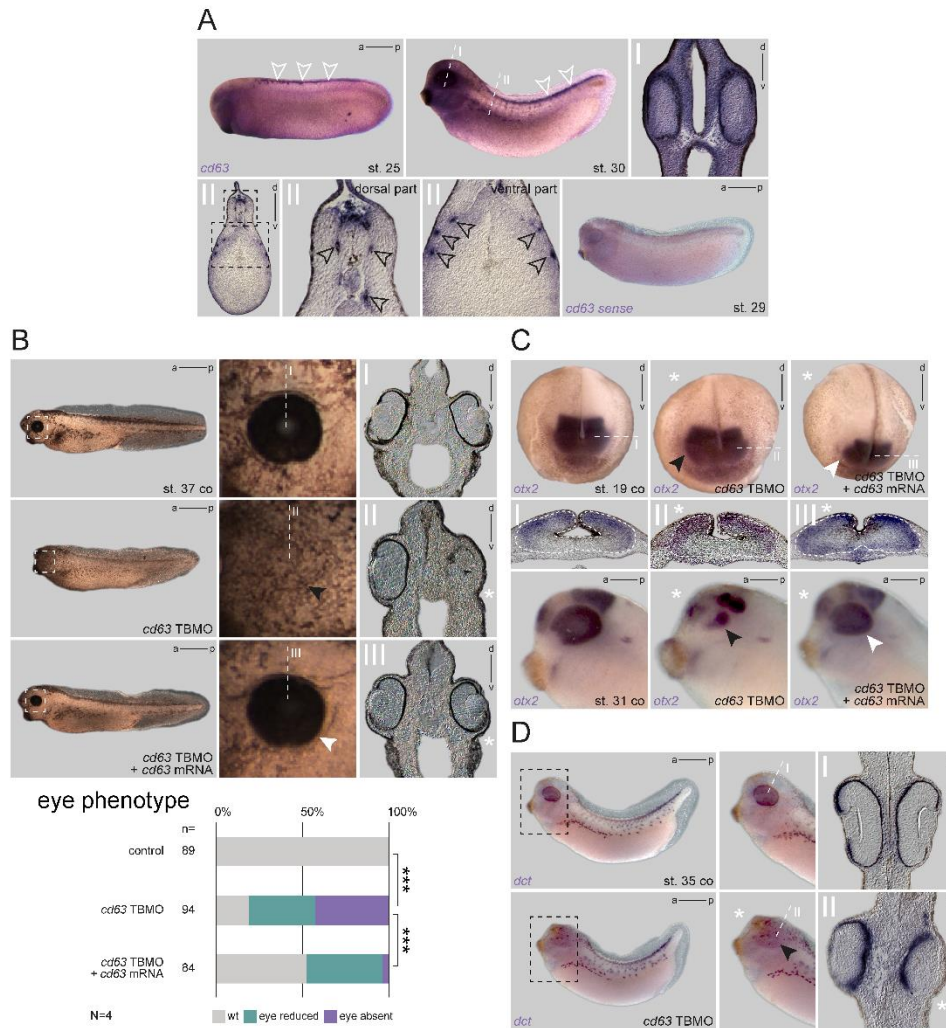


Figure 1. Loss of Cd63 in the neural ectoderm caused defects in eye morphogenesis: **A** Expression pattern of *cd63* during tailbud stages. Enrichment of transcripts in the TNC of st. 25 (white arrowheads). At st. 30, *cd63* was additionally detected in eyes and cement gland. Transversal sections highlighted signals in the eyes, head mesenchyme, brain, premigratory TNC, dorsal fin mesenchyme, medially and laterally migrating TNC cells (black arrowheads). *cd63* sense control specimen of st. 29 did not show any signal. **B** Knockdown of *cd63* in one dorsal animal blastomere resulted in impaired eye development, which was rescued by co-injection of *cd63* mRNA. Sections illustrated normal eye structures in control and rescue specimen, whereas morphant embryos depicted disturbed optic cup formation on the injected side. Quantification of eye phenotypes illustrates significance of the effect. **C** Unilateral loss of *cd63* in the eye field lineage revealed altered expression pattern of *otx2* in neurula and later tailbud stages. At neurulation, *otx2* showed no reduction in intensity but indicated alterations of the targeted eye vesicle (black arrowhead). Sections revealed defects in medial forebrain closure and lateral optic vesicle formation. In tailbud stages, loss of *cd63* resulted in partial reduction of eye

11/25/2020 - Open Access

tissues (black arrowhead) compared to matching controls. Both effects were reduced by co-injection of *cd63* mRNA (white arrowheads). **D** *cd63* TBMO injection did not block TNC migration or *dct* expression in eyes or melanophores of unilateral morphants. Sections revealed massively impaired formation of eye tissue (black arrowhead) compared to WT eyes of controls. Asterisks mark the injected side. a, anterior; co, control; d, dorsal; p, posterior; TBMO, translation blocking Morpholino oligomer; TNC, trunk neural crest; st., stage; v, ventral; wt, wild type.

Description

Tetraspanins (TSPAN) are a family of (33 in humans) scaffold proteins consisting of the name-giving four membrane-spanning domains, two extracellular loops, and an intracellular N- and C-terminus. By forming 'tetraspanin-enriched microdomains' they participate in organizing the plasma membrane and serve as multipurpose adapters. Some can be found ubiquitously in most cells, while others are specific to certain cell types. On a subcellular level, enrichment in distinct membrane-associated organelles has been documented for several members (Termini and Gillette, 2017).

One member, Cd63, shows such specific enrichment in intraluminal vesicles (ILV) of late endosomes (LE; also called multivesicular bodies, MVB). Further, it is found in exosomes, small extracellular vesicles created from ILV of specialized MVB, which become released after fusion of the MVB with the plasma membrane (Piper and Katzmann, 2007; Pols and Klumperman, 2009; Simons and Raposo, 2009). Another specialized form of LE are melanosomes, which are dedicated for pigment (types of melanin) production in all vertebrates. They are mainly found in two types of tissue, the melanin producing melanocytes ('melanophores' in basal vertebrates like amphibians), and in the retinal pigment epithelium (RPE), the outer, light-shielding layer of the vertebrate optic cup (Raposo and Marks, 2007). In amphibians, melanophores derive from trunk neural crest (TNC) cells at the dorsal neural tube, from where they migrate to their lateral, mostly dermal destination during later embryogenesis (Collazo *et al.*, 1993). Cd63 also localizes to early melanosomes, and was shown to be required for melanogenesis in human melanoma cells (Basrur *et al.*, 2003; van Niel *et al.*, 2011).

The externally developing frog *Xenopus* represents a great vertebrate model system for developmental analyses, especially true for the neural crest and its derivatives. However, neither the tissue-specific developmental expression, nor the functional requirement of a specific TSPAN have been tested *in vivo*. Therefore, in this study, we analyzed the expression and function of the *Xenopus cd63* orthologue during tailbud stages, i.e. when major tissue differentiation processes and organ development take place. We were interested if *cd63* showed specific enrichment in melanosome-associated tissues like TNC cells, melanophores or the retinal pigment epithelium (Collazo *et al.*, 1993; Sinn and Wittbrodt, 2013). Further, we tested if loss of *cd63* affected development and function of these tissues.

Expression analysis by *in situ* hybridization (ISH) using a *cd63*-specific probe revealed a striking specific enrichment of mRNA in certain tissues. At early tailbud stages (Figure 1A; st. 25), *cd63* showed strong expression in premigratory TNC cells. This tissue was still positive at later tailbud stage, then localized mRNA signals were also found in the cement gland, head mesenchyme, brain, dermis, dorsal fin mesenchyme, migrating TNC cells and eyes, including the RPE (Figure 1A; st. 30). At this stage, transcript enrichment could also be detected laterally in putative melanophores, i.e. before start of pigment synthesis (Figure 1A). A sense probe control did not detect any signal in these tissues (Figure 1A). These analyses demonstrated that *cd63* was expressed in a tissue-specific manner, indicating a spatial requirement for certain embryonic processes. Moreover, the mRNA distribution suggested a potential role in pigment-associated tissues, i.e. melanophores and RPE.

Thus, we next wanted to test a potential functional requirement of Cd63 for melanogenesis in tadpoles. We designed a translation-blocking morpholino oligomer (TBMO) that binds the 5'UTR of both homeologs of the *X. laevis cd63* mRNA, to block protein synthesis. Embryos were injected unilaterally into the neural lineage to target the eyes, TNC, and melanophores. When control embryos or internal control side of morphants showed normal eye and melanophore formation, the targeted side of morphants displayed strong defects in eye morphology (Figure 1B). Most morphant halves displayed reduced or lacking eyes when analyzed externally. Transversal sections confirmed defects in optic cup formation, with defects ranging from partial to nearly complete lack of most major structures (RPE, retina and lens). This effect was partially rescued by co-injection of wild type (WT) *cd63* mRNA lacking the 5'UTR, i.e. insensitive to the MO, demonstrating specificity of the observed phenotype. Rescued halves showed WT or milder phenotypes (Figure 1B). Interestingly, no obvious phenotype was detected in morphant melanophores. Migration appeared not to be altered, and neither number, nor the shape of melanophores was significantly different from control halves. To understand the temporal basis of this eye phenotype, a subset of injected specimens was fixed at late neurula or tailbud stages to check for expression of *otx2*, a forebrain marker highlighting eye tissues (optic vesicle/cup or differentiated eyes, respectively). At neurulation, expression was not reduced after *cd63* knockdown but revealed alterations in prosencephalon shapes on the injected side, indicating a morphogenetic effect (Figure 1C). Transversal sections of such embryos revealed an inhibition of medial closure of the prosencephalon, and impairment of optic vesicle formation (sections I-III in 1C), together causing widening of the *otx2* expression domain on the injected half. Later, when embryos reached tailbud stages, this morphogenetic phenotype appeared more pronounced, resulting in partial reduction of optic *otx2* expression. Again, the severity of both phenotypes was milder in rescued embryos.

11/25/2020 - Open Access

Finally, some embryos were checked for expression of *dopachrome tautomerase* (*dct*), a gene coding for a tyrosinase-related enzyme participating in melanin synthesis in the RPE and in melanocytes, and which is highly expressed in these tissues in *Xenopus* as well (Kumasaka *et al.*, 2003). As reported before, expression was highly reminiscent of *cd63* at tailbud stages (cf. Figure 1A). We did not detect any effect on TNC formation, number or migration ability of melanophore precursors, or expression intensity, indicating correct specification of melanophores (Figure 1D). Using *dct* to highlight the RPE, embryos showed again a clear reduction in optic tissues, though, sections revealed remnant RPE expression even in severely affected specimen. Thus, knockdown of *cd63* did not affect melanophore development in our approach. Altogether, from these analyses we conclude that Cd63 is required for correct eye morphogenesis, but surprisingly dispensable for melanophore specification and melanogenesis in *Xenopus*.

While the observed phenotypes were shown to be specific to the loss of *cd63*, we cannot exclude a compensatory effect taking place in the melanophore lineage. In some cases, including Cd63-dependent melanosome formation in mice, it has been shown that the RPE is more sensitive to alterations in the process of melanogenesis as compared to melanocytes, as this process is much more dynamic in the latter (cf. Lopes *et al.*, 2007; van Niel *et al.*, 2011). Nearly no TSPAN gene has ever been analyzed in *Xenopus* development so far; therefore, the loss of *cd63* in melanophores might also be compensated by other TSPAN potentially expressed in these cells as well. Alternatively, in contrast to mouse melanocytes, Cd63 might not directly participate in amphibian melanogenesis (van Niel *et al.*, 2011). It could participate in other cellular processes, not directly related to melanin production, e.g. regulation of exosomes. The lack of impact on migration of TNC derivatives is in agreement with another known role of Cd63, namely its inhibitory effect on cell migration. While known as a factor elevated in early stage melanomas, it has been shown to be a negative driver of advanced stages by inhibiting epithelial-mesenchymal transition, and thus invasive behavior (Radford *et al.*, 1997; Jang and Lee, 2003; Lupia *et al.*, 2014). Therefore, in our knockdown approach, migration behavior of TNC should rather be promoted. Finally, the role of Cd63 in cell migration is tightly associated with its regulatory function of integrin abundance at the plasma membrane, an influence on cell adhesion shared with other TSPAN (Termini and Gillette, 2017). Concerning the morphogenetic phenotypes we observed in the early tadpole eyes, it is interesting to note that correct integrin localization has been demonstrated to be essential for eye morphogenesis in fish, providing an interesting link to our observations (Martinez-Morales *et al.*, 2009).

Methods

[Request a detailed protocol](#)

Xenopus laevis care and maintenance

Frogs were purchased from Nasco (Fort Atkinson, WI, USA). Handling, care and experimental manipulations of animals was approved by the Regional Government Stuttgart, Germany (V349/18ZO 'Xenopus Embryonen in der Forschung'), according to German regulations and laws (§6, article 1, sentence 2, nr. 4 of the animal protection act). Female frogs (between 4 and 12 years old) were injected subcutaneously with 300-700 units of human chorionic gonadotropin (Sigma), depending on weight and age, to induce ovulation. Sperm of male frogs was obtained by maceration of testes (stored at 4°C in 1x Modified Barth's saline with HEPES). Embryos were staged according to Nieuwkoop and Faber (1994). Only clutches of embryos from healthy females were used for the experiments and early embryonic stages were chosen only if survival rates were normal. For experiments, individual embryos from one batch were randomly picked and used as control or tested specimens. If control groups displayed unusual or high percentage of developmental defects later in development, such clutches and experiments were excluded as well, based on empirical judgement.

Morpholino design, mRNA synthesis and microinjections

The *cd63* TBMO (sequence: 5'TTCTCCTCTCCAGTAACTTGTAACG 3') targeting the 5'UTR of both *X. laevis* homeologs was designed using the S-sequence (5'UTR position -40 to -16 distance from the start), as deposited in gene bank (accession: NM_001087051). For rescue experiments, RFP-*cd63*/CS2 plasmid (Lee *et al.*, 2007) containing the *cd63* coding sequence without 5'UTR was linearized with NotI and transcribed *in vitro* (Sp6 polymerase) using Ambion message machine kit. Drop size was calibrated to four nl per injection. One pmol of MO was injected unilaterally into the animal hemisphere at four cell stages with or without rescue mRNA (260 pg per injection), targeting predominantly the neural half of the embryo. The opposite side was used as an internal control.

In situ Hybridization

Partial ISH probes for *X. laevis* *cd63* (accession: NM_001087051) and *dct* (accession: BC073623.1) were cloned using standard RT-PCR with the following primer pairs:

(F) 5'-TTCTTCAACTTCGTTCTGG-3'/(R) 5'-CCGTGATATTACTTGTTGC-3' (*cd63*), and

(F) 5'-GCCGCTGAAGTTCTTTAACTC-3'/(R) 5'-GGTAAAGGTAGCATTATCAAGG-3' (*dct*).

For *in situ* mRNA detection, ISH was performed after fixation in MEMFA for 2-3h at room temperature and processed following a standard protocols (Sive *et al.*, 2000). RNA *in situ* probes were transcribed using SP6 or T7 polymerases.

11/25/2020 - Open Access

Embryo sections

For vibratome sections (thickness: 30–35 μm), embryos were embedded in a glutaraldehyde-cross-linked gelatin-albumin mix (Embedding medium: 2.2 g gelatine, 135 g bovine serum albumin, 90 g sucrose dissolved in 450 ml PBS) and razor blade-sectioned as indicated in whole-mount panels using a Leica VT1000S vibratome.

Photo Documentation

Pictures were taken with a Zeiss SteREO Discovery.V12 (for whole embryos) or an Axioplan2 inverted (for sections) microscope using AxioVision 4.6. Adobe Photoshop CS6 was used for cropping and careful brightness adjustments. All figures were arranged using Adobe Illustrator CS6.

Statistical analysis

Statistical calculations of marker gene expression were performed using Pearson's chi-square test. $*=p<0.05$, $**=p<0.01$, $***=p<0.001$ were used for all statistical analyses. 'N' represents the number of experiments (i.e. number of biological replicates of batches of embryos from different fertilizations), and 'n' the number of embryos analyzed (i.e. number of biological replicates of embryos).

Acknowledgments: We like to thank V. Andre, A. Schäfer-Kosulja and W. Möller for technical assistance, K. Feistel and the Blum Lab members for continuous valuable feedback. The *otx2* plasmid was a kind gift of Dr. R. Harland, the RFP-cd63/CS2 of Dr. N. Kinoshita.

References

- Basrur, V., Yang, F., Kushimoto, T., Higashimoto, Y., Yasumoto, K.-I., Valencia, J., Muller, J., Vieira, W. D., Watabe, H., Shabanowitz, J., et al. (2003). Proteomic analysis of early melanosomes: identification of novel melanosomal proteins. *J. Proteome Res.* 2, 69–79. PMID: 12643545.
- Collazo, A., Bronner-Fraser, M. and Fraser, S. E. (1993). Vital dye labelling of *Xenopus laevis* trunk neural crest reveals multipotency and novel pathways of migration. *Development* 118, 363–376. PMID: 7693414.
- Jang, H.-I. and Lee, H. (2003). A decrease in the expression of CD63 tetraspanin protein elevates invasive potential of human melanoma cells. *Exp Mol Med* 35, 317–323. PMID: 14508073.
- Kumasaka, M., Sato, S., Yajima, I. and Yamamoto, H. (2003). Isolation and developmental expression of tyrosinase family genes in *Xenopus laevis*. *Pigment Cell Res.* 16, 455–462. PMID: 12950720.
- Lee, R. H. K., Iioka, H., Ohashi, M., Iemura, S.-I., Natsume, T. and Kinoshita, N. (2007). XRab40 and XCullin5 form a ubiquitin ligase complex essential for the noncanonical Wnt pathway. *The EMBO Journal* 26, 3592–3606. PMID: 17627283.
- Lopes, V. S., Wasmeier, C., Seabra, M. C. and Futter, C. E. (2007). Melanosome maturation defect in Rab38-deficient retinal pigment epithelium results in instability of immature melanosomes during transient melanogenesis. *Mol. Biol. Cell* 18, 3914–3927. PMID: 17671165.
- Lupia, A., Peppicelli, S., Witort, E., Bianchini, F., Carloni, V., Pimpinelli, N., Urso, C., Borgognoni, L., Capaccioli, S., Calorini, L., et al. (2014). CD63 Tetraspanin Is a Negative Driver of Epithelial-to-Mesenchymal Transition in Human Melanoma Cells. *Journal of Investigative Dermatology* 134, 2947–2956. PMID: 24940653.
- Martinez-Morales, J. R., Rembold, M., Greger, K., Simpson, J. C., Brown, K. E., Quiring, R., Pepperkok, R., Martin-Bermudo, M. D., Himmelbauer, H. and Wittbrodt, J. (2009). ooplano-mediated basal constriction is essential for optic cup morphogenesis. *Development* 136, 2165–2175. PMID: 19502481.
- Nieuwkoop, P. D. and Faber, J. (1994). *Normal Table of Xenopus laevis (Daudin)* Garland Publishing Inc, New York ISBN 0-8153-1896-0
- Piper, R. C. and Katzmann, D. J. (2007). Biogenesis and Function of Multivesicular Bodies. *Annu. Rev. Cell Dev. Biol.* 23, 519–547. PMID: 17506697.
- Pols, M. S. and Klumperman, J. (2009). Trafficking and function of the tetraspanin CD63. *Experimental Cell Research* 315, 1584–1592. PMID: 18930046.
- Radford, K. J., Thorne, R. F. and Hersey, P. (1997). Regulation of tumor cell motility and migration by CD63 in a human melanoma cell line. *J. Immunol.* 158, 3353–3358. PMID: 9120293.
- Raposo, G. and Marks, M. S. (2007). Melanosomes--dark organelles enlighten endosomal membrane transport. *Nat Rev Mol Cell Biol* 8, 786–797. PMID: 17878918.
- Simons, M. and Raposo, G. (2009). Exosomes--vesicular carriers for intercellular communication. *Current Opinion in Cell Biology* 21, 575–581. PMID: 19442504.

11/25/2020 - Open Access

Sinn, R. and Wittbrodt, J. (2013). An eye on eye development. *Mechanisms of Development* 130, 347–358. PMID: 23684892.

Sive, H. L., Grainger, R. M. and Harland, R. M. (2000). *Early Development of Xenopus Laevis*. Cold Spring Harbor Laboratory Press. ISBN: 9780879695040

Termini, C. M. and Gillette, J. M. (2017). Tetraspanins Function as Regulators of Cellular Signaling. *Front Cell Dev Biol* 5, 163. PMID: 28428953.

van Niel, G., Charrin, S., Simoes, S., Romao, M., Rochin, L., Saftig, P., Marks, M. S., Rubinstein, E. and Raposo, G. (2011). The Tetraspanin CD63 Regulates ESCRT-Independent and -Dependent Endosomal Sorting during Melanogenesis. *Developmental Cell* 21, 708–721. PMID: 21962903.

Funding: J.K. was a recipient of a Ph.D. fellowship from the Landesgraduiertenförderung Baden-Württemberg.

Author Contributions: Jennifer Kreis: Investigation, Validation, Visualization, Writing - review and editing, Formal analysis. Ramona Bonß: Investigation, Validation. Philipp Vick: Conceptualization, Methodology, Project administration, Supervision, Validation, Writing - original draft, Data curation.

Reviewed By: Thomas Hollemann and Anonymous

History: Received August 19, 2020 **Revision received** October 30, 2020 **Accepted** November 23, 2020 **Published** November 25, 2020

Copyright: © 2020 by the authors. This is an open-access article distributed under the terms of the Creative Commons Attribution 4.0 International (CC BY 4.0) License, which permits unrestricted use, distribution, and reproduction in any medium, provided the original author and source are credited.

Citation: Kreis, J; Bonß, R; Vick, P (2020). The tetraspanin Cd63 is required for eye morphogenesis in *Xenopus*. *microPublication Biology*. <https://doi.org/10.17912/micropub.biology.000335>

Expression of an endosome-excluded Cd63 prevents axis elongation in *Xenopus*

11/25/2020 - Open Access

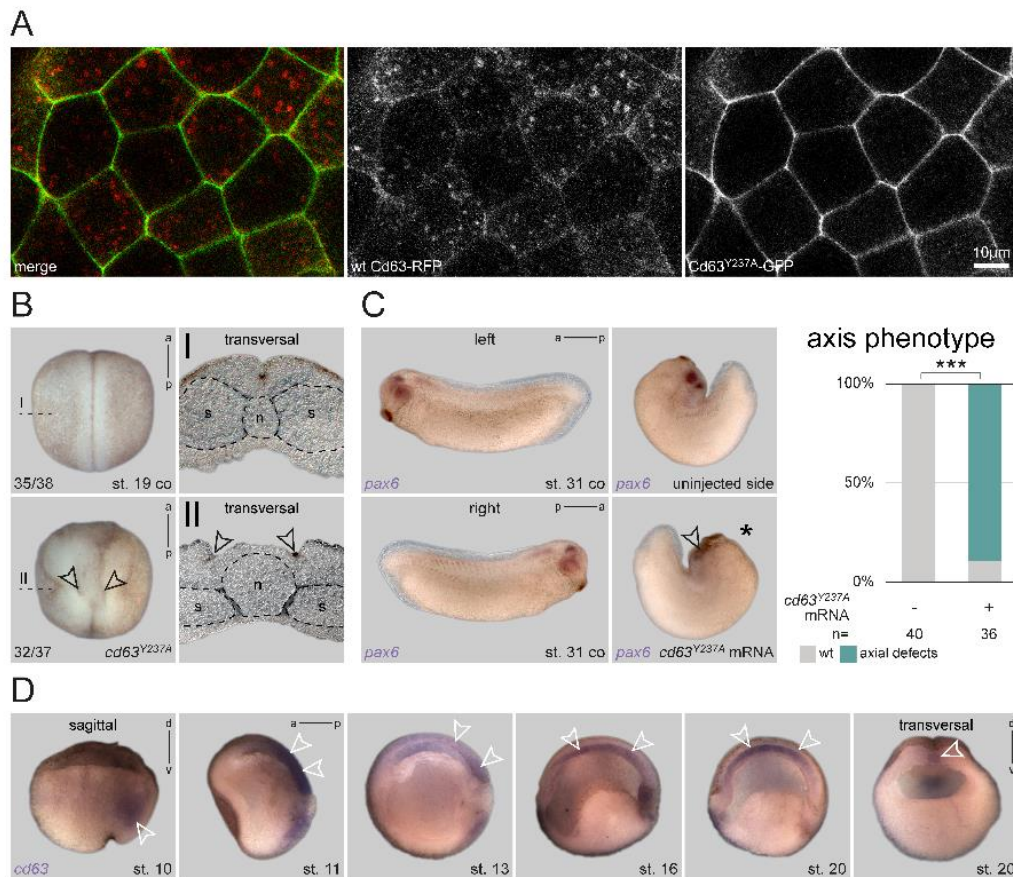
Expression of an endosome-excluded Cd63 prevents axis elongation in *Xenopus*Jennifer Kreis¹, Ramona Bonk¹, Kerstin Feistel¹ and Philipp Vick^{1,§}¹Institute of Biology, University of Hohenheim, 70599 Stuttgart, Germany[§]To whom correspondence should be addressed: philipp.vick@uni-hohenheim.de

Figure 1. Overexpressed Cd63 mutant does not localize to late endosomes but blocks axis elongation: A Overexpressed RFP-tagged wt Cd63 (red) localizes to plasma membrane and endosomes in animal cap cells, whereas Cd63^{Y237A} (green) accumulates only in the plasma membrane. **B** Control specimen depicted normal neurulation and normal sized notochords (n, outlined by black dashed line) in transversal section. Overexpression of *cd63^{Y237A}* mRNA in dorsal lineage caused defects in neural tube closure. Sections revealed strongly expanded notochordal tissue (outlined by black dashed line) and widened floorplate tissue, as indicated by apparently unaltered apical constriction at the hinge points lateral of it (arrowheads). **C** Untreated specimen of st. 31 established wt AP axis extension and wt expression of *pax6* indicating normal eye development. Unilateral overexpression (injected side marked by asterisk) of *cd63^{Y237A}* mRNA resulted in embryos with shortened AP axis and reduced neural and optical expression of *pax6*. Quantification of axis phenotype. **D** Sagittal sections of st. 10 specimens revealed *cd63* transcripts in deep dorsal mesoderm (arrowhead). With ongoing gastrulation, expression was detected in the posterior neuroectoderm and notochordal mesoderm (st. 11; arrowheads). During neurulation (st. 13, 16, 20) *cd63* vanished from the neuroectoderm and became restricted to the notochord (arrowheads). Sagittal and transversal sections of late neurulas confirmed notochordal expression (arrowheads). a, anterior; AP, antero-posterior; co, control; d, dorsal; p, posterior; s, somites; st., stage; v, ventral; wt, wildtype.

11/25/2020 - Open Access

Description

Cd63 is an adapter protein belonging to the tetraspanin family. As other members, it possesses four membrane-spanning domains, two extracellular loops, and the N- and C-terminus both face the cytoplasm. Cd63 is highly enriched in intraluminal vesicles (ILV) of late endosomes (LE; also called multivesicular bodies, MVB; Termini and Gillette, 2017). Cd63 trafficking to LE occurs via classical routes, i.e. from the ER to the Golgi complex, then to the plasma membrane, from where it is endocytosed and incorporated into ILV (Kobayashi *et al.*, 2000; Pols and Klumperman, 2009). As an ILV-enriched component, Cd63 is a marker of exosomes, as these small extracellular vesicles are created from ILV of certain types of MVB (Pols and Klumperman, 2009; Simons and Raposo, 2009). Finally, Cd63 localizes to early melanosomes, highly specialized organelles that originate from LE-type precursors, and was shown to be required for melanogenesis in human melanoma cells (Basrur *et al.*, 2003; van Niel *et al.*, 2011). In our preceding analysis (Kreis *et al.*, 2020), using *Xenopus* embryos we found the orthologous gene expressed in the trunk neural crest (TNC) and in melanosome-associated tissues such as the retinal pigment epithelium and melanophores (pigment producing cells of poikilotherm vertebrates; Raposo and Marks, 2007). Neural knockdown of *cd63* specifically caused eye morphogenesis defects in early tadpole stages, surprisingly without impacting TNC formation and migration, nor melanophore specification and melanogenesis (Kreis *et al.*, 2020).

To analyze the cellular basis of this eye phenotype, we asked whether endosomal localization of Cd63 was required for correct eye development. Endocytosis and incorporation of Cd63 into ILV is mediated by a C-terminal 'lysosomal targeting motif', comprised of the last five amino acids (AA), GYEVN (Rous *et al.*, 2002). Single AA mutagenesis combined with indirect immunofluorescence screening had determined a tyrosine-to-alanine replacement (GYEVN to GAEVN) to be most efficient in preventing translocation from the plasma membrane to LE in rat kidney cells (Rous *et al.*, 2002). We generated two equivalent constructs using *Xenopus cd63*: one comprising the mutated coding sequence (*cd63*^{Y237A}/CS2+), and a second one fused N-terminally to eGFP (*cd63*^{Y237A}/eGFP/CS2+) for localization testing. To verify that the *Xenopus* mutant construct mimicked the published mis-localization in embryos *in vivo*, we injected mRNA of *cd63*^{Y237A}/eGFP together with an RFP-tagged wt *cd63* (Lee *et al.*, 2007) into the animal hemisphere and compared their subcellular localization by confocal microscopy. While WT Cd63 localized to both plasma membrane and endosomal structures as published (Lee *et al.*, 2007), mutant Cd63^{Y237A} was not found in endosomal structures, but was strongly enriched in the plasma membrane (Figure 1A). Thus, our construct provided a valuable tool to analyze the function of Cd63 localization to LE during *Xenopus* development.

Next, we injected the construct into the dorsal lineage of 4-cell stage embryos to analyze potential phenotypes. Surprisingly, injected embryos developed strong axial phenotypes during neurulation, resulting in an open neural tube at late neurula stages. Transversal sections of such specimens at the trunk level revealed that bilateral hinge points elevating the neural folds had formed correctly. However, the floorplate between these hinge points was extremely wide, preventing neural fold apposition and fusion (Figure 1B). Additionally, the notochord appeared amorphous in these specimens, not displaying a regular round shape as in control embryos, i.e. notochord morphogenesis was severely compromised. Together, the observed phenotype indicated a failure of proper axial elongation. This phenotype became even more pronounced, when injected embryos were reared to tailbud stages. Even in unilaterally injected specimens, axial extension of dorsal tissues was significantly inhibited, resulting in an extreme dorsal curvature in most embryos (Figure 1C). When such embryos were processed for *in situ* hybridization (ISH) to highlight eye development using a *pax6* probe, optic *pax6* expression was strongly reduced on the injected side (Figure 1C), indicating impairment of eye morphogenesis, and reminiscent of the morpholino (MO)-mediated knockdown of *cd63* (Kreis *et al.*, 2020).

As these phenotypes suggested a possible role of Cd63 in tissues important for axial convergent extension (CE) behavior (Keller and Sutherland, 2020), we next performed ISH to analyze the expression patterns of *cd63* during gastrulation and neurulation. *cd63* was expressed in both the axial mesoderm and the neuroectoderm (Figure 1D), i.e. germ layers exhibiting CE and extensive axial elongation. In bisected embryos, neural plate expression was visible during late gastrulation and early neurulation and vanished afterwards. Mesodermal expression was found continuously throughout this embryonic time-frame. *cd63* was first expressed in the deep mesoderm during early gastrulation, later, during formation and elongation of the notochord, these tissues showed intense mRNA enrichment as well. Together, these results support the conclusion that localization of Cd63 to LE is involved in regulation of embryonic axial extension during late gastrulation and/or early neurulation.

While the observed phenotype is striking, it also reveals a significant difference to our previous *cd63* loss-of-function approach (Kreis *et al.*, 2020). By inhibiting translation, we found *cd63* to be required for eye morphogenesis, with aberrant optic vesicle formation during late neurulation being the first visible phenotype. While such knockdown embryos did not show early axis elongation phenotypes, both approaches resulted in later eye defects. Therefore, the early defects presented here, indicate a dominant-inhibitory effect caused by plasma membrane retention of Cd63 (cf. Figure 1A). Therefore, the lack of endosomal trafficking of Cd63^{Y237A}, which partially mimics the loss of *cd63*, could indicate a specific requirement for correct eye morphogenesis. In this work, we have not directly assessed if Cd63^{Y237A} mislocalized to the plasma membrane in the dorsal mesoderm or posterior neural ectoderm as well, i.e. in those tissues

11/25/2020 - Open Access

performing axis elongation behavior. However, if this was the case, as expected, this might also result in aberrant accumulation of Cd63 binding partners, which in turn caused Cd63^{Y237A}-specific interference with CE behavior in these early stages.

Tetraspanins are well-known to serve as multipurpose adapters by forming ‘tetraspanin-enriched microdomains’. In this way, they have been reported to influence cell adhesion properties, and thus to alter cellular morphology and migratory behavior (Termini and Gillette, 2017). Supporting this notion, Cd63 is considered a negative driver of advanced stages of melanoma, as it inhibits epithelial-mesenchymal transition (EMT), and thus invasive migratory behavior (Radford *et al.*, 1997; Jang and Lee, 2003; Lupia *et al.*, 2014). The role of Cd63 in cell migration is also associated with its well-known regulatory function on integrin abundance at the membrane (Pols and Klumperman, 2009). In turn, correct integrin function and localization has been demonstrated to be required for CE movements in *Xenopus* (Marsden and DeSimone, 2003; Davidson *et al.*, 2006; Keller *et al.*, 2008). Thus, Cd63^{Y237A} might indirectly inhibit axial elongation and CE by negatively influencing integrin dynamics, potentially also in tissues normally not expressing *cd63* endogenously (i.e. in the neural plate during late neurula stages). In this context, it is important to mention that the observed phenotype (Figure 1B) is highly reminiscent of a CE defect as observed after blocking dishevelled (*dvl*) function specifically in the neural ectoderm. Upon *dvl* perturbation, neural folds also show apical constriction and medial movement at mid neurulation, but CE is not occurring in the midline in between (Wallingford and Harland, 2002). *Dvl* regulates CE in both floorplate and notochord by participating in the planar cell polarity pathway (PCP) via its PDZ protein interaction domain (Wallingford and Harland, 2001). Interestingly, Cd63 possesses a PDZ-binding motif in its C-terminus, which has been demonstrated to bind the PDZ domain of Syntenin-1 (Latysheva *et al.*, 2006; Pols and Klumperman, 2009). Syntenin-1, on the other hand, has been shown to interact with PDZ-binding domains of Syndecans, and Syndecan-4, a well-known regulator of PCP, is also involved in recycling of integrins, i.e. sharing a similar role with Cd63 (Grootjans *et al.*, 1997; Muñoz *et al.*, 2006; Morgan *et al.*, 2013). Future analyses will reveal whether there is a direct or indirect interaction of Cd63 with *Dvl* or Syntenin-1, which would also explain its effect on axial elongation during *Xenopus* neurulation.

Methods

[Request a detailed protocol](#)

Xenopus laevis care and maintenance

Frogs were purchased from Nasco (Fort Atkinson, WI, USA). Handling, care and experimental manipulations of animals was approved by the Regional Government Stuttgart, Germany (V349/18ZO ‘*Xenopus* Embryonen in der Forschung’), according to German regulations and laws (§6, article 1, sentence 2, nr. 4 of the animal protection act). To induce ovulation, female frogs were injected subcutaneously with 300-700 units of human chorionic gonadotropin (Sigma). Embryos were staged according to Nieuwkoop and Faber (1994). Only clutches of healthy embryos from healthy females were used for the experiments shown. Embryos from one batch were randomly picked and used as control or tested specimens.

Construct cloning, mRNA synthesis and microinjections

To generate an endosome-excluded version of *cd63*, the full-length *X. laevis* L-homeolog was isolated and the lysosomal targeting motif GYEVN was mutated to GAEVN by changing the codon TAT to GCT using the following primer pairs:

F1_5'-GAATTCATGGCGGTGGAAGG-3' (for both plasmids)

R1_5'-CTCGAGCGGTACATGACTTCAGCTCCA-3' (for CS2+ plasmid)

R2_5'-CTCGAGCGGTCCCATGACTTCAGCTCCA-3' (for CS2+/c-terminal eGFP plasmid)

PCR products were introduced into CS2+ or CS2+/c-terminal eGFP plasmids using *EcoRI* and *XhoI* enzymes. For mRNA synthesis, plasmids were linearized with *NotI* and transcribed *in vitro* (Sp6 polymerase) using Ambion message machine kit. Drop size was calibrated to 4 nl per injection. 560pg (for double injections in B) or 400pg (for single injections in A, C) of mRNA was injected.

In situ Hybridization

ISH probes for *X. laevis cd63* was used as described (Kreis *et al.*, 2020). For *in situ* mRNA detection, ISH was performed after fixation in MEMFA for 2-3 h at room temperature and processed following a standard protocol (Sive *et al.*, 2000). RNA *in situ* probes were transcribed using SP6 or T7 polymerases.

Embryo sections

For vibratome sections (thickness: 30-35 μ m), embryos were embedded in a glutaraldehyde-crosslinked gelatin-albumin mix (embedding medium: 2.2 g gelatine, 135 g bovine serum albumin, 90 g sucrose dissolved in 450 ml PBS) and razor blade-sectioned as indicated in whole-mount panels using a Leica VT1000S vibratome.

Photo Documentation

11/25/2020 - Open Access

Confocal images of fluorescence were taken with a Zeiss LSM 700 and adjusted using the Zeiss Zen 2012 Blue edition. Embryo pictures were taken with a Zeiss SteREO Discovery.V12 (whole embryos), or an Axioplan2 (sections) microscope using AxioVision 4.6. Adobe Photoshop CS6 was used for cropping and careful brightness adjustments. All figures were arranged using Adobe Illustrator CS6.

Statistical analysis

Statistical calculations were performed using Pearson's chi-square test. *= $p < 0.05$, **= $p < 0.01$, ***= $p < 0.001$ were used.

Acknowledgments: We like to thank V. Andre, A. Schäfer-Kosulja and S. Vogel for technical assistance, and the Blum Lab members for valuable feedback. The pax6 plasmid was a kind gift of Dr. T. Hollemann, the rfp-cd63/CS2 plasmid of Dr. N. Kinoshita.

References

- Basrur V, Yang F, Kushimoto T, Higashimoto Y, Yasumoto K, Valencia J, Muller J, Vieira WD, Watabe H, Shabanowitz J, Hearing VJ, Hunt DF, Appella E. 2003. Proteomic analysis of early melanosomes: identification of novel melanosomal proteins. *J Proteome Res* 2: 69-79. PMID: 12643545.
- Davidson LA, Marsden M, Keller R, Desimone DW. 2006. Integrin alpha5beta1 and fibronectin regulate polarized cell protrusions required for *Xenopus* convergence and extension. *Curr Biol* 16: 833-44. PMID: 16682346.
- Grootjans JJ, Zimmermann P, Reekmans G, Smets A, Degeest G, Dürr J, David G. 1997. Syntenin, a PDZ protein that binds syndecan cytoplasmic domains. *Proc Natl Acad Sci U S A* 94: 13683-8. PMID: 9391086.
- Jang HI, Lee H. 2003. A decrease in the expression of CD63 tetraspanin protein elevates invasive potential of human melanoma cells. *Exp Mol Med* 35: 317-23. PMID: 14508073.
- Keller R, Sutherland A. 2020. Convergent extension in the amphibian, *Xenopus laevis*. *Curr Top Dev Biol* 136: 271-317. PMID: 31959291.
- Keller R, Shook D, Skoglund P. 2008. The forces that shape embryos: physical aspects of convergent extension by cell intercalation. *Phys Biol* 5: 015007. PMID: 18403829.
- Kobayashi T, Vischer UM, Rosnoble C, Lebrand C, Lindsay M, Parton RG, Kruihof EK, Gruenberg J. 2000. The tetraspanin CD63/lamp3 cycles between endocytic and secretory compartments in human endothelial cells. *Mol Biol Cell* 11: 1829-43. PMID: 10793155.
- Kreis, J; Bonß, R; Vick, P (2020), The tetraspanin Cd63 is required for eye morphogenesis in *Xenopus*. *microPublication Biology*. DOI: 10.17912/micropub.biology.000335
- Latysheva N, Muratov G, Rajesh S, Padgett M, Hotchin NA, Overduin M, Berdichevski F. 2006. Syntenin-1 is a new component of tetraspanin-enriched microdomains: mechanisms and consequences of the interaction of syntenin-1 with CD63. *Mol Cell Biol* 26: 7707-18. PMID: 16908530.
- Lee RH, Iioka H, Ohashi M, Iemura S, Natsume T, Kinoshita N. 2007. XRab40 and XCullin5 form a ubiquitin ligase complex essential for the noncanonical Wnt pathway. *EMBO J* 26: 3592-606. PMID: 17627283.
- Lupia A, Peppicelli S, Witort E, Bianchini F, Carloni V, Pimpinelli N, Urso C, Borgognoni L, Capaccioli S, Calorini L, Lulli M. 2014. CD63 tetraspanin is a negative driver of epithelial-to-mesenchymal transition in human melanoma cells. *J Invest Dermatol* 134: 2947-2956. PMID: 24940653.
- Marsden M, DeSimone DW. 2003. Integrin-ECM interactions regulate cadherin-dependent cell adhesion and are required for convergent extension in *Xenopus*. *Curr Biol* 13: 1182-91. PMID: 12867028.
- Morgan MR, Hamidi H, Bass MD, Warwood S, Ballestrem C, Humphries MJ. 2013. Syndecan-4 phosphorylation is a control point for integrin recycling. *Dev Cell* 24: 472-85. PMID: 23453597.
- Muñoz R, Moreno M, Oliva C, Orbenes C, Larraín J. 2006. Syndecan-4 regulates non-canonical Wnt signalling and is essential for convergent and extension movements in *Xenopus* embryos. *Nat Cell Biol* 8: 492-500. PMID: 16604063.
- Nieuwkoop, P. D. and Faber, J. (1994). *Normal Table of Xenopus laevis (Daudin)* Garland Publishing Inc, New York ISBN 0-8153-1896-0
- Pols MS, Klumperman J. 2009. Trafficking and function of the tetraspanin CD63. *Exp Cell Res* 315: 1584-92. PMID: 18930046.
- Radford KJ, Thorne RF, Hersey P. 1997. Regulation of tumor cell motility and migration by CD63 in a human melanoma cell line. *J Immunol* 158: 3353-8. PMID: 9120293.
- Raposo G, Marks MS. 2007. Melanosomes--dark organelles enlighten endosomal membrane transport. *Nat Rev Mol Cell Biol* 8: 786-97. PMID: 17878918.

11/25/2020 - Open Access

Rous BA, Reaves BJ, Ihrke G, Briggs JA, Gray SR, Stephens DJ, Banting G, Luzio JP. 2002. Role of adaptor complex AP-3 in targeting wild-type and mutated CD63 to lysosomes. *Mol Biol Cell* 13: 1071-82. PMID: 11907283.

Simons M, Raposo G. 2009. Exosomes--vesicular carriers for intercellular communication. *Curr Opin Cell Biol* 21: 575-81. PMID: 19442504.

Sive, H. L., Grainger, R. M. and Harland, R. M. (2000). *Early Development of Xenopus Laevis*. Cold Spring Harbor Laboratory Press. ISBN: 9780879695040

Termini CM, Gillette JM. 2017. Tetraspanins Function as Regulators of Cellular Signaling. *Front Cell Dev Biol* 5: 34. PMID: 28428953.

Van Niel G, Charrin S, Simoes S, Romao M, Rochin L, Saftig P, Marks MS, Rubinstein E, Raposo G. 2011. The tetraspanin CD63 regulates ESCRT-independent and -dependent endosomal sorting during melanogenesis. *Dev Cell* 21: 708-21. PMID: 21962903.

Wallingford JB, Harland RM. 2001. *Xenopus* Dishevelled signaling regulates both neural and mesodermal convergent extension: parallel forces elongating the body axis. *Development* 128: 2581-92. PMID: 11493574.

Wallingford JB, Harland RM. 2002. Neural tube closure requires Dishevelled-dependent convergent extension of the midline. *Development* 129: 5815-25. PMID: 12421719.

Funding: J.K. was a recipient of a Ph.D. fellowship from the Landesgraduiertenförderung Baden-Württemberg.

Author Contributions: Jennifer Kreis: Formal analysis, Investigation, Validation, Writing - review and editing, Visualization. Ramona Bonß: Investigation, Validation. Kerstin Feistel: Writing - review and editing, Investigation. Philipp Vick: Conceptualization, Investigation, Methodology, Project administration, Supervision, Validation, Writing - original draft.

Reviewed By: Anonymous

History: Received August 26, 2020 **Revision received** November 17, 2020 **Accepted** September 22, 2020 **Published** November 25, 2020

Copyright: © 2020 by the authors. This is an open-access article distributed under the terms of the Creative Commons Attribution 4.0 International (CC BY 4.0) License, which permits unrestricted use, distribution, and reproduction in any medium, provided the original author and source are credited.

Citation: Kreis, J; Bonß, R; Feistel, K; Vick, P (2020). Expression of an endosome-excluded Cd63 prevents axis elongation in *Xenopus*. *microPublication Biology*. <https://doi.org/10.17912/micropub.biology.000334>

Discussion

This compilation of studies provides an insight in the versatile function of Rab7 and LEs during early embryonic development. Analyses during mesoderm specification revealed that Rab7 acts as essential mediator in Wnt and FGF signal transduction in distinct mesodermal tissues. After mesoderm specification Cd63, another LE-related protein, suggests the importance of these compartments in axial and eye development.

Rab7 knockdown does not affect development before zygotic gene activation

All data acquisitions presented here share a common feature, none of the knockdown approaches interfered with early maternal signal transduction to set up the dorsoventral body axis. Neither deficiency of Rab7 nor that of Cd63 resulted in dorsalized or ventralized embryos. Proper axis establishment, especially dorsal specification requires Wnt signaling activity (Heasman et al., 1994; Moon, 2005; Yost et al., 1996). As Wnt signal transduction was linked to late endosomal compartments (Taelman et al., 2010), the lack of an early altered axis phenotype was unexpected. Thus two different scenarios are conceivable: oocytes contain deposited Rab7 protein capable to associate with endosomes to mediate maternal Wnt signaling or endosomes are circumvented as signaling platforms in such early stages.

Along the lines of the first scenario, already present MO-insensitive Rab7 protein could allow regular endosome maturation, thus ensuring destruction complex internalization in LEs/MVBs to maintain Wnt signaling. One could also hypothesize that maternal Rab7 protein exists on already mature endosomes in agreement with Dobrowolski and De Robertis who assumed MVBs opposite to the sperm entry point. Upon fertilization Wnt determinants tethered to maternally deposited EEs could travel along microtubules from vegetal to the future dorsal side. As MVBs and EEs meet, EE

incorporation would occur and sequestration of captured Gsk3 takes places. Hence, Wnt signal transduction is ensured due to spatial separation of the destruction complex from cytoplasmic Ctnnb1 (Dobrowolski and De Robertis, 2012).

The second scenario postulated by Li and colleagues excludes endosomes in signal transduction, due to a fast acting response of an incoming Wnt signal. In this model Wnt stimulation results in Ctnnb1 saturation at destruction complexes accompanied by blocked ubiquitination. Since Ctnnb1 would then remain at the destruction complexes without being tagged for degradation by the proteasome, newly synthesized Ctnnb1 could accumulate (Clevers and Nusse, 2012; Li et al., 2012). In either case, *rab7* knockdown could not interfere in Wnt signal transduction and therefore normal axis determination as observed.

Dorsal organizer induction is a result of early dorsoventral axis establishment. This signaling center originates upon joint pathway activity of Wnt and TGF- β signaling (Nishita et al., 2000). However, Rab7 deficiency did not impact on organizer formation, either. The above mentioned settings provide an explanation, why loss of *rab7* is not able to interfere with the Wnt-dependent induction. As there is no indication of Rab7-associated LEs in TGF- β signal transduction so far, alterations in organizer induction in terms of this pathway were unexpected anyhow. Nonetheless, one cannot exclude a still undiscovered function of LEs as signaling platforms for TGF- β signaling. Maybe, such signal transduction is required in other developmental contexts, which have not been investigated yet.

LE-associated Rab7 facilitates mesoderm specification after midblastula transition

The first severe phenotypic alterations in the absence of Rab7 occurred at the onset of gastrulation. *rab7*-depleted embryos suffered from GDs, as depicted by suppressed

mesodermal gene expression. Since Wnt signaling activity is downregulated dorsally in favor of neural development after organizer induction, the following conclusions were related to the emerging ventrolateral Wnt activity. Zygotic Wnt activity, which participates in mesoderm patterning, is substantiated by *wnt family member 8 (wnt8)* expression in the ventrolateral mesoderm (Smith and Harland, 1991). Analyses of mesodermal markers in *rab7*-morphant specimens revealed impaired expression of Wnt-dependent genes, apposite to the requirement of LEs in Wnt signal transduction. Expression of ventrolateral *myod1* and lateral *myogenic factor 5 (myf5)* is subjected to Wnt8 regulation and it was shown that inhibition of Wnt pathway components diminished transcripts of both transcription factors (Hoppler et al., 1996; Shi et al., 2002) in a similar manner as in the *rab7* LOF. Further, epistatic analyses with downstream *Ctnnb1* underlined Rab7-mediated Wnt-dependent specification of the ventrolateral mesoderm. The partial rescue capacity by lithium chloride of dorsolateral fates in morphant embryos suggested a regulative function of Rab7 in other pathways, participating in dorsal mesoderm specification, as well. One putative relevant signaling pathway is FGF signaling, as its activity contributes to mesodermal development as well as in anteroposterior patterning (Christen and Slack, 1997; Harland, 2004). An overlapping and/or intertwining function of Wnt and FGF signaling has been described in several scenarios (Domingos et al., 2001; Hong et al., 2008; Kjolby et al., 2019; ten Berge et al., 2008), which is also true for some of the here analyzed genes during gastrulation. *forkhead J1 (foxj1)* and *tbxt*, two known Wnt targets are likewise dorsally regulated by *Fgfr1* activity downstream of Nodal homolog 3 (Nodal3) (Glinka et al., 1996; Kjolby and Harland, 2017; Schneider et al., 2019; Smith et al., 1995; Vick et al., 2018; Walentek et al., 2012; Yamaguchi et al., 1999; Yokota et al., 2003). Even paraxial Wnt-dependent *myf5* and *myod1* require additional FGF signals for induction in the somitic/dorsolateral mesoderm (Hoppler et al., 1996; Osborn et al., 2020; Shi et

al., 2002). Kjolby and colleagues recently demonstrated that Wnt-dependent ring- and horseshoe-shaped mesodermal genes, all harbor additional Ets2 binding sites, making them responsive to FGF signaling. However, binding sites of the transcription factor and nuclear adaptor for Ctnnb1 T-cell factor (TCF) is located more proximal in the promoter region of horseshoe genes compared to ring-shaped genes. As TCFs usually act as transcriptional repressors in absence of Wnt i.e. nuclear Ctnnb1, repression of ring-shaped genes can be overcome by FGF components whereas the stronger repressive state in the dorsal most region leading to the horseshoe pattern cannot be overruled by Ets2 (Kjolby et al., 2019). Based on these perceptions one can conclude that Rab7 LOF in the dorsal most/axial regions caused a mere FGF phenotype, whereas knockdown in the dorsolateral/paraxial domains affects Wnt and FGF signaling equally. This could provide an explanation of the strong rescue capacity of the downstream FGF pathway components Ets2 and Erk/Mapk1 of ring- and horseshoe-shaped *tbxt* and *myod1* in the axial and paraxial domains of Rab7-deficient embryos.

Rab7-mutant mice likewise depict conditions of failed mesoderm specification during gastrulation (Kawamura et al., 2012 and 2020), which could imply a conserved cross-species function of LE-associated Rab7 in such developmental processes in general. Analyses in the mouse model confirmed that mesoderm specification depends on Rab7-mediated Wnt signaling as well. The authors showed that endocytic clearance of the Wnt antagonist Dickkopf (Dkk) was essential to facilitate spatial pathway activity thereby promoting mesodermal patterning. Knockout mice failed to remove Dkk proteins via endocytosis and delivery to vacuoles for degradation. Of note, these vacuoles are the equivalent to the late endosomal compartments and seemed to be impaired as these structures are fragmented in the absence Rab7 (Kawamura et al., 2020). Unfortunately, the authors did not investigate the intracellular signal

transduction of Wnt or other pathways. The fragmentation of vacuoles in Rab7-mutant mice could likewise indicate lost integrity of the endosomal machinery, thus compromising the ability of signal propagation on their endosomal platforms. As suggested by our data this might not only have implications for the Wnt signal transduction but for other pathways as well. Although the authors did not rule out other pathways entirely (Kawamura et al., 2012 and 2020), they did not test for a specific role of Rab7 in FGF signaling, but instead analyzed the expression of *fgf8* and *sprouty RTK signaling antagonist 2 (spry2)*, which were unaffected. Importantly, similar to our results pan-mesodermal *tbxt* was severely affected in the absence of Rab7 (Kawamura et al., 2012 and 2020) and expression of this gene is regulated by Wnt and FGF signaling as mentioned before (Glinka et al., 1996; Kjolby and Harland, 2017; Schneider et al., 2019; Smith et al., 1995; Vick et al., 2018; Walentek et al., 2012; Yamaguchi et al., 1999; Yokota et al., 2003). Our data depicted that impaired *tbxt* expression in *Xenopus* could be rescued by FGF pathway components. If there is a conserved function across species, FGF/MAPK signaling could also be impaired in mice during mesoderm development. This assumption would even be more plausible as the results of another research group showed that knockout of the lipid raft adaptor Lamtor1/p18, a scaffold to anchor components of the MAPK signaling to LEs, caused a similar phenotype as Rab7 deficiency in mice. Knockout of either Rab7 or Lamtor1/p18 led to embryonic death during gastrulation in corresponding stages. In both knockout scenarios, this early lethality was a result of severely affected endosomal transport in the visceral endoderm as the intracellular compartment composition was disturbed (Kawamura et al., 2012 and 2020; Nada et al., 2009). Such defects of intracellular endosomal transport in the visceral endoderm prevented elongation of the primitive streak and anteroposterior patterning failed (Kawamura et al., 2012 and 2020).

The data from this study clearly depict the requirement of Rab7-mediated Wnt and FGF signaling in mesoderm specification and subsequent axial elongation. Since both pathways are active during gastrulation in the same tissue, it seems to be of great interest how such signals are orchestrated or intertwined. Stulberg and colleagues investigated crosstalk between these pathways and stated that a hierarchical placement to each other is difficult. Wnt as well as FGF signaling positively regulate each other. Phosphorylation of the Wnt pathway member Gsk3 increased Erk/Mapk1 phosphorylation and conversely FGF signals promoted Wnt signaling by inhibiting the pathways antagonists such as Dkk. Although, they ascertained that genes which are accessed by both pathways are mostly regulated contrarily. Therefore, a balanced regulation of Wnt and FGF is crucial to maintain a reciprocal signaling activity in order to ensure axial elongation and somitogenesis (Stulberg et al., 2012). Hence, integrity of Rab7-associated LEs as signaling platforms contributes to maintain balanced activity levels of both pathways.

In summary, mesoderm specification during gastrulation relies on Rab7-mediated signal activity of the Wnt and FGF pathways: ventral mesoderm is primarily regulated by Wnt activity and dorsolateral mesoderm most likely requires intracellular signal transduction of both pathways, whereas dorsal mesoderm putatively depends on FGF signals.

LEs as crucial signaling platforms of Wnt and FGF pathway activation during mesoderm specification

Wnt as well as FGF signaling are two essential pathways in mesoderm specification and proper signal transduction of these pathways is linked to Rab7. Besides its cytoplasmic and mostly inactive fraction, Rab7 commonly exerts its function associated to LEs (Rink et al., 2005; Zerial and McBride., 2001; Zhang et al., 2009). LEs are

characterized by their multivesicular structure, which is mediated by members of the ESCRT machinery. A connection to Wnt signaling was established for two of them: Hepatocyte growth factor-regulated tyrosine kinase substrate (Hrs) and Vacuolar protein sorting 4 homolog (Vps4) (Taelman et al., 2010). The first initiates complex formation of an ESCRT protein and the latter is essential for complex disassembly allowing excision of vesicles into LEs (Katzmann et al., 2002). Dysfunction of either component prevents ILV formation and therefore separation of the destruction complexes to propagate Wnt signaling. Attenuation of Hrs and Vps4 depicted a similar alteration of Wnt-dependent genes like in a *rab7* knockdown situation. Additionally, epistatic analyses revealed that the Wnt-dependent mesoderm specification facilitated by Rab7 is mediated via LEs.

In terms of FGF signal transduction, LEs are likely involved as signaling platforms, too. Components of the related EGF pathway have been shown to colocalize with (early) endosomal membranes (Jiang and Sorkin, 2002; Lu et al., 2009). Increasing size of Ras aggregates upon FGF stimulation implies an activated endosomal machinery. Ras was distributed to the same vesicular structures as GPI-anchored GFP used in our analyses, indicating an internalization to endosomal compartments (Chatterjee and Mayor, 2001; Sabharanjak et al., 2002). Rab7 deficiency inhibits GFP accumulation in larger intracellular structures, which may indicate a similar scenario as reported in mice. As endocytic uptake was blocked upon *rab7* knockout in mice (Kawamura et al., 2020), lost distribution of Ras in larger aggregates could as well be due to malfunctioning endocytosis. Interestingly, pathway components like Ras and Erk/Mapk1 were also noticed at late endosomal membranes to exert signaling activity (Lu et al., 2009; Nada et al., 2009). Our investigations of Rab7 placed its function between these two FGF pathway components, indicating signal transduction via LEs. Since the outer limiting membranes of LEs are crucial in correct FGF/MAPK signal

transduction, an involvement of the ESCRT machinery as shown for Wnt signaling seems elusive here (Katzmann et al., 2002; Taelman et al., 2010). Nevertheless, a requirement of ESCRTs could theoretically be conceivable for FGF signaling in terms of spatial separation of an inhibitor, too. Thus intraluminal incorporation of Spry, an inhibitor of MAPK signaling, could likewise promote FGF signal transduction as the relocalization of Gsk3 from the cytoplasm into ILVs in Wnt signaling does (Platta and Stenmark, 2011; Taelman et al., 2010; Vinyoles et al., 2014). However, neither MAPK components nor Spry have been reported inside of LEs, i.e. colocalized with ILV markers. Taken together, this creates a line of evidence that Rab7-regulated LEs constitute a crucial signaling platform not only for Wnt but also FGF signaling to ensure mesoderm specification.

Cd63 suggests a requirement of LEs in development beyond mesoderm specification

cd63 encodes a tetraspanin and exhibits an expression pattern mainly similar to *rab7* (Kreis et al., 2020a; 2020b and 2021). Both proteins exert regulative functions associated with LEs, indicating a requirement of this compartment for developmental processes. Indeed, Cd63 protein not only localizes to LEs and lysosomes, moreover, it is present in TEMs at the cell surface (Pols and Klumperman, 2009). This broad cellular abundance of Cd63 provides various regulative functions. Nonetheless, first alterations of embryonic development were detected during neurulation, when a mutant *cd63* construct was introduced. Overexpression of an endosome-excluded *cd63* resulted in impaired dorsal mesoderm elongation, whereas MO-mediated knockdown did not induce an axial phenotype. In our notion, knockdown of Cd63 should affect LE functionality and thus preventing necessary signal transduction to promote axis elongation, presumably similar to Rab7 deficiency as previously noted

(Kreis et al., 2021). The lack of a comparable knockdown phenotype could be the result of a compensatory effect by another tetraspanin family member. Cd9, a tetraspanin present on RNA and protein level in the corresponding stages, could likely compensate a loss of Cd63 (Peshkin et al., 2019). Silencing of Cd9 in T-cells attenuated phosphorylation of Erk/Mapk1 (Rocha-Perugini et al., 2014), thus providing an interesting link between tetraspanins and FGF-dependent axial development. Structural analyses of the promotor region of *cd63* revealed potential Ras-responsive elements (Hotta et al., 1992), which could allow a positive feedback loop as seen with countless other signaling pathway components in general. If LEs acted as operative signaling platforms, mutant Cd63 retained at the plasma membrane could intercept Cd63 interactors needed for normal LE-associated function, ultimately resulting in inhibited axial elongation. Additionally, retention at the plasma membrane could promote signaling by binding several adaptors, which otherwise would not have been accessed. Such pathway activations might also explain phenotypic differences to the *cd63* LOF.

The emerging eye phenotype in tadpoles caused by *cd63* deficiency was phenocopied by the mutant Cd63. As *rab7* knockdown impaired correct eye development as well, one can hypothesize that such defects are likewise occurring by a malfunctioning late endosomal compartment. This could indicate a compromised function of specialized LEs, namely melanosomes, which contribute to the formation of the optic system and retinal function. Apart from their function in eye development melanosomes constitute intracellular compartments of melanophores, the equivalent of higher vertebrates' melanocytes (Raposo and Marks, 2007). In amphibians, these specific cell types originate from trunk neural crests and migrate laterally to their destination during development (Colazzo et al. 1993). Although *cd63* expression analysis revealed a high enrichment in trunk neural crests, loss of this tetraspanin did not change their migratory

behavior nor their appearance. This may also be caused by a compensational effect, which was put forward before in skin melanocytes of mice suffering from defects in melanogenesis (Lopes et al., 2007). Conversely, this implies that eye formation probably lacks such a compensatory mechanism in terms of Cd63, and thus is more sensitive to alterations of normal development.

In contrast to the *rab7* LOF, analyses concerning a gain or loss of Cd63 did not reveal phenotypic alterations which could be clearly associated to impaired Wnt or FGF signal transduction. To date, evidence is scarce for a Cd63 participation in FGF signaling. This could be due to the fact, that the LE-associated fraction of Cd63 is primarily found in ILVs of these MVBs and FGF signal transduction occurs at the outer limiting membrane of such LEs. Thus, there may not be any level of interaction, even if there is a common localization at the same endosomal compartment. The lack of an early phenotype made it puzzling to draw conclusions in terms of Wnt signaling. Again, a connection to Wnt signaling could be obscured by the absence of a phenotype due to compensation by another tetraspanin during gastrulation.

However, the disturbed eye morphogenesis of tadpoles upon Cd63 LOF may offer a link to Wnt signaling, as retinal stem cell properties are provided by signals of this pathway (Denayer et al., 2008; Van Raay and Vetter, 2004).

Even though, Rab7 and Cd63 are both associated to LEs and thus exert functions in the same tissues and processes. The here noted investigations clearly demonstrated interesting differences in their mode of action. The variety of knockdown phenotypes could be the outcome of interactions with a number of different adaptors, effectors and/or binding partners to facilitate specific functions at a specific time.

Conclusion

The objective of this study was to investigate the necessity of the late endosomal machinery to mediate intracellular signal transduction. The presented examples here demonstrate the requirement of LE-associated Rab7 in various mesodermal tissues in *Xenopus laevis*. Rab7-regulated LEs operate as signaling platforms to facilitate Wnt and FGF signals to promote correct mesoderm specification. Further analyses regarding Cd63 revealed that signal transduction via LEs could constitute a crucial feature of early developmental processes more generally.

References

- Agius, E., Oelgeschläger, M., Wessely, O., Kemp, C., De Robertis, E. M. (2000). Endodermal Nodal-related signals and mesoderm induction in *Xenopus*. *Development* 127 (6), 1173-1183.
- Amaya, E., Musci, T. J. and Kirschner, M. W. (1991). Expression of a dominant negative mutant of the FGF receptor disrupts mesoderm formation in *Xenopus* embryos. *Cell* 66 (2), 257-270.
- Amaya, E., Stein, P. A., Musci, T. J. and Kirschner, M. W. (1993). FGF signalling in the early specification of mesoderm in *Xenopus*. *Development* 118, 447-487.
- Arjonen, A., Alanko, J., Veltel, S. and Ivaska, J. (2012). Distinct recycling of active and inactive $\beta 1$ integrins. *Traffic* 13, 610-625.
- Auciello, G., Cunningham, D. L., Tatar, T., Heath, J. K. and Rappoport, J. Z. (2013). Regulation of fibroblast growth factor receptor signalling and trafficking by Src and Eps8. *Journal of Cell Science* 126, 613-624.
- Babst, M. (2011). MVB vesicle formation: ESCRT-dependent, ESCRT-independent and everything in between. *Current Opinion in Cell Biology* 23, 452-457.
- Basrur, V., Yang, F., Kushimoto, T., Higashimoto, Y., Yasumoto, K.-I., Valencia, J., Muller, J., Vieira, W. D., Watabe, H., Shabanowitz, J., Hearing, V. J., Hunt, D. F., Appella, E. (2003). Proteomic analysis of early melanosomes: identification of novel melanosomal proteins. *J. Proteome Res.* 2, 69-79.
- Beyer, T., Danilchik, M., Thumberger, T., Vick, P., Tisler, M., Schneider, I., Bogusch, S., Andre, P., Ulmer, B., Walentek, P., Niesler, B., Blum, M., Schweickert, A. (2012). Serotonin Signaling Is Required for Wnt-Dependent GRP Specification and Leftward Flow in *Xenopus*. *Current Biology* 22, 33-39.
- Biechele, T. L., Adams, A. M. and Moon, R. T. (2009). Transcription-based reporters of Wnt/beta-catenin signaling. *Cold Spring Harbor Protocols*, pdb.prot5223.
- Bilić, J., Huang, Y.-L., Davidson, G., Zimmermann, T., Cruciat, C.-M., Bienz, M. and Niehrs, C. (2007). Wnt Induces LRP6 Signalosomes and Promotes Dishevelled-Dependent LRP6 Phosphorylation. *Science* 316 (5831), 1619-1622.
- Bishop, N. and Woodman, P. (2000). ATPase-defective mammalian VPS4 localizes to aberrant endosomes and impairs cholesterol trafficking. *Mol. Biol. Cell* 11, 227-239.
- Böttcher, R. T. and Niehrs, C. (2005). Fibroblast growth factor signaling during early vertebrate development. *Endocr Rev* 26 (1), 63-77.

- Borday, C., Parain, K., Thi Tran, H., Vleminckx, K., Perron, M. and Monsoro-Burq, A. H. (2018). An atlas of Wnt activity during embryogenesis in *Xenopus tropicalis*. PLoS ONE 13, e0193606.
- Bruce, A. E. E. and Winklbauer, R. (2020). Brachyury in the gastrula of basal vertebrates. Mechanisms of Development 163, 103625.
- Brunt, L. and Scholpp, S. (2018). The function of endocytosis in Wnt signaling. Cell. Mol. Life Sci. 75, 785-795.
- Burke, P., Schooler, K., Wiley, H. S. (2001). Regulation of epidermal growth factor receptor signaling by endocytosis and intracellular trafficking. Mol Biol Cell 12 (6), 1897-1910.
- Burstyn-Cohen, T., Stanleigh, J., Sela-Donenfeld, D. and Kalcheim, C. (2004). Canonical Wnt activity regulates trunk neural crest delamination linking BMP/noggin signaling with G1/S transition. Development 131, 5327-5339.
- Butler, M. T. and Wallingford, J. B. (2017). Planar cell polarity in development and disease. Nat Rev Mol Cell Biol 18, 375-388.
- Chatterjee, S. and Mayor, S. (2001). The GPI-anchor and protein sorting. Cell Mol Life Sci 58 (14), 1969-1987.
- Christen, B. and Slack, J. M. (1997). FGF-8 is associated with anteroposterior patterning and limb regeneration in *Xenopus*. Dev Biol 192 (2), 455-466.
- Clevers, H. and Nusse, R. (2012). Wnt/ β -catenin signaling and disease. Cell 149, 1192-1205.
- Collazo, A., Bronner-Fraser, M. and Fraser, S. E. (1993). Vital dye labelling of *Xenopus laevis* trunk neural crest reveals multipotency and novel pathways of migration. Development 118, 363-376.
- Conlon, F. L., Sedgwick, S. G., Weston, K. M., Smith, J. C. (1996). Inhibition of Xbra transcription activation causes defects in mesodermal patterning and reveals autoregulation of Xbra in dorsal mesoderm. Development 122 (8), 2427-2435.
- Cullen, P. J. and Steinberg, F. (2018). To degrade or not to degrade: mechanisms and significance of endocytic recycling. Nat Rev Mol Cell Biol 19 (11), 679-696.
- Cuykendall, T. N. and Houston, D. W. (2009). Vegetally localized *Xenopus* trim36 regulates cortical rotation and dorsal axis formation. Development 136 (18), 3057-3065.
- Dale, L. (1997). Development: morphogen gradients and mesodermal patterning. Curr Biol 7 (11), 698-700.

- Dale, L. and Jones C. M. (1999). BMP signalling in early *Xenopus* development. *BioEssays* 21, 751-760.
- Davidson, L. A., Marsden, M., Keller, R., Desimone, D. W. (2006). Integrin alpha5beta1 and fibronectin regulate polarized cell protrusions required for *Xenopus* convergence and extension. *Curr Biol* 16, 833-844.
- Denayer, T., Locker, M., Borday, C., Deroo, T., Janssens, S., Hecht, A., van Roy, F., Perron, M., Vleminckx, K. (2008). Canonical Wnt signaling controls proliferation of retinal stem/progenitor cells in postembryonic *Xenopus* eyes. *Stem Cells* 26 (8), 2063-2074.
- Dessaud, E., McMahon, A. P. and Briscoe, J. (2008). Pattern formation in the vertebrate neural tube: a sonic hedgehog morphogen-regulated transcriptional network. *Development* 135, 2489-2503.
- De Robertis, E. M. (2009). Spemann's organizer and the self-regulation of embryonic fields. *Mech Dev* 126 (11-12), 925-941.
- De Robertis, E. M. and Kuroda, H. (2004). Dorsal-ventral patterning and neural induction in *Xenopus* embryos. *Annu Rev Cell Dev Biol* 20, 285-308.
- Di Guglielmo, G. M., Baass, P. C., Ou, W. J., Posner, B. I., Bergeron, J. J. (1994). Compartmentalization of SHC, GRB2 and mSOS, and hyperphosphorylation of Raf-1 by EGF but not insulin in liver parenchyma. *EMBO J* 13 (18), 4269-4277.
- Dobrowolski, R. and De Robertis, E. M. (2011). Endocytic control of growth factor signalling: multivesicular bodies as signalling organelles. *Nature Publishing Group* 13, 53-60.
- Domingos, P. M., Itasaki, N., Jones, C. M., Mercurio, S., Sargent, M. G., Smith, J. C., Krumlauf, R. (2001). The Wnt/beta-catenin pathway posteriorizes neural tissue in *Xenopus* by an indirect mechanism requiring FGF signaling. *Dev Biol* 239 (1), 148-160.
- Dorey, K. and Amaya, E. (2010). FGF signalling: diverse roles during early vertebrate embryogenesis. *Development* 137 (22), 3731-3742.
- Dosch, R., Gawantka, V., Delius, H., Blumenstock, C., Niehrs, C. (1997). Bmp-4 acts as a morphogen in dorsoventral mesoderm patterning in *Xenopus*. *Development* 124 (12), 2325-2334.
- Elkin, S. R., Lakoduk, A. M. and Schmid, S. L. (2016). Endocytic pathways and endosomal trafficking: a primer. *Wien Med Wochenschr* 166 (7-8), 196-204.
- Fagotto, F. (2020). Tissue segregation in the early vertebrate embryo. *Seminars in Cell & Developmental Biology* 107, 130-146.

- Fagotto, F., Guger, K. and Gumbiner, B. M. (1997). Induction of the primary dorsalizing center in *Xenopus* by the Wnt/GSK/beta-catenin signaling pathway, but not by Vg1, Activin or Noggin. *Development* 124, 453-460.
- Fehrenbacher, N., Bar-Sagi, D. and Philips, M. (2009). Ras/MAPK signaling from endomembranes. *Molecular Oncology* 3, 297-307.
- Fletcher, R. B. and Harland, R. M. (2008). The Role of FGF Signaling in the Establishment and Maintenance of Mesodermal Gene Expression in *Xenopus*. *Developmental Dynamics* 237, 1243-1254.
- Fürthauer, M. and González-Gaitán, M. (2009). Endocytic Regulation of Notch Signalling During Development. *Traffic* 10, 792-802.
- Fürthauer, M., Thisse, C., Thisse, B. (1997). A role for FGF-8 in the dorsoventral patterning of the zebrafish gastrula. *Development* 124 (21), 4253-4264.
- Gallwitz, D., Donath, C., Sander, C. (1983). A yeast gene encoding a protein homologous to the human c-has/bas proto-oncogene product. *Nature* 306 (5944), 704-707.
- Gawantka, V., Delius, H., Hirschfeld, K., Blumenstock, C., Niehrs, C. (1995). Antagonizing the Spemann organizer: role of the homeobox gene *Xvent-1*. *EMBO* 14 (24), 6268-6279.
- Glinka, A., Delius, H., Blumenstock, C. and Niehrs, C. (1996). Combinatorial signalling by *Xwnt-11* and *Xnr3* in the organizer epithelium. *Mechanisms of Development* 60, 221-231.
- Glinka, A., Wu, W., Delius, H., Monaghan, A. P., Blumenstock, C. and Niehrs, C. (1998). *Dickkopf-1* is a member of a new family of secreted proteins and functions in head induction. *Nature* 391, 357-362.
- Glinka, A., Wu, W., Onichtchouk, D., Blumenstock, C., Niehrs, C. (1997). Head induction by simultaneous repression of *Bmp* and *Wnt* signalling in *Xenopus*. *Nature* 389 (6650), 517-519.
- Grootjans, J. J., Zimmermann, P., Reekmans, G., Smets, A., Degeest, G., Dürr, J., David, G. (1997). Syntenin, a PDZ protein that binds syndecan cytoplasmic domains. *Proc Natl Acad Sci U S A* 94, 13683-13688.
- Guerra, F. and Bucci, C. (2016). Multiple Roles of the Small GTPase Rab7. *Cells* 5 (3), 34.
- Hanson, P. I. and Cashikar, A. (2012). Multivesicular Body Morphogenesis. *Annu. Rev. Cell Dev. Biol.* 28, 337-362.
- Harland, R. M. (2004). Dorsoventral patterning of the mesoderm. In *Gastrulation: from Cells to Embryo*. Cold Spring Harbor Laboratory Press, 373-388.

- Heasman, J., Crawford, A., Goldstone, K., Garner-Hamrick, P., Gumbiner, B., McCrea, P., Kintner, C., Noro, C. Y. and Wylie, C. (1994). Overexpression of cadherins and underexpression of beta-catenin inhibit dorsal mesoderm induction in early *Xenopus* embryos. *Cell* 79, 791-803.
- Heasman, J., Kofron, M. and Wylie, C. (2000). Beta-catenin signaling activity dissected in the early *Xenopus* embryo: a novel antisense approach. *Developmental Biology* 222, 124-134.
- Hikasa, H. and Sokol, S. Y. (2013). Wnt Signaling in Vertebrate Axis Specification. *Cold Spring Harbor Perspectives in Biology* 5 (1), a007955.
- Hoepfner, S., Severin, F., Cabezas, A., Habermann, B., Runge, A., Gillyooly, D., Stenmark, H., Zerial, M. (2005). Modulation of receptor recycling and degradation by the endosomal kinesin KIF16B. *Cell* 121 (3), 437-450.
- Hotta, H., Miyamoto, H., Hara, I., Takahashi, N., Homma, M. (1992). Genomic structure of the ME491/CD63 antigen gene and functional analysis of the 5'-flanking regulatory sequences. *Biochem Biophys Res Commun* 185 (1), 436-442.
- Hemmati-Brivanlou, A. and Thomsen, G. H. (1995). Ventral mesodermal patterning in *Xenopus* embryos: expression patterns and activities of BMP-2 and BMP-4. *Dev Genet* 17 (1), 78-89.
- Hong, C.-S., Park, B.-Y., Saint-Jeannet, J.-P. (2008). Fgf8a induces neural crest indirectly through the activation of Wnt8 in the paraxial mesoderm. *Development* 135 (23), 3903-3910.
- Honoré, S. M., Aybar, M. J. and Mayor, R. (2003). Sox10 is required for the early development of the prospective neural crest in *Xenopus* embryos. *Developmental Biology* 260, 79-96.
- Hoppler, S., Brown, J. D. and Moon, R. T. (1996). Expression of a dominant-negative Wnt blocks induction of MyoD in *Xenopus* embryos. *Genes & Development* 10, 2805-2817.
- Hoppler, S. and Moon, R. T. (1998). BMP-2/-4 and Wnt-8 cooperatively pattern the *Xenopus* mesoderm. *Mechanisms of Development* 71, 119-129.
- Horner, D. S., Pasini, M. E., Beltrame, M., Mastrodonato, V., Morelli, E. and Vaccari, T. (2018). ESCRT genes and regulation of developmental signaling. *Seminars in Cell & Developmental Biology* 74, 29-39.
- Huotari, J. and Helenius, A. (2011). Endosome maturation. *The EMBO Journal* 30, 3481-3500.
- Hurley, J. H., Hanson, P. I. (2010). Membrane budding and scission by the ESCRT machinery: it's all in the neck. *Nat Rev Mol Cell Biol* 11 (8), 556-566.
- Hurwitz, S. N., Cheerathodi, M. R., Nkosi, D., York, S. B. and Meckes, D. G. Jr. (2018). Tetraspanin CD63 Bridges Autophagic and Endosomal Processes To Regulate Exosomal

Secretion and Intracellular Signaling of Epstein-Barr Virus LMP1. *Journal of Virology* 92 (5), e01969-17.

Iemura, S., Yamamoto, T. S., Takagi, C., Uchiyama, H., Natsume, T., Shimasaki, S., Sugino, H., Ueno, N. (1998). Direct binding of follistatin to a complex of bone-morphogenetic protein and its receptor inhibits ventral and epidermal cell fates in early *Xenopus* embryo. *Proc Natl Acad Sci U S A* 95 (16), 9337-9342.

Itoh, K. and Sokol, S. Y. (1999). Axis determination by inhibition of Wnt signaling in *Xenopus*. *Genes & Development* 13, 2328-2336.

Jang, H.-I. and Lee, H. (2003). A decrease in the expression of Cd63 tetraspanin protein elevates invasive potential of human melanoma cells. *Exp Mol Med* 35, 317-323.

Jiang, X. and Sorkin, A. (2002). Coordinated traffic of Grb2 and Ras during epidermal growth factor receptor endocytosis visualized in living cells. *Mol Biol Cell* 13 (5), 1522-1535.

Joseph, E. M. and Melton, D. A. (1998). Mutant Vg1 ligands disrupt endoderm and mesoderm formation in *Xenopus* embryos. *Development* 125 (14), 2677-2685.

Katzmann, D. J., Odorizzi, G. and Emr, S. D. (2002). Receptor downregulation and multivesicular-body sorting. *Nat Rev Mol Cell Biol* 3, 893-905.

Kawamura, N., Sun-Wada, G.-H., Aoyama, M., Harada, A., Takasuga, S., Sasaki, T. and Wada, Y. (2012). Delivery of endosomes to lysosomes via microautophagy in the visceral endoderm of mouse embryos. *Nat Commun* 3, 1071.

Kawamura, N., Takaoka, K., Hamada, H., Hadjantonakis, A.-K., Sun-Wada, G.-H. and Wada, Y. (2020). Rab7-Mediated Endocytosis Establishes Patterning of Wnt Activity through Inactivation of Dkk Antagonism. *CellReports* 31, 107733.

Keller, R. and Sutherland, A. (2020). Convergent extension in the amphibian, *Xenopus laevis*. *Curr Top Dev Biol* 136, 271-317.

Keller, R., Shook, D., Skoglund, P. (2008). The forces that shape embryos: physical aspects of convergent extension by cell intercalation. *Phys Biol* 5, 015007.

Kiecker, C. and Niehrs, C. (2001). A morphogen gradient of Wnt/beta-catenin signalling regulates anteroposterior neural patterning in *Xenopus*. *Development* 128 (21), 4189-4201.

Kim, K., Lake, B. B., Haremake, T., Weinstein, D. C. and Sokol, S. Y. (2012). Rab11 regulates planar polarity and migratory behavior of multiciliated cells in *Xenopus* embryonic epidermis. *Dev. Dyn.* 241, 1385-1395.

- Kimelman, D. and Kirschner, M. (1987). Synergistic induction of mesoderm by FGF and TGF-beta and the identification of an mRNA coding for FGF in the early *Xenopus* embryo. *Cell* 51 (5), 869-877.
- Kinoshita, N., Hashimoto, Y., Yasue, N., Suzuki, M., Cristea, I. M., Ueno, N. (2020). Mechanical Stress Regulates Epithelial Tissue Integrity and Stiffness through the FGFR/Erk2 Signaling Pathway during Embryogenesis. *Cell Rep* 30(11), 3875-3888.
- Kishigami, S. and Mishina, Y. (2005). BMP signaling and early embryonic patterning. *Cytokine Growth Factor Rev* 16 (3), 265-278.
- Kjolby, R. A. S. and Harland, R. M. (2017). Genome-wide identification of Wnt/ β -catenin transcriptional targets during *Xenopus* gastrulation. *Developmental Biology* 426, 165-175.
- Kobayashi, T., Vischer, U. M., Rosnoblet, C., Lebrand, C., Lindsay, M., Parton, R. G., Kruithof, E. K., Gruenberg, J. (2000). The tetraspanin CD63/lamp3 cycles between endocytic and secretory compartments in human endothelial cells. *Mol Biol Cell* 11 (5), 1829-1843.
- Kolch, W. (2000). Meaningful relationships: the regulation of the Ras/Raf/MEK/ERK pathway by protein interactions. *Biochem. J.* 351, 289-305.
- Kreis, J., Bonß, R., Vick, P. (2020a). The tetraspanin Cd63 is required for eye morphogenesis in *Xenopus*. *MicroPubl Biol*, doi: 10.17912/micropub.biology.000335.
- Kreis, J., Bonß, R., Feistel, K.; Vick, P. (2020b). Expression of an endosome-excluded Cd63 prevents axis elongation in *Xenopus*. *MicroPubl Biol*, doi: 10.17912/micropub.biology.000334.
- Kreis, J., Wielath, F. M., Vick, P. (2021). Rab7 is required for mesoderm patterning and gastrulation in *Xenopus*. *Biol Open* 10 (7), bio056887.
- Kumar S., Umair Z., Yoon J., Lee U., Kim S. C., Park J. B., Lee J. Y., Kim J. (2018). Xbra and Smad-1 cooperate to activate the transcription of neural repressor ventx1.1 in *Xenopus* embryos. *Sci. Rep.* 8, 11391.
- Kumar, V., Goutam, R. S., Park, S., Lee, U., Kim, J. (2021). Functional Roles of FGF Signaling in Early Development of Vertebrate Embryos. *Cells* 10 (8), 2148.
- Kumasaka, M., Sato, S., Yajima, I. and Yamamoto, H. (2003). Isolation and developmental expression of tyrosinase family genes in *Xenopus laevis*. *Pigment Cell Res.* 16, 455-462.
- Kurth, T. and Hausen, P. (2000). Bottle cell formation in relation to mesodermal patterning in the *Xenopus* embryo. *Mech Dev* 97 (1-2), 117-131.

- Langemeyer, L., Borchers, A.-C., Herrmann, E., Füllbrunn, N., Han, Y., Perz, A., Auffarth, K., Kümmel, D. and Ungermann, C. (2020). A conserved and regulated mechanism drives endosomal Rab transition. *eLife* 11 (9), e56090.
- Latysheva, N., Muratov, G., Rajesh, S., Padgett, M., Hotchin, N.A., Overduin, M., Berditchevski, F. (2006). Syntenin-1 is a new component of tetraspanin-enriched microdomains: mechanisms and consequences of the interaction of syntenin-1 with CD63. *Mol Cell Biol* 26, 7707-7718.
- Lee, J.-Y. and Harland, R. M. (2010). Endocytosis Is Required for Efficient Apical Constriction during *Xenopus* Gastrulation. *Current Biology* 20, 253-258.
- Lee, R. H. K., Iioka, H., Ohashi, M., Iemura, S.-I., Natsume, T. and Kinoshita, N. (2007). XRab40 and XCullin5 form a ubiquitin ligase complex essential for the noncanonical Wnt pathway. *The EMBO Journal* 26, 3592-3606.
- Li, V. S. W., Ng, S. S., Boersema, P. J., Low, T. Y., Karthaus, W. R., Gerlach, J. P., Mohammed, S., Heck, A. J. R., Maurice, M. M., Mahmoudi, T., et al. (2012). Wnt Signaling through Inhibition of β -Catenin Degradation in an Intact Axin1 Complex. *Cell* 149, 1245-1256.
- Lopes, V. S., Wasmeier, C., Seabra, M. C. and Futter, C. E. (2007). Melanosome maturation defect in Rab38-deficient retinal pigment epithelium results in instability of immature melanosomes during transient melanogenesis. *Mol. Biol. Cell* 18, 3914-3927.
- Lu, A., Tebar, F., Alvarez-Moya, B., López-Alcalá, C., Calvo, M., Enrich, C., Agell, N., Nakamura, T., Matsuda, M., Bachs, O. (2009). A clathrin-dependent pathway leads to KRas signaling on late endosomes en route to lysosomes. *J Cell Biol* 184 (6), 863-879.
- Lupia, A., Peppicelli, S., Witort, E., Bianchini, F., Carloni, V., Pimpinelli, N., Urso, C., Borgognoni, L., Capaccioli, S., Calorini, L. and Lulli, M. (2014). CD63 Tetraspanin Is a Negative Driver of Epithelial-to-Mesenchymal Transition in Human Melanoma Cells. *Journal of Investigative Dermatology* 134, 2947-2956.
- Margiotta, A., Progida, C., Bakke, O. and Bucci, C. (2017). Rab7a regulates cell migration through Rac1 and vimentin. *BBA - Molecular Cell Research* 1864, 367-381.
- Marsden, M., DeSimone, D.W. (2003). Integrin-ECM interactions regulate cadherin-dependent cell adhesion and are required for convergent extension in *Xenopus*. *Curr Biol* 13, 1182-91.
- Martinez, O. and Goud, B. (1998). Rab proteins. *Biochimica et Biophysica Acta*, 1404, 101-112.

- Martinez-Morales, J. R., Rembold, M., Greger, K., Simpson, J. C., Brown, K. E., Quiring, R., Pepperkok, R., Martin-Bermudo, M. D., Himmelbauer, H. and Wittbrodt, J. (2009). ojoplano-mediated basal constriction is essential for optic cup morphogenesis. *Development* 136, 2165-2175.
- Mellman, I. (1996). Endocytosis and Molecular Sorting. *Annu. Rev. Cell Dev. Biol.*, 12, 575-625.
- Miller, J. R., Rowning, B. A., Larabell, C. A., Yang-Snyder, J. A., Bates, R. L., Moon, R. T. (1999). Establishment of the dorsal-ventral axis in *Xenopus* embryos coincides with the dorsal enrichment of dishevelled that is dependent on cortical rotation. *J Cell Biol* 146 (2), 427-437.
- Moon, R. T. (2005). *Xenopus* Embryo: β -catenin and Dorsal-Ventral Axis Formation. *Encyclopedia of Life Sciences*, doi.org/10.1038/npg.els.0004185.
- Morgan, M. R., Hamidi, H., Bass, M. D., Warwood, S., Ballestrem, C., Humphries, M. J. (2013). Syndecan-4 phosphorylation is a control point for integrin recycling. *Dev Cell* 24, 472-485.
- Morrison, D. K. (2012). MAP kinase pathways. *Cold Spring Harb Perspect Biol* 4 (11), a011254.
- Muñoz, R., Moreno, M., Oliva, C., Orbenes, C., Larraín, J. (2006). Syndecan-4 regulates non-canonical Wnt signalling and is essential for convergent and extension movements in *Xenopus* embryos. *Nat Cell Biol* 8, 492-500.
- Nada, S., Hondo, A., Kasai, A., Koike, M., Saito, K., Uchiyama, Y., Okada, M. (2009). The novel lipid raft adaptor p18 controls endosome dynamics by anchoring the MEK-ERK pathway to late endosomes. *EMBO J* 28 (5), 477-489.
- Nakamura, Y., de Paiva Alves, E., Veenstra, G. J. C. and Hoppler, S. (2016). Tissue- and stage-specific Wnt target gene expression is controlled subsequent to β -catenin recruitment to cis-regulatory modules. *Development* 143, 1914-1925.
- Neilson, K. M. and Friesel, R. (1996). Ligand-independent activation of fibroblast growth factor receptors by point mutations in the extracellular, transmembrane, and kinase domains. *J Biol Chem* 271 (40), 25049-25057.
- Niehrs, C. (2004). Regionally specific induction by the Spemann-Mangold organizer. *Nat Rev Genet* 5 (6), 425-434.
- Niehrs, C. (2010). On growth and form: a Cartesian coordinate system of Wnt and BMP signaling specifies bilaterian body axes. *Development* 137 (6), 845-857.

- Niehrs, C. and Acebron, S. P. (2010). Wnt signaling: multivesicular bodies hold GSK3 captive. *Cell* 143, 1044-1046.
- Niehrs, C. and Pollet, N. (1999). Synexpression groups in eukaryotes. *Nature* 402 (6761), 483-487.
- Nielsen, E., Severin, F., Backer, J. M., Hyman, A. A., Zerial, M. (1999). Rab5 regulates motility of early endosomes on microtubules. *Nat Cell Biol* 1 (6), 376-382.
- Nieuwkoop, P. D. and Faber, J. (1994). Normal table of *Xenopus laevis* (Daudin): a systematical and chronological survey of the development from the fertilized egg till the end of metamorphosis. Garland Publishing Inc.
- Nishita, M., Hashimoto, M. K., Ogata, S., Laurent, M. N., Ueno, N., Shibuya, H., Cho, K. W. (2000). Interaction between Wnt and TGF-beta signalling pathways during formation of Spemann's organizer. *Nature* 403 (6771), 781-785.
- Oksvold, M. P., Skarpen, E., Wierød, L., Paulsen, R. E., Huitfeldt, H. S. (2001). Re-localization of activated EGF receptor and its signal transducers to multivesicular compartments downstream of early endosomes in response to EGF. *Eur J Cell Biol* 80 (4), 285-294.
- Osborn, D. P. S., Li, K., Cutty, S. J., Nelson, A. C., Wardle, F. C., Hinitz, Y., Hughes, S. M. (2020). Fgf-driven Tbx protein activities directly induce myf5 and myod to initiate zebrafish myogenesis. *Development* 147 (8), dev184689.
- Parr, B. A. and McMahon, A. P. (1995). Dorsalizing signal Wnt-7a required for normal polarity of D-V and A-P axes of mouse limb. *Nature* 374, 350-353.
- Paterno, G. D. and Gillespie, L. L. (1989). Fibroblast growth factor and transforming growth factor beta in early embryonic development. *Prog Growth Factor Res* 1 (2), 79-88.
- Pera, E. M., Acosta, H., Gougnard, N., Climent, M., Arregi, I. (2014). Active signals, gradient formation and regional specificity in neural induction. *Exp Cell Res* 321 (1), 25-31.
- Peshkin, L., Lukyanov, A., Kalocsay, M., Gage, R. M., Wang, D., Pells, T. J., Karimi, K., Vize, P. D., Wühr, M. and Kirschner, M. W. (2019). The protein repertoire in early vertebrate embryogenesis. Preprint, bioRxiv 1865, 571174.
- Piccolo, S., Sasai, Y., Lu, B., De Robertis, E. M. (1996). Dorsoventral patterning in *Xenopus*: inhibition of ventral signals by direct binding of chordin to BMP-4. *Cell* 86 (4), 589-598.
- Piper, R. C. and Katzmann, D. J. (2007). Biogenesis and Function of Multivesicular Bodies. *Annu. Rev. Cell Dev. Biol.* 23, 519-547.

- Pla, P. and Monsoro-Burq, A. H. (2018). The neural border: Induction, specification and maturation of the territory that generates neural crest cells. *Developmental Biology* 444 Suppl 1, S36-S46.
- Platta, H. W. and Stenmark, H. (2011). Endocytosis and signaling. *Current Opinion in Cell Biology* 23, 393-403.
- Ploper, D. and De Robertis, E. M. (2015). The MITF family of transcription factors: Role in endolysosomal biogenesis, Wnt signaling, and oncogenesis. *Pharmacol. Res.* 99, 36-43.
- Ploper, D., Taelman, V. F., Robert, L., Perez, B. S., Titz, B., Chen, H.-W., Graeber, T. G., Euv, von, E., Ribas, A. and De Robertis, E. M. (2015). MITF drives endolysosomal biogenesis and potentiates Wnt signaling in melanoma cells. *Proc. Natl. Acad. Sci. U.S.A.* 112, E420-429.
- Pols, M. S. and Klumperman, J. (2009). Trafficking and function of the tetraspanin CD63. *Experimental Cell Research* 315, 1584-1592.
- Poteryaev, D., Datta, S., Ackema, K., Zerial, M. and Spang, A. (2010). Identification of the Switch in Early-to-Late Endosome Transition. *Cell* 141, 497-508.
- Radford, K. J., Thorne, R. F. and Hersey, P. (1997). Regulation of tumor cell motility and migration by Cd63 in a human melanoma cell line. *J. Immunol.* 158, 3353-3358.
- Ramel, M.-C. and Lekven, A. C. (2004). Repression of the vertebrate organizer by Wnt8 is mediated by Vent and Vox. *Development* 131, 3991-4000.
- Raposo, G. and Marks, M. S. (2007). Melanosome – dark organelles enlighten endosomal membrane transport. *Nat Rev Mol Cell Biol* 8, 786-797.
- Rink, J., Ghigo, E., Kalaidzidis, Y. and Zerial, M. (2005). Rab Conversion as a Mechanism of Progression from Early to Late Endosomes. *Cell* 122, 735-749.
- Rocha-Perugini, V., González-Granado, J. M., Tejera, E., López-Martín, S., Yañez-Mó, M., Sánchez-Madrid, F. (2014). Tetraspanins CD9 and CD151 at the immune synapse support T-cell integrin signaling. *Eur J Immunol* 44 (7), 1967-1975.
- Rodaway, A., Takeda, H., Koshida, S., Broadbent, J., Price, B., Smith, J. C., Patient, R., Holder, N. (1999). Induction of the mesendoderm in the zebrafish germ ring by yolk cell-derived TGF-beta family signals and discrimination of mesoderm and endoderm by FGF. *Development* 126 (14), 3067-3078.
- Rodman, J. S. and Wandinger-Ness, A. (2000). Rab GTPases coordinate endocytosis. *Journal of Cell Science* 113, 183-192.

- Rous, B. A., Reaves, B. J., Ihrke, G., Briggs, J. A., Gray, S. R., Stephens, D. J., Banting, G., Luzio, J. P. (2002). Role of adaptor complex AP-3 in targeting wild-type and mutated CD63 to lysosomes. *Mol Biol Cell* 13, 1071-1082.
- Sabharanjak, S., Sharma, P., Parton, R. G., Mayor, S. (2002). GPI-anchored proteins are delivered to recycling endosomes via a distinct cdc42-regulated, clathrin-independent pinocytic pathway. *Dev Cell* 2 (4), 411-423.
- Saksena, S., Sun, J., Chu, T., Emr, S. D. (2007). ESCRTing proteins in the endocytic pathway. *Trends Biochem Sci* 32 (12), 561-573.
- Sardiello, M., Palmieri, M., di Ronza, A., Medina, D. L., Valenza, M., Gennarino, V. A., Di Malta, C., Donaudy, F., Embrione, V., Polishchuk, R. S., Banfi, S., Parenti, G., Cattaneo, E., Ballabio, A. (2009). A Gene Network Regulating Lysosomal Biogenesis and Function. *Science* 325, 473-477.
- Scherz, P. J., Harfe, B. D., McMahon, A. P. and Tabin, C. J. (2004). The Limb Bud Shh-Fgf Feedback Loop Is Terminated by Expansion of Former ZPA Cells. *Science* 305, 396-399.
- Schlessinger, J. (2000). Cell Signaling by Receptor Tyrosine Kinases. *Cell* 103, 211-225.
- Schneider, I., Kreis, J., Schweickert, A., Blum, M. and Vick, P. (2019). A dual function of FGF signaling in *Xenopus* left-right axis formation. *Development* 146, dev173575.
- Schneider, S., Steinbeisser, H., Warga, R. M., Hausen, P. (1996). β -catenin translocation into nuclei demarcates the dorsalizing centers in frog and fish embryos. *Mechanism of Development* 57, 191-198.
- Schuh, A. L. and Audhya, A. (2014). The ESCRT machinery: from the plasma membrane to endosomes and back again. *Crit Rev Biochem Mol Biol* 49 (3), 242-261.
- Schulte-Merker, S. and Smith, J. C. (1995). Mesoderm formation in response to Brachyury requires FGF signaling. *Curr Biol* 5 (1), 62-67.
- Session, A. M., Uno, Y., Kwon, T., Chapman, J. A., Toyoda, A., Takahashi, S., Fukui, A., Hikosaka, A., Suzuki, A., Kondo, M., et al. (2016). Genome evolution in the allotetraploid frog *Xenopus laevis*. *Nature* 538, 336-343.
- Shi, D.-L., Bourdelas, A., Umbhauer, M. and Boucaut, J.-C. (2002). Zygotic Wnt/beta-catenin signaling preferentially regulates the expression of Myf5 gene in the mesoderm of *Xenopus*. *Developmental Biology* 245, 124-135.

- Sigismund, S., Confalonieri, S., Ciliberto, A., Polo, S., Scita, G. and Di Fiore, P. P. (2012). Endocytosis and signaling: cell logistics shape the eukaryotic cell plan. *Physiological Reviews* 92, 273-366.
- Simons, M. and Raposo, G. (2009). Exosomes – vesicular carriers for intercellular communication. *Current Opinion in Cell Biology* 21, 575-581.
- Sinn, R. and Wittbrodt, J. (2013). An eye on eye development. *Mechanisms of Development* 130, 347-358.
- Sive, H. L., Grainger, R. M. and Harland, R. M. (2000). *Early Development of Xenopus Laevis*. CSHL Press.
- Skirkanich, J., Luxardi, G., Yang, J., Kodjabachian, L., Klein, P.S. (2011). An essential role for transcription before the MBT in *Xenopus laevis*. *Dev Biol* 357 (2), 478-491.
- Skjeldal, F. M., Hofstad Haugen, L., Mateus, D., Frei, D. M., Vik Rødseth, A., Hu, X. and Bakke, O. (2021). De novo formation of early endosomes during Rab5-to-Rab7a transition. *Journal of Cell Science* 134 (8), jcs254185.
- Slack, J.M., Darlington, B. G., Gillespie, L. L., Godsave, S. F., Isaacs, H. V., Paterno, G. D. (1990). Mesoderm induction by fibroblast growth factor in early *Xenopus* development. *Philos Trans R Soc Lond B Biol Sci* 327 (1239), 75-84.
- Smith, J. C. (1989). Induction and early amphibian development. *Curr Opin Cell Biol* 1 (6), 1061-1070.
- Smith, J. C., Cunliffe, V., Green, J. B., New, H. V. (1993). Intercellular signalling in mesoderm formation during amphibian development. *Philos Trans R Soc Lond B Biol Sci* 340 (1293), 287-296.
- Smith, J. C., Price, B. M., Green, J. B., Weigel, D., Herrmann, B. G. (1991). Expression of a *Xenopus* homolog of Brachyury (T) is an immediate-early response to mesoderm induction. *Cell* 67 (1), 79-87.
- Smith, W. C. and Harland, R. M. (1991). Injected Xwnt-8 RNA acts early in *Xenopus* embryos to promote formation of a vegetal dorsalizing center. *Cell* 67, 753-765.
- Smith, W. C., McKendry, R., Ribisi, S. and Harland, R. M. (1995). A nodal-related gene defines a physical and functional domain within the Spemann organizer. *Cell* 82, 37-46.
- Sokol, S., Christian, J. L., Moon, R. T. and Melton, D. A. (1991). Injected Wnt RNA induces a complete body axis in *Xenopus* embryos. *Cell* 67, 741-752.

- Sorkin, A., McClure, M., Huang, F., Carter, R. (2000). Interaction of EGF receptor and grb2 in living cells visualized by fluorescence resonance energy transfer (FRET) microscopy. *Curr Biol* 10 (21), 1395-1398.
- Sorkin, A. and Von Zastrow, M. (2002). Signal transduction and endocytosis: close encounters of many kinds. *Nat Rev Mol Cell Biol* 3 (8), 600-614.
- Stenmark, H. (2009). Rab GTPases as coordinators of vesicle traffic. *Nature reviews* 10, 513-525.
- Stenmark, H. and Olkkonen, V. M. (2001). The Rab GTPase family. *Genome Biology* 2 (5).
- Stennard, F., Ryan, K., Gurdon, J. B. (1997). Markers of vertebrate mesoderm induction. *Curr Opin Genet Dev* 7 (5), 620-627.
- Strong, C. F., Barnett, M. W., Hartman, D., Jones, E. A., Stott, D. (2000). Xbra3 induces mesoderm and neural tissue in *Xenopus laevis*. *Dev Biol* 222 (2), 405-419.
- Stubbs, J. L., Oishi, I., Izpisua-Belmonte, J. C. and Kintner, C. (2008). The forkhead protein Foxj1 specifies node-like cilia in *Xenopus* and zebrafish embryos. *Nat Genet* 40, 1454-1460.
- Symes, K. and Smith, J. C. (1987). Gastrulation movements provide an early marker of mesoderm induction in *Xenopus laevis*. *Development* 101, 339-349.
- Tada, M. and Smith, J. C. (2000). Xwnt11 is a target of *Xenopus* Brachyury: regulation of gastrulation movements via Dishevelled, but not through the canonical Wnt pathway. *Development* 127, 2227-2238.
- Taelman, V. F., Dobrowolski, R., Plouhinec, J.-L., Fuentealba, L. C., Vorwald, P. P., Gumper, I., Sabatini, D. D. and De Robertis, E. M. (2010). Wnt Signaling Requires Sequestration of Glycogen Synthase Kinase 3 inside Multivesicular Endosomes. *Cell* 143, 1136-1148.
- Tao, Q., Yokota, C., Puck, H., Kofron, M., Birsoy, B., Yan, D., Asashima, M., Wylie, C. C., Lin, X., Janet Heasman, J. (2005). Maternal wnt11 activates the canonical wnt signaling pathway required for axis formation in *Xenopus* embryos. *Cell* 120 (6), 857-871.
- Teis, D., Wunderlich, W. and Huber, L. A. (2002). Localization of the MP1-MAPK scaffold complex to endosomes is mediated by p14 and required for signal transduction. *Developmental Cell* 3, 803-814.
- ten Berge, D., Brugmann, S. A., Helms, J. A., Nusse, R. (2008). Wnt and FGF signals interact to coordinate growth with cell fate specification during limb development. *Development*, 135 (19), 3247-3257.

- Termini, C. M. and Gillette, J. M. (2017). Tetraspanins Function as Regulators of Cellular Signaling. *Front. Cell Dev. Biol.* 5 (34).
- Trajkovic, K., Hsu, C., Chiantia, S., Rajendran, L., Wenzel, D., Wieland, F., Schwille, P., Brügger, B. and Simons, M. (2008). Ceramide triggers budding of exosome vesicles into multivesicular endosomes. *Science* 319 (5867), 1244-1247.
- Ukita, K., Hirahara, S., Oshima, N., Imuta, Y., Yoshimoto, A., Jang, C.-W., Oginuma, M., Saga, Y., Behringer, R. R., Kondoh, H., et al. (2009). Wnt signaling maintains the notochord fate for progenitor cells and supports the posterior extension of the notochord. *Mechanisms of Development* 126, 791-803.
- van Niel, G., Charrin, S., Simoes, S., Romao, M., Rochin, L., Saftig, P., Marks, M. S., Rubinstein, E. and Raposo, G. (2011). The Tetraspanin CD63 Regulates ESCRT-Independent and -Dependent Endosomal Sorting during Melanogenesis. *Developmental Cell* 21, 708-721.
- Van Raay, T. J., and Vetter, M. L. (2004). Wnt/frizzled signaling during vertebrate retinal development. *Dev Neurosci* 26 (5-6), 352-358.
- Vick, P., Kreis, J., Schneider, I., Tingler, M., Getwan, M., Thumberger, T., Beyer, T., Schweickert, A. and Blum, M. (2018). An Early Function of Polycystin-2 for Left-Right Organizer Induction in *Xenopus*. *iScience* 2, 76-85.
- Villanueva, S., Glavic, A., Ruiz, P. and Mayor, R. (2002). Posteriorization by FGF, Wnt, and retinoic acid is required for neural crest induction. *Developmental Biology* 241, 289-301.
- Vinyoles, M., Del Valle-Pérez, B., Curto, J., Viñas-Castells, R., Alba-Castellón, L., García de Herreros, A. and Duñach, M. (2014). Multivesicular GSK3 sequestration upon Wnt signaling is controlled by p120-catenin/cadherin interaction with LRP5/6. *Molecular Cell* 53, 444-457.
- Vogel, A., Rodriguez, C. and Izpisua Belmonte, J. C. (1996). Involvement of FGF-8 in initiation, outgrowth and patterning of the vertebrate limb. *Development* 122, 1737-1750.
- von Dassow, G., Schmidt, J. E., Kimelman, D. (1993). Induction of the *Xenopus* organizer: expression and regulation of *Xnot*, a novel FGF and activin-regulated homeo box gene. *Genes Dev* 7 (3), 355-366.
- Vonderheit, A. and Helenius, A. (2005). Rab7 associates with early endosomes to mediate sorting and transport of Semliki forest virus to late endosomes. *PLoS Biol* 3 (7), 1225-1238.
- Vonica, A. and Gumbiner, B. M. (2002). Zygotic Wnt activity is required for Brachyury expression in the early *Xenopus laevis* embryo. *Developmental Biology* 250, 112-127.

- Walentek, P., Beyer, T., Thumberger, T., Schweickert, A., Blum, M. (2012). ATP4a is required for Wnt-dependent Foxj1 expression and leftward flow in *Xenopus* left-right development. *Cell Rep* 1 (5), 516-527.
- Walentek, P., Schneider, I., Schweickert, A. and Blum, M. (2013). Wnt11b Is Involved in Cilia-Mediated Symmetry Breakage during *Xenopus* Left-Right Development. *PLoS ONE* 8, e73646-73649.
- Wallingford, J. B., Harland, R. M. (2001). *Xenopus* Dishevelled signaling regulates both neural and mesodermal convergent extension: parallel forces elongating the body axis. *Development* 128, 2581-2592.
- Wallingford, J. B., Harland, R. M. (2002). Neural tube closure requires Dishevelled-dependent convergent extension of the midline. *Development* 129, 5815-5825.
- Wallingford, J. B., Fraser, S. E., Harland, R. M. (2002). Convergent extension: the molecular control of polarized cell movement during embryonic development. *Dev Cell* 2 (6), 695-706.
- Weaver, C., Farr 3rd, G. H., Pan, W., Rowning, B. A., Wang, J., Mao, J., Wu, D., Li, L., Larabell, C. A., Kimelman, D. (2003). GBP binds kinesin light chain and translocates during cortical rotation in *Xenopus* eggs. *Development* 130 (22), 5425-5436.
- Weaver, C. and Kimelman, D. (2004). Move it or lose it: axis specification in *Xenopus*. *Development* 131, 3491-3499.
- Wessely, O. and Tran, U. (2011). *Xenopus* pronephros development – past, present, and future. *Pediatr Nephrol* 26, 1545-1551.
- Whitman, M., Melton, D. A. (1992). Involvement of p21ras in *Xenopus* mesoderm induction. *Nature* 357 (6375), 252-254.
- Wilson, P. A. and Hemmati-Brivanlou, A. (1995). Induction of epidermis and inhibition of neural fate by Bmp-4. *Nature* 376 (6538), 331-333.
- Wilson, V., Olivera-Martinez, I. and Storey, K. G. (2009). Stem cells, signals and vertebrate body axis extension. *Development* 136, 1591-1604.
- Wouters, F. S. and Bastiaens, P. I. (1999). Fluorescence lifetime imaging of receptor tyrosine kinase activity in cells. *Curr Biol* 9 (19), 1127-1130.
- Yamaguchi, T. P., Takada, S., Yoshikawa, Y., Wu, N., McMahon, A. P. (1999). T (Brachyury) is a direct target of Wnt3a during paraxial mesoderm specification. *Genes Dev* 13 (24), 3185-3190.

- Yamamoto, Y. and Oelgeschläger, M. (2004). Regulation of bone morphogenetic proteins in early embryonic development. *Naturwissenschaften* 91 (11), 519-534.
- Yang, Y. and Niswander, L. (1995). Interaction between the signaling molecules WNT7a and SHH during vertebrate limb development: dorsal signals regulate anteroposterior patterning. *Cell* 80, 939-947.
- Yokota, C., Kofron, M., Zuck, M., Houston, D. W., Isaacs, H., Asashima, M., Wylie, C. C. and Heasman, J. (2003). A novel role for a nodal-related protein; Xnr3 regulates convergent extension movements via the FGF receptor. *Development* 130, 2199-2212.
- Yokota, C., Mukasa, T., Higashi, M., Odaka, A., Muroya, K., Uchiyama, H., Eto, Y., Asashima, M. and Momoi, T. (1995). Activin Induces the Expression of the *Xenopus* Homolog of Sonic hedgehog during Mesoderm Formation in *Xenopus* Explants. *Biochem. Biophys. Res. Commun.* 207, 1-7.
- Yost, C., Torres, M., Miller, J. R., Huang, E., Kimelman, D., Moon, R. T. (1996). The axis-inducing activity, stability, and subcellular distribution of beta-catenin is regulated in *Xenopus* embryos by glycogen synthase kinase 3. *Genes Dev* 10 (12), 1443-1454.
- Zerial, M. and McBride, H. (2001). Rab proteins as membrane organizers. *Nature Rev. Mol. Cell Biol.* 2, 107-117.
- Zhang, J., Houston, D. W., King, M. L., Payne, C., Wylie, C., Heasman, J. (1998). The Role of Maternal VegT in Establishing the Primary Germ Layers in *Xenopus* Embryos. *Cell* 94, 515-524.
- Zhang, M., Chen, L., Wang, S. and Wang, T. (2009). Rab7: roles in membrane trafficking and disease. *Biosci. Rep.* 29, 193-209.
- Zhang, B., Tran, U. and Wessely, O. (2011). Expression of Wnt signaling components during *Xenopus* pronephros development. *PLoS ONE* 6, e26533.
- Zhao, J., Cao, Y., Zhao, C., Postlethwait, J., Meng, A. (2003). An SP1-like transcription factor Spr2 acts downstream of Fgf signaling to mediate mesoderm induction. *EMBO J* 22 (22), 6078-6088.
- Zimmermann, L. B., De Jesús-Escobar, J. M., Harland, R. M. (1996). The Spemann organizer signal noggin binds and inactivates bone morphogenetic protein 4. *Cell* 86 (4), 599-606.

Author's contribution

Rab7 is required for mesoderm patterning and gastrulation in *Xenopus*

Investigation, validation, visualization, formal analysis, data curation, conceptualization in parts and writing: review and editing.

The late endosomal regulator Rab7 is required for FGF dependent mesoderm specification by regulating Ras mediated MAPK activation

Investigation, validation, visualization, formal analysis, data curation, conceptualization in parts and writing.


The tetraspanin Cd63 is required for eye morphogenesis in *Xenopus*

Investigation, validation, visualization, formal analysis and writing: review and editing.

Expression of an endosome-excluded Cd63 prevents axis elongation in *Xenopus*

Investigation, validation, visualization, formal analysis and writing: review and editing.

Stuttgart, 22.06.2022
Place and date


Signature (PD Dr. Kerstin Feistel)

Curriculum vitae

Name: Jennifer Kreis
 Date of birth: 12.06.1985
 Place of birth: Herdecke, Germany
 Place of Residence: Stuttgart, Germany
 Nationality: German

Education and Scientific Career

Since 2016 Doctoral student at the University of Hohenheim, Germany
 in the laboratory of Prof. Dr. M. Blum, in the group of
 Dr. P. Vick
 Funded (3 years) by the Landesgraduiertenförderung of
 Baden-Württemberg

2010 – 2016 Study of Biology at the University of Hohenheim, Germany
 M.Sc. Thesis in the laboratory of Prof. Dr. M. Blum, in the
 group of Dr. P. Vick
 B.Sc. Thesis in the laboratory and group of
 Prof. Dr. M. Blum

2009 – 2010 Study of Library- and Informationmanagement at
 Hochschule der Medien in Stuttgart, Germany

2006 – 2009 Bookseller apprenticeship at Buchhandlung Friedlein in
 Singen Hohentwiel, Germany

1996 – 2005 Highschool “Friedrich Wöhler Gymnasium“ in Singen
 Hohentwiel, Germany

Qualifications

12/2016 – 02/2021 Humboldt reloaded seminars “Forschendes Lernen“
 University of Hohenheim, Germany

07/2016 Seminar “Aquatische Modellsysteme“ and practical course
 “Arbeiten mit aquatischen Modellsystemen“
 University of Ulm, Germany

03/2016 Seminar and practical course "FELASA B"
University of Hohenheim, Germany

Conference Participations

12/2019 5. German *Xenopus* Meeting
Albert-Ludwigs-University & University Freiburg Medical
Centre, Germany

10/2019 6th Tri-regional stem cell and developmental biology
meeting
Illkirch, France

06/2019 2. European Amphibian Club 2019
Lutherstadt Wittenberg, Germany

06/2017 1. European Amphibian Club 2017
Rennes, France

03/2017 Joint Meeting of the German and Japanese Societies of
Developmental Biologists
Christian-Albrechts-University Kiel, Germany

12/2016 3. German *Xenopus* Meeting
University of Hohenheim, Germany

10/2016 11th GfE School, Cell Dynamics in Development &
Evolution
Schloss Reisenburg/Günzburg, Germany

10/2015 2. German *Xenopus* Meeting
Karlsruhe Institute of Technology, Germany

04/2013 1. *Xenopus* Regio Meeting
University of Hohenheim, Germany

Stuttgart, 02.06.2022

Place and date


Signature

Danksagung

Das erfolgreiche Erstellen dieser Arbeit wurde mir durch das Zutun vieler toller Menschen in meinem Umfeld ermöglicht. So ist die Unterstützung von Seiten meines sozialen Umfelds in vielerlei Hinsicht vergleichbar mit den Kapazitäten der hier eruierten endosomalen Maschinerie. Aufgrund des perfekten Zusammenspiels der mir wohlwollend entgegengebrachten Zuwendung in Form von Rückhalt, Freundschaft, gemeinsam verbrachter Zeit, konstruktiver Kritik, gut gemeinten Ratschlägen, Motivation, freundlichen Worten, wissenschaftlichem Input, Begeisterung für die Biologie und noch vielem mehr, war diese Promotion möglich. Ähnlich, wie die kleinen Rab GTPasen im endosomalen Netzwerk, hat jeder sowohl im privaten als auch beruflichen Kreis seinen kleinen oder großen Beitrag zum entsprechenden Zeitpunkt geleistet um die Maschinerie „Promotion“ voran zu treiben. Dafür kann ich nicht annähernd genügend Dank aussprechen. Damit niemand vergessen wird, bedanke ich mich von ganzem Herzen bei allen, die Anteil an meiner persönlichen Reifung und diesem für mich herausfordernden und unfassbar spannenden Abschnitt meines Lebens genommen haben!